

**TIGHT-BINDING MODEL FOR ELECTRON
TRANSPORT THROUGH FERROMAGNETIC
METAL/SPACER/FERROMAGNETIC METAL
JUNCTIONS**



Natthagrittha Nakhonthong

A Thesis Submitted in Partial Fulfillment of the Requirements for the

Degree of Master in Applied Physics

Suranaree University of Technology

Academic Year 2018

แบบจำลองแบบโททบายดิงสำหรับการขนส่งอิเล็กตรอนผ่านรอยต่อของโลหะ
เฟอร์โรแมกเนติก/ตัวกั้นกลาง/โลหะเฟอร์โรแมกเนติก



นางสาวณัฐกฤตา นาก้อนทอง

วิทยานิพนธ์นี้เป็นส่วนหนึ่งของการศึกษาตามหลักสูตรปริญญาวิทยาศาสตรมหาบัณฑิต

สาขาวิชาฟิสิกส์ประยุกต์

มหาวิทยาลัยเทคโนโลยีสุรนารี

ปีการศึกษา 2561

**TIGHT-BINDING MODEL FOR ELECTRON TRANSPORT
THROUGH FERROMAGNETIC METAL/ SPACER/
FERROMAGNETIC METAL JUNCTIONS**

Suranaree University of Technology has approved this thesis submitted in partial fulfillment of the requirements for a Master's Degree.

Thesis Examining Committee

Sirichok
(Assoc. Prof. Dr. Sirichok Jungthawan)

Chairperson

Puangratana Pairor
(Assoc. Prof. Dr. Puangratana Pairor)

Member (Thesis Advisor)

Michael F. Smith
(Asst. Prof. Dr. Michael F. Smith)

Member

Wittawat Saenrang
(Dr. Wittawat Saenrang)

Member

Kontorn Chamniprasart
(Assoc. Prof. Ft. Lt. Dr. Kontorn Chamniprasart)

Vice Rector for Academic Affairs
and Internationalization

Worawat Meevasana
(Assoc. Prof. Dr. Worawat Meevasana)

Dean of Institute of Science

ฉัฐกฤตา นาก่อนทอง : แบบจำลองแบบโททับายคิงสำหรับการขนส่งอิเล็กตรอนผ่านรอยต่อ
ของโลหะเฟอร์โรแมกเนติก/ตัวกั้นกลาง/โลหะเฟอร์โรแมกเนติก (TIGHT-BINDING
MODEL FOR ELECTRON TRANSPORT THROUGH FERROMAGNETIC METAL/
SPACER/ FERROMAGNETIC METAL JUNCTIONS). อาจารย์ที่ปรึกษา :
รองศาสตราจารย์ ดร.พวงรัตน์ ไพเราะ, 100 หน้า.

ค่าสภาพต้านทานเชิงแม่เหล็ก, แบบจำลองแบบโททับายคิง, เฟอร์โรแมกเนต

วิทยานิพนธ์นี้เป็นการประยุกต์แบบจำลองแบบโททับายคิงในหนึ่งมิติสำหรับการศึกษาการ
ขนส่งอิเล็กตรอนในระบบรอยต่อโลหะเฟอร์โรแมกเนติก/ตัวกั้นกลาง/โลหะเฟอร์โรแมกเนติก โดยที่
ได้รวมค่าสนามแม่เหล็กภายนอกขนาดเล็กซึ่งตั้งฉากกับแนวการเรียงตัวของอะตอมในหนึ่งมิติ โดยใช้
รูปแบบเดียวกับปรากฏการณ์ซีมานอันเนื่องมาจากอันตรกิริยาระหว่างสปินของอิเล็กตรอนกับ
สนามแม่เหล็ก ในการศึกษานี้ได้คำนวณค่าความน่าจะเป็นในการส่งผ่านและการสะท้อนกลับของ
อิเล็กตรอนผ่านรอยต่อ และนำค่าความน่าจะเป็นดังกล่าวมาคำนวณหาค่าความนำไฟฟ้าและค่าสภาพ
ความต้านทานสนามแม่เหล็ก โดยที่ค่าสภาพความต้านทานของสนามแม่เหล็กมีค่าขึ้นอยู่กับปัจจัยทาง
กายภาพหลายประการ ซึ่งการศึกษานี้มุ่งเน้นไปที่คุณสมบัติทางกายภาพของตัวกั้นกลาง เมื่อมี
คุณสมบัติเป็นโลหะหรือฉนวน นอกจากนี้ยังศึกษาความหนาของตัวกั้นกลางและคุณภาพของรอยต่อ
อีกด้วย จากการศึกษาและวิเคราะห์คุณสมบัติดังกล่าว พบว่า ค่าอัตราส่วนสภาพความต้านทาน
สนามแม่เหล็กมีค่าเป็นลบในกรณีที่ตัวกั้นกลางมีคุณสมบัติโลหะเมื่อคุณภาพของรอยต่อนั้นดี ซึ่งค่าที่
เป็นลบนี้ ยังไม่มีการพบเห็นในการทดลอง อย่างไรก็ตามค่าอัตราส่วนสภาพความต้านทาน
สนามแม่เหล็กนี้มีค่าเพิ่มขึ้นตามค่าช่องว่างพลังงานของฉนวนที่เป็นตัวกั้นกลาง และค่าอัตราส่วน
สภาพความต้านทานนี้มีการเปลี่ยนแปลงแบบกวัดแกว่งตามค่าความหนาของฉนวน

สาขาวิชาฟิสิกส์
ปีการศึกษา 2561

ลายมือชื่อนักศึกษา ฉัฐกฤตา
ลายมือชื่ออาจารย์ที่ปรึกษา พวงรัตน์ ไพเราะ

ACKNOWLEDGEMENTS

First of all, I would like to express my sincere gratitude to my thesis advisor Ajarn Puangratana for her guidance and patience throughout my years at SUT. I could not have imagined having a better advisor and mentor for my M.Sc. study. I also would like to thank the rest of my thesis committee: Assoc. Prof. Dr. Sirichok Jungthawan, Asst. Prof. Dr. Michael F. Smith, and Dr. Wittawat Saenrang for their critical reviews and insightful comments on my thesis.

Secondly, I would like to thank my lovely friends: Mr. Thananuwat Suyupron, Mr. Kittipong Wangnok, Mr. Adithep Butraburi, Miss. Watcharaporn Moonsap, Miss. Jaruchit Siripak and Mr. Theerawee Thiwatwaranikul. They have been by on my side, enjoying all the happy moments and helping me through many tough times. In particular, I am grateful to thank P'Thananuwat for helpful advice, extensive knowledge, and inspiring me to do the research. I would also like to extend my gratitude to P'Kittipong for his friendship, empathy, and great take care of many things.

Thirdly, no graduate students would graduate without Mrs. Phenkhae Petchmai. I would like to thank her and all School of Physics staff for their help with support. They can handle all problems for us grad students from the very tiny to the very enormous. I am eternally grateful

Last but not least, I would like to thank my family: my parents, my brothers and sister for their never-ending supporting in all aspects of my life, understanding, and always standing by my side.

Natthagrittha Nakhonthong

CONTENTS

	Page
ABSTRACT IN THAI	I
ABSTRACT IN ENGLISH	II
ACKNOWLEDGEMENTS	III
CONTENTS	IV
LIST OF TABLES	VII
LIST OF FIGURES	VIII
LIST OF ABBREVIATIONS	XIII
CHAPTER	
I INTRODUCTION	1
1.1 Motivation	1
1.2 Literature Review	5
1.2.1 Experimental Studies of Magnetoresistance	5
1.2.2 Theoretical Models for Tunneling Magnetoresistance	10
1.2.2.1 One-electron Models	10
1.2.2.2 First Principles Calculations	15
1.3 Outline of Thesis	17
II TIGHT-BINDING MODEL FOR ONE-DIMENSIONAL TUNNELING SYSTEM	18
2.1 Hydrogen Molecule Ion	19
2.2 One-dimensional chain of metallic atoms	22
2.3 One-dimensional metal/spacer/metal junction	25

CONTENTS (Continued)

	Page
2.3.1 The Hamiltonian	26
2.3.2 The Electron State in Each Region and Matching Conditions	27
2.3.3 The Conductance	30
III ONE-DIMENSIONAL TUNNELING FOR FERROMAGNET/SPACER/FERROMAGNET JUNCTION IN A SMALL MAGNETIC FIELD	32
3.1 The Hamiltonian	33
3.2 The Electron States	35
3.3 The Electron State in Each Region and Matching Conditions . .	39
3.4 Transmission and Reflection Probabilities	42
IV RESULTS AND DISCUSSION	44
4.1 Ferromagnetic metal/ Normal metal /Ferromagnet metal Structure	45
4.1.1 Transmission probability for different metals	45
4.1.2 The effect of a metal thickness on magnetoresistance . . .	47
4.1.3 The effect of the hopping energy between two atoms of two interfaces on magnetoresistance	51
4.2 Ferromagnetic metal/Insulating/Ferromagnet metal Structure . .	53
4.2.1 Transmission probability for insulating	53
4.2.2 The effect of insulating thickness on magnetoresistance . .	54
4.2.3 The effect of the band gap on magnetoresistance	58
4.2.4 The effect of the hopping energy between two atoms of two interfaces on magnetoresistance	60
V CONCLUSION	63

CONTENTS (Continued)

	Page
REFERENCES	65
APPENDICES	73
APPENDIX A WOLFRAM MATHEMATICA PROGRAM CAL- CULATION RELATED TO METAL/SPACER/ METAL JUNCTION	73
APPENDIX B WOLFRAM MATHEMATICA PROGRAM CAL- CULATION RELATED TO FERROMAGNETIC /METAL/SPACER/FERROMAGNETIC ME- TAL JUNCTION	78
CURRICULUM VITAE	100

LIST OF TABLES

Table		Page
1.1	The conductance for parallel and antiparallel magnetization of majority and minority electrons and tunneling magnetoresistance ratio for the Fe/MgAl ₂ O ₄ /Fe (001) and the Fe/MgO/Fe (001) MTJs with the same thickness of barrier ~ 1.2 nm (taken from Miura et al., 2012).	16



LIST OF FIGURES

Figure		Page
1.1	The resistance measurements of (a) multilayers of $(\text{Fe}/\text{Cr})_n$ from Fert's group and (b) $\text{Fe}/\text{Cr}/\text{Fe}$ junction from Grünberg's group as a function of external magnetic field. (Taken from Binasch et al., 1989 and Baibich et al., 1988)	6
1.2	The change in resistance of $\text{CoFe}/\text{Al}_2\text{O}_3/\text{Co}$ junction (bottom graphs) plotted as a function of magnetic field at temperature 295 K. Also shown are the variations in the CoFe (middle graphs) and Co (top graphs) film resistance. The arrows are the direction of magnetization in the two films. (Taken from Moodera et al., 1995)	7
1.3	Tunneling magnetoresistance varies strongly with thickness ($d_{\text{Al}_2\text{O}_3}$) of Al_2O_3 layer. (Taken from Yuasa et al., 2000)	8
1.4	The magnetoresistance of $\text{Fe}(001)/\text{MgO}(001)/\text{Fe}(001)$ junction as a function of the thickness of the MgO layer. (a) is taken from Yuasa et al. (2005). (b) is from Matsumoto et al. (2009). (c) The magnetoresistance of $\text{CoFeB}/\text{MgO}/\text{CoFeB}$ junction as a function of the thickness of MgO . (taken from Zhu et al., 2015)	9
1.5	Spin polarization of the tunneling conductance as a function of the normalized potential barrier height for various values of $k_{\uparrow}/k_{\downarrow}$, taken from Slonczewski (Slonczewski, 1989).	12

LIST OF FIGURES (Continued)

Figure		Page
1.6	Angular dependence of the resistance of a CoFe/Al ₂ O ₃ /Co junction measured in an external magnetic field lower than the exchange energy of one electrode but higher than the exchange energy of the other electrode. Taken from Moodera and Kinder (Moodera et al., 1995).	13
1.7	Schematic plot of the Fe (100)/MgO (100)/Fe (100) junction in an atomic scale (Waldron et al., 2006).	16
2.1	The figure shows the geometry of hydrogen molecule (H ₂ ⁺) consisting two protons and single electron.	19
2.2	Chain of $N + 1$ ions in a one-dimensional.	23
2.3	The energy dispersion of the electron in the metal with wave vector are between $-\pi/a$ and π/a	24
2.4	Chains of ions representing one-dimensional metal/spacer/metal junction. Each ion is a distance a apart. ϵ 's and t 's are on-site and hopping energies.	26
2.5	The sketch of the energy dispersion relation of an electron in each region in the case where the spacer is a metal.	29
3.1	One-dimensional of ferromagnetic metal/spacer/ferromagnetic metal junction is displayed for (a) the chains of ions and (b) the geometry in a small external magnetic field perpendicular to into the model.	33

LIST OF FIGURES (Continued)

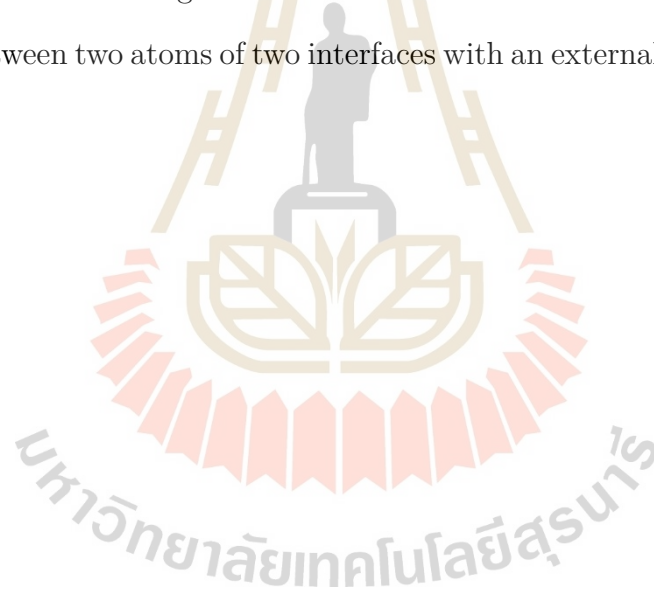
Figure		Page
3.2	The sketches of the energy dispersion relation of an electron in each region. Notice the splits of the relation for spin-up and spin-down electrons. In this picture we take the spacer to be insulating. . . .	36
3.3	The sketches of the energy dispersion relation of a ferromagnet in left side. The arrows depict the directions of the electron spins and J_L are the spin exchange energy with (a) spin-up incident and (b) spin-down incident electron.	37
3.4	The sketches of the energy dispersion relation of the insulating and Δ is the band gap.	38
3.5	The sketches of the energy dispersion relation of a ferromagnet in right side with two transmission of electron scattering. The arrows depict the directions of the electron spins and J_R are the spin exchange energy.	39
4.1	The sketches of the energy dispersion relation of a metallic spacer at (a) $\varepsilon_M = \mu$ (half-filling), (b) $\varepsilon_M - \mu < 0$ (more than half filling) and (c) $\varepsilon_M - \mu > 0$ (less than half filling).	45
4.2	The transmission probability as a function of energy (E_n/t_L) with 7 metallic spacer atoms.	46
4.3	The magnetoresistance ratio as a function of magnetic field with various thicknesses of the metal layers (a) $N_M = 5,7,9$ and 11 atoms and (b) $N_M = 4,6,8$ and 10 atoms.	47

LIST OF FIGURES (Continued)

Figure		Page
4.4	The magnetoresistance of Fe/metal/Fe junction plotted as a function of the thickness of metal with the magnetic field at 1.0 and 1.5 times t_L	49
4.5	The magnetoresistance of Fe/Cr/Fe junction plotted as a function of the thickness of Cr. Also shown are the oscillation magnetoresistance (a) in at low temperature of experimental work and (b) our model, when $\varepsilon_M = \mu$ and $cB = 1.5t_L$	50
4.6	Show the result of magnetoresistance as a function of external magnetic field (cB/t_L) with (a) $t' = t''$ and (b) $t' \neq t''$	51
4.7	The result of magnetoresistance as a function of the hopping energy between two atoms of two interfaces with the magnetic field. . . .	52
4.8	The transmission probability as a function of the energy (E_n/t_L) with thickness of the insulating layer as 7 atoms.	54
4.9	The magnetoresistance ratio as a function of magnetic field with thickness of the insulating layer for various thickness (a) $N_M = 5,7,9$ and 11 atoms and (b) $N_M = 4,6,8$ and 10 atoms.	55
4.10	The magnetoresistance ratio as a function of thickness of the insulating layer for as $cB = 0.1t_L$ and $0.15t_L$ and $\varepsilon_M - \mu = 2.01t_L$. . .	56
4.11	The magnetoresistance of Fe(001)/MgO (001)/Fe(001) junction plotted as a function of the thickness of MgO (t_{MgO}). Also shown are (a) the oscillation in 1.2 to 3.2 nm at temperature 293 K and 20 K and (b) the magnetoresistance as a function of the number of atoms, when $\varepsilon_M - \mu = 2.004t_L$	57

LIST OF FIGURES (Continued)

Figure		Page
4.12	The transmission probability as the on-site energy of the spacer at the thickness layer as 7 atoms.	59
4.13	The result of the magnetoresistance as a function of band gap energy (Δ/t_L) at the thickness layer as 7 atoms.	60
4.14	Show the result of magnetoresistance a function of external magnetic field (cB/t_L) with (a) $t' = t''$ and (b) $t' \neq t''$	61
4.15	The result of magnetoresistance as a function of the hopping energy between two atoms of two interfaces with an external magnetic field.	62



LIST OF ABBREVIATIONS

TMR	Tunneling magnetoresistance ratio
RKKY	Ruderman-Kittel-Kasuya-Yosida interaction
Δ	Band gap energy
μ_B	Bohr magneton
ε_F	Fermi energy
\vec{v}_s	Velocity of the spin- s electron
\mathbb{E}	Electric field
G	Conductance

CHAPTER I

INTRODUCTION

In this master thesis, we aspire to use a one-dimensional tight-binding model in a theoretical study of the electron transport through a ferromagnetic metal/spacer/ferromagnetic metal junction in a small applied magnetic field. In this first chapter, we will present the reasons why we find this system interesting and why we will use one-dimensional tight-binding model to investigate this system. We will also recount, with our best ability, both experimental effort and theoretical endeavor that have been done so far to gain more understanding about this junction.

1.1 Motivation

Electronic devices like diodes and transistors contain junctions acting as barriers for charge carriers in the devices to tunnel through. The flow of these carriers through junctions is characterized by the electronic properties of the materials of the devices and can be manipulated by applied external fields for the purpose of system control and information processing. In conventional electronics, we have controlled particle flow by making use of its charge property and applying electric field.

In 1988, Grünberg's and Fert's research groups showed us that we can control particle transport through junctions with magnetic field as well. In that year both groups independently discovered giant magnetoresistance in thin film multilayered structures of alternating ferromagnetic metals separated by a metallic

non-magnetic spacer (Binasch et al., 1989; Baibich et al., 1988). That is, they found that the resistances of their samples can be significantly changed by applied magnetic field.

In the absence of the field, the resistance of the system is high, because the magnetizations of two adjacent ferromagnetic layers are in opposite direction. When the field is turned on and strong enough, the magnetizations become in parallel resulting in much lower resistance. This effect allows us to control the current flow, by making use of the spin degree of freedom. This discovery marked the birth of the field of spintronics that studies the manipulation and control of spin degree of freedom in electronic devices by means of electric and magnetic field. From the point of view of practical application, giant magnetoresistance has since attracted interest from makers of magnetic sensors, switches, logical devices, read heads for hard disc drives, and random-access memory devices, and spin-field effect transistors (Chappert and Van Dau, 2007; Katine et al., 2000; Grollier et al., 2001; van 't Erve et al., 2006; Awschalom and Flatté, 2007).

Many experimental research works have shown that there are several factors impacting on the change in resistance with the field, or the magnetoresistance ratio. For instance, to be able to observe the giant magnetoresistance, the thickness of the metallic non-magnetic layer between two adjacent ferromagnetic layers has to be in the order of nanometers (Parkin et al., 1990), because at these distances only does the Ruderman-Kittel-Kasuya-Yosida interaction between the two ferromagnetic layers cause their magnetizations to be antiparallel in zero magnetic fields (Ruderman and Kittel, 1954; Kasuya, 1956; Yosida, 1957) and a strong enough field will force them to be in parallel. The reduction of resistance with the field usually hits a plateau at some value of field strength H_S , which depends on the thickness of the spacer and the number of spacer layers (Fert and Campbell,

1968; Mosca et al., 1991; Grollier et al., 2003). Also, if one replaces the metallic non-magnetic spacer with an insulating layer, the percentage of the magnetoresistance ratio (called tunneling magnetoresistance ratio) is more pronounced (Butler et al., 2001; Mathon and Umerski, 2001; LeClair et al., 2002; Parkin et al., 2004; Yuasa et al., 2005).

Theoretically, we can understand the experimental results through quantum mechanics. In 1975, Jullière used the result from transfer Hamiltonian method, sometimes called Bardeen's approach, to explain his experimental results. He measured the conductance of the junction of two different ferromagnetic electrodes separated by insulating layer in applied magnetic field. In the absence of the field, the magnetizations of both electrodes were in parallel, because the thickness of the insulating layer was too big for the Ruderman-Kittel-Kasuya-Yosida interaction to cause them to be antiparallel. However, once the field was turned on and its strength was between the two coercive fields of the two ferromagnets, the magnetizations would be in opposite directions and he observed the reduction of 14% in the conductance (Julliere, 1975). He quantitatively explained the experimental results, using the transfer Hamiltonian method. In this approach, high insulating barrier potential (or low tunneling regime) and elastic tunneling are assumed. As a result, the conductance is proportional to product of the densities of states for majority spin and minority spin of the two ferromagnetic electrodes (Bardeen, 1961). In Jullière's case, the magnetic field causes the shift in the densities of the states and hence the reduction of the conductance. Due to the low tunneling regime assumption, which are valid in Jullière's case, the quantitative results from this approach are limited to cases of insulating barriers, whereas other aspects, like the effects of non-insulating barriers and barrier thickness, cannot be explored.

To examine such effects of the thickness insulating layer and also that of relative directions of the magnetizations of the two electrodes in the absence of applied field, Slonczewski (Slonczewski, 1989) modeled the same type of junction using a one-electron model for ferromagnetic electrons. He solved the Schrödinger equation for the system to obtain the transmission probability in the elastic scattering process. He found that the thickness and the potential barrier would affect the conductance. Also, the conductance would depend on the angles between the two magnetizations. The Slonczewski model works well with the junction consisting of the metallic ferromagnets with electronic parabolic energy dispersion. It was shown by Qi and coworkers (Qi et al., 1998) that Slonczewski's model can be applied to a wider range of cases than Julliere's model, and it gives the same results as Julliere's model, when the barrier potential is very high (Qi et al., 1998).

When the effect of realistic energy band structure of either ferromagnetic layers or the spacer on this type of junction is of interest, researchers turn to first-principles calculation. Once they obtain the realistic band structures, they use the Green's function technique to calculate the conductance. For instance, Waldron et al. (2006) studied the transport of electrons through clean Fe (100)/MgO (100)/Fe (100) structure (Waldron et al., 2006) and found that the zero-bias tunnel magnetoresistance of this junction could be many thousand percent. However, the effect can be reduced when the Fe/MgO interface is oxidized. The results are limited to the case of low tunneling regime and in zero applied magnetic field.

Another method of calculation used to study this type of junction in the literature is a tight-binding model. It is used to obtain a non-parabolic energy dispersion relation of electrons in the system. It is not as realistic as the first-principles calculation, but similar to that in Slonczewski's model, it allows us to include arbitrary barrier potential into the calculation of transmission probability.

However, like in Slonczewski's model, most studies of the magnetic tunneling junction with a tight-binding model, the direct inclusion of the effect of the magnetic field has not much been studied.

In summary, the physics related to tunneling through a magnetic multilayered structure is quite rich. There are still many theoretical and experimental aspects that are worth being explored. Even though the real system is complicated, one can use a simple theoretical model to understand the particle transport through the system.

In this thesis, applying a tight-binding model, we theoretically investigate the dependence on the type and thickness of the spacer and applied magnetic field on the tunneling magnetoresistance ratio. We also compare and contrast the final results with a continuous model, like Slonczewski's.

1.2 Literature Review

1.2.1 Experimental Studies of Magnetoresistance

Giant magnetoresistance was discovered by Fert's and Grünberg's groups, after they were both able to systematically produce multilayer systems with precise thickness in the order of nanometers. Grünberg's group measured the resistance as a function of applied field of Fe/Cr/Fe junction, whereas Fert's group did the measurement for $(\text{Fe/Cr})_n$ multilayer system, where $n \geq 30$. In Figure 1.1, we show some of the results from both groups. Fert's group found that the resistance at 4.2 K of multilayers of $(\text{Fe/Cr})_n$ could drop up to 55% in the saturation magnetic fields H_S . Both the reduction of resistance and H_S depended strongly on the number of Fe/Cr layers and the thickness of Cr layers. When the field is smaller than H_S , the magnetizations of the adjacent layers of Fe are antiparallel leading to high

resistance. When the field is stronger than H_S , the magnetizations become parallel and hence lowering the resistance (Baibich et al., 1988). Grünberg's group did similar experiment but at room temperature for trilayer system Fe/Cr/Fe. They found the resistance dropped to 1.5% in the field stronger than H_S (Binasch et al., 1989). The change in electrical resistance with the applied field is essentially due to spin-dependent tunneling effect.

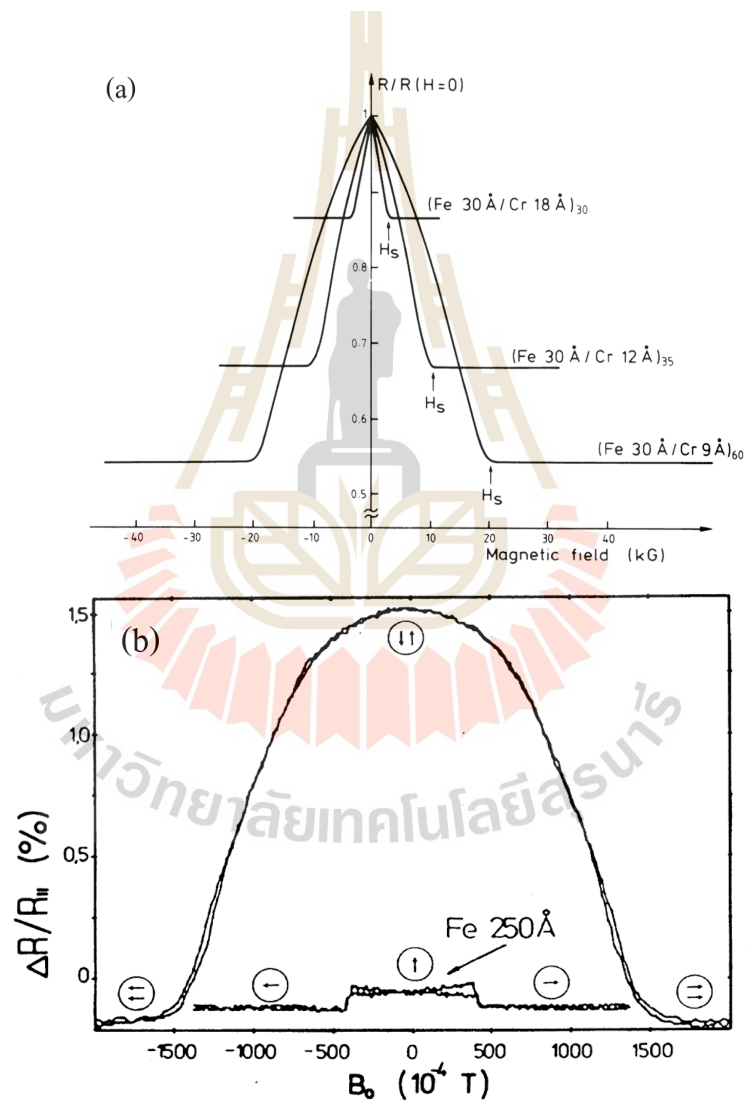


Figure 1.1 The resistance measurements of (a) multilayers of $(Fe/Cr)_n$ from Fert's group and (b) Fe/Cr/Fe junction from Grünberg's group as a function of external magnetic field. (Taken from Binasch et al., 1989 and Baibich et al., 1988)

As soon as giant magnetoresistance was discovered, researchers tried to find ways to obtain higher value of the magnetoresistance ratio. One way is to use insulators as spacers. In Figure 1.2, we show the magnetoresistances of CoFe/Al₂O₃/Co junction, CoFe film, and Co film at 295 K. As can be seen, when the system is either CoFe film or Co film, the magnetoresistance ratio is small, no more than 0.15%, but when the system is CoFe/Al₂O₃/Co junction, the magnetoresistance ratio is as high as 10% (Moodera et al., 1995).

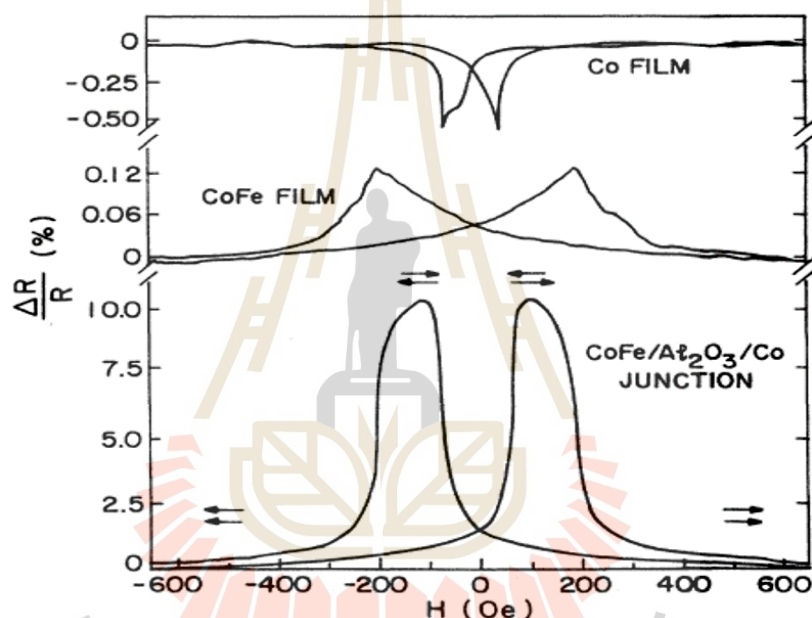


Figure 1.2 The change in resistance of CoFe/Al₂O₃/Co junction (bottom graphs) plotted as a function of magnetic field at temperature 295 K. Also shown are the variations in the CoFe (middle graphs) and Co (top graphs) film resistance. The arrows are the direction of magnetization in the two films. (Taken from Moodera et al., 1995)

There have been other works showing that the thickness of insulating layers can have big impact on the magnetoresistance ratio. Wang and co-workers showed that they could achieve the tunneling magnetoresistance value of 70.4% at room temperature in Si(100)/Si₃N₄/Ru/CoFeB/Al₂O₃/CoFeB/Ru/FeCo/CrMnPt junction.

tion, when the Al_2O_3 layer is very thin, in the range of 1 nm (Dexin Wang et al., 2004). Yuasa and co-workers also reported, for $\text{Fe}/\text{Al}_2\text{O}_3/\text{CoFe}$ magnetic tunneling junction, the tunneling magnetoresistance strongly varies with Al_2O_3 thickness for $\text{Fe}(211)$, $\text{Fe}(110)$, and $\text{Fe}(100)$ epitaxial electrodes at 2 K in Figure 1.3 (Yuasa et al., 2000).

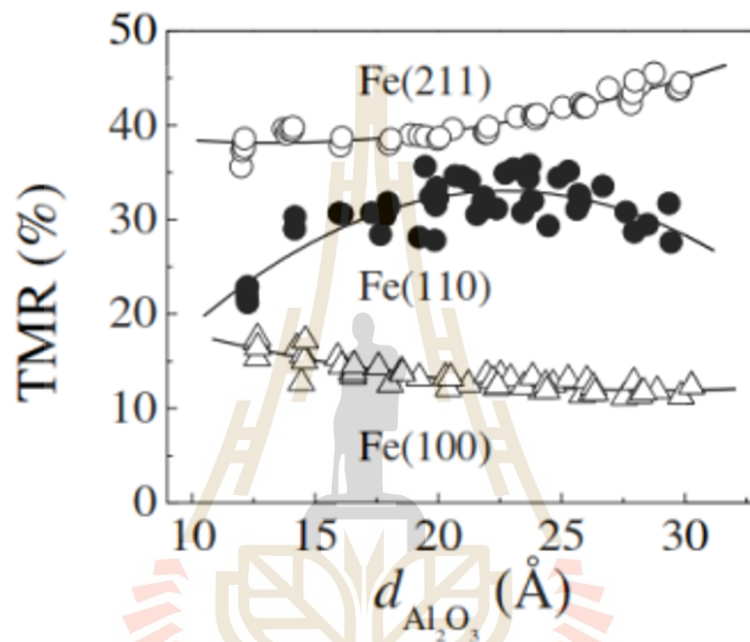


Figure 1.3 Tunneling magnetoresistance varies strongly with thickness ($d_{\text{Al}_2\text{O}_3}$) of Al_2O_3 layer. (Taken from Yuasa et al., 2000)

The same effect can also be found when MgO is used as a spacer. Yuasa and co-workers (Yuasa et al., 2005) studied $\text{Fe}(001)/\text{MgO}(001)/\text{Fe}(001)$ junctions with varying MgO-layer thickness between 1.2 nm and 3.2 nm. They found that the tunneling magnetoresistance can reach up to 180% at 293 K and 247% at 20 K. They also reported that there is an oscillation of the magnetoresistance ratio with the thickness of the MgO layer as depicted in Figure 1.4(a). Although not seen as prominent as Yuasa and co-workers result, similar oscillation was seen in the same system by Matsumoto and co-workers as shown in Figure 1.4(b) (Matsumoto et al.,

2009). Zhu and co-workers did not observe the oscillation, but they did see that the thickness of MgO layer causes a large variation of the tunneling magnetoresistance in CoFeB/MgO/CoFeB magnetic tunnel junction as shown in Figure 1.4(c) (Zhu et al., 2015).

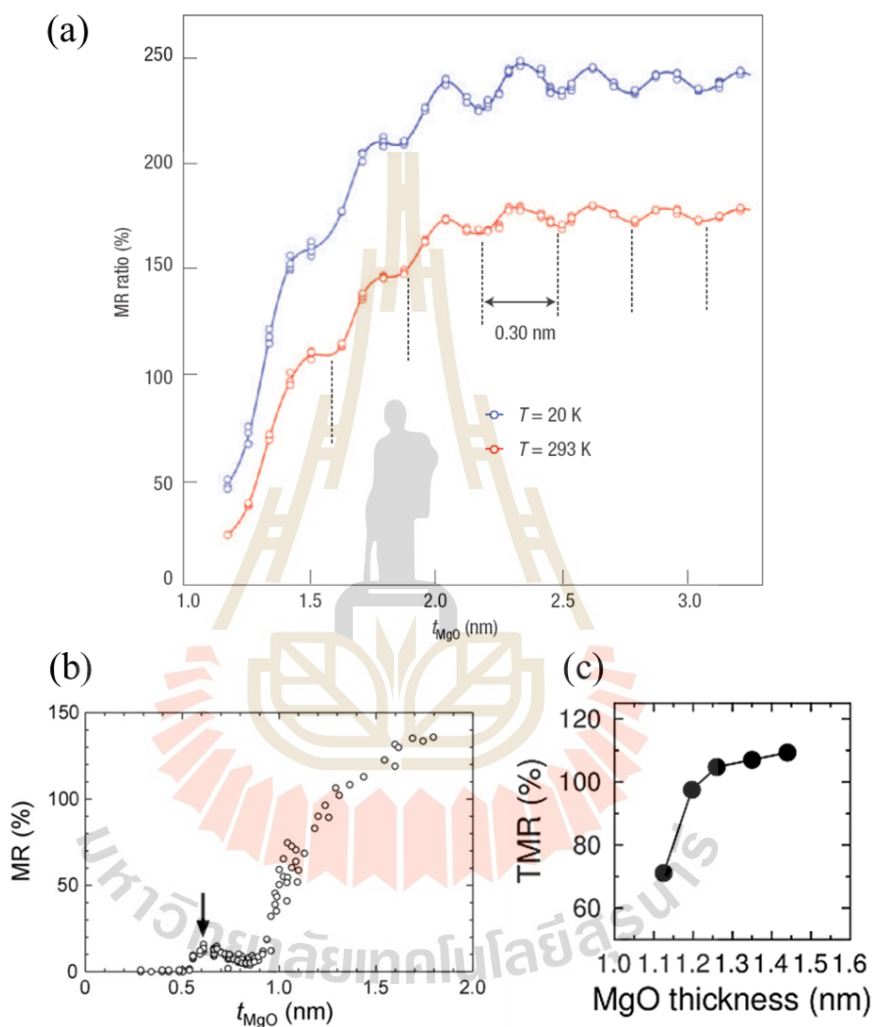


Figure 1.4 The magnetoresistance of Fe(001)/MgO(001)/Fe (001) junction as a function of the thickness of the MgO layer. (a) is taken from Yuasa et al. (2005). (b) is from Matsumoto et al. (2009). (c) The magnetoresistance of CoFeB/MgO/CoFeB junction as a function of the thickness of MgO. (taken from Zhu et al., 2015)

1.2.2 Theoretical Models for Tunneling Magnetoresistance

In this section, we will describe two theoretical models used to study tunneling magnetoresistance of the ferromagnetic metal/spacer/ferromagnetic metal junction: one-electron model, and first-principles calculation.

1.2.2.1 One-electron Models

There are many approaches with one-electron approximation, which one can use to theoretically study the tunneling magnetoresistance. Here, we will focus on three of them: Jullière's, Slonczewski's, and tight-binding.

In 1975, Jullière, who did the first experiment on the tunneling magnetoresistance of Fe/Ge/Co junctions, was also the first to use a simple theoretical model to describe it. He used Bardeen's description of tunneling across an insulating barrier. In the Bardeen approach, which was based on the standard time-dependent perturbation theory, the tunneling current density is equal to the net rate of transfer of electrons between the electrodes (Bardeen, 1961):

$$J = \frac{2\pi e}{\hbar} \sum_{ij} |b_{ij}|^2 [f(\varepsilon_i - \mu_L) - f(\varepsilon_j - \mu_R)] \delta(\varepsilon_i - \varepsilon_j) \quad (1.1)$$

where i, j respectively label the electron states of the left and right electrodes, b_{ij} is the tunneling matrix element between these states, $f(\varepsilon - \mu)$ is the Fermi-Dirac distribution function, and μ is the associated chemical potential. Using Bardeen's expression for the current and two assumptions: the electron spin is conserved and b_{ij} are the same for all states, Jullière obtained the conductances, G_P and G_{AP} , for the parallel and antiparallel magnetizations of the two electrodes at zero temperature respectively as follows:

$$G_P = \frac{1}{R_P} = \frac{e^2}{\hbar} |b|^2 [D_L^\uparrow(\varepsilon_F) D_R^\uparrow(\varepsilon_F) + D_L^\downarrow(\varepsilon_F) D_R^\downarrow(\varepsilon_F)] \quad (1.2)$$

$$G_{AP} = \frac{1}{R_{AP}} = \frac{e^2}{h} |b|^2 [D_L^\uparrow(\varepsilon_F) D_R^\downarrow(\varepsilon_F) + D_L^\downarrow(\varepsilon_F) D_R^\uparrow(\varepsilon_F)] \quad (1.3)$$

where $D_i^s(\varepsilon_F)$ is the density of states of electrode i for spin s and R_P , R_{AP} are the corresponding resistance. Jullière tunneling magnetoresistance ratio is defined as

$$TMR \equiv \frac{G_P - G_{AP}}{G_{AP}} \equiv \frac{R_{AP} - R_P}{R_P} \quad (1.4)$$

In term of spin polarization, $P \equiv \frac{D^\uparrow - D^\downarrow}{D^\uparrow + D^\downarrow}$,

$$TMR \equiv \frac{2P_L P_R}{1 - P_L P_R}. \quad (1.5)$$

This formula gave a value of 26% for Fe/Ge/Co junctions, which is higher than the maximum measured value of 14%. The discrepancy may be due to the spin-flip scattering and the magnetic coupling between the two electrodes (Julliere, 1975).

In 1989, Slonczewski (Slonczewski, 1989) approximated the electron energy dispersion relation of two ferromagnetic metals as two parabolic bands shifted rigidly by the exchange splitting of the spin bands. He solved the Schrödinger equation of two identical ferromagnetic films separated by a rectangular potential barrier, and obtained the conductance G as a function of the relative magnetization direction of the two films, specified by an angle θ .

$$G(\theta) = G_0(1 + P^2 \cos\theta), \quad (1.6)$$

where P is the effective spin polarization of tunneling electrons:

$$P = \left(\frac{k^\uparrow - k^\downarrow}{k^\uparrow + k^\downarrow} \right) \left(\frac{\kappa^2 - k^\uparrow k^\downarrow}{\kappa^2 + k^\uparrow k^\downarrow} \right) \quad (1.7)$$

where $\kappa = \sqrt{(2m/\hbar^2)(U - \varepsilon_F)}$, m is the electron effective mass, U is the barrier potential, ε_F is the Fermi energy of each ferromagnetic metal, and k_\uparrow, k_\downarrow are the

Fermi wave vectors of the bands for the spin-up and spin-down electrons: $k_{\uparrow} = \sqrt{(2m/\hbar^2)(E - h_0 + \varepsilon_{F1})}$, $k_{\downarrow} = \sqrt{(2m/\hbar^2)(E + h_0 + \varepsilon_{F2})}$. In the $U \gg \varepsilon_F$ limit, Slonczewski's model provides the same results as Jullière's model. When U is not large, the spin polarization is decreased with decreasing U and flips its sign for small enough barrier potential (Figure 1.5). This result was the first to indicate that the spin polarization of the tri-layered system can be affected significantly by the physical properties of the middle layer.

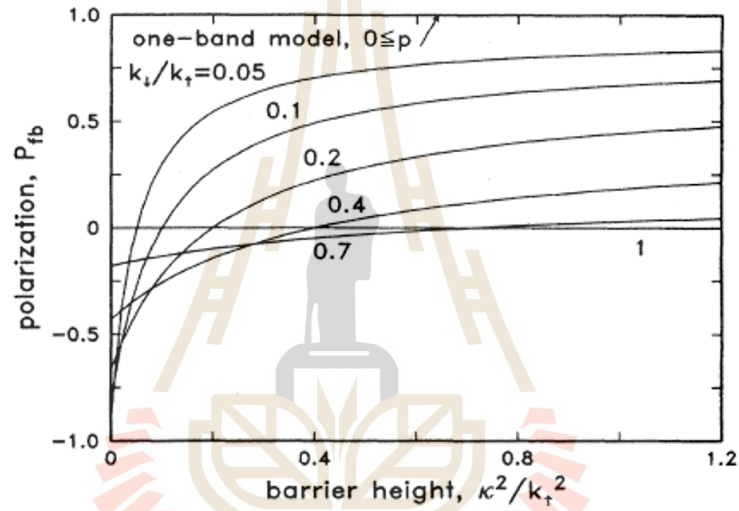


Figure 1.5 Spin polarization of the tunneling conductance as a function of the normalized potential barrier height for various values of $k_{\uparrow}/k_{\downarrow}$, taken from Slonczewski (Slonczewski, 1989).

The cosine dependence of the conductance, predicted by Slonczewski's model, was experimentally confirmed by Moodera and Kinder (Moodera et al., 1995). They performed a tunneling experiment on a tri-layered system containing different ferromagnetic films in an external field stronger than the coercive field of one electrode but lower than that of the other. This condition made the magnetization of the harder electrode point in a particular direction during the experiment and made it possible to control the direction of the magnetization of

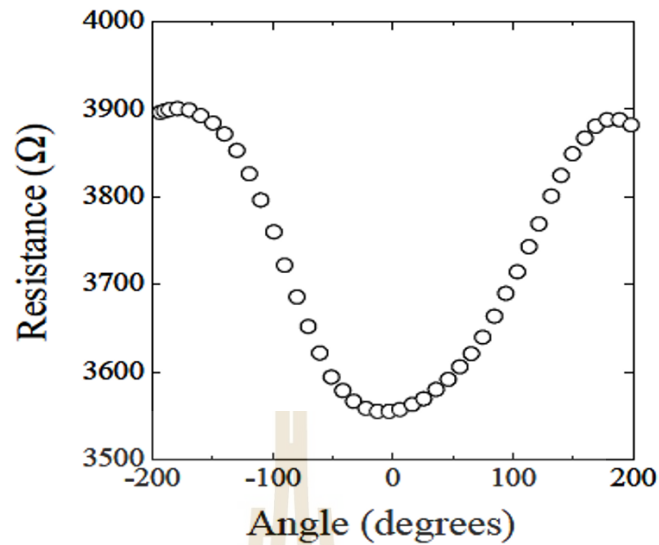


Figure 1.6 Angular dependence of the resistance of a CoFe/Al₂O₃/Co junction measured in an external magnetic field lower than the exchange energy of one electrode but higher than the exchange energy of the other electrode. Taken from Moodera and Kinder (Moodera et al., 1995).

the softer electrode by the external field. Their resistance measurements showed dependence on the field direction with respect to the magnetization of the harder electrode as $\cos\theta$ (see Figure 1.6).

In 1998, Yunong Qi, D. Y. Xing, and Jinming Dong showed that the results from the Slonczewski's model with the delta-function as the barrier potential and those from the Julliere formula have the same form in the tunneling limit. They confirmed the results, which were also obtained by Slonczewski, that tunneling magnetoresistance ratio is sensitive to the angle between the magnetization of the two adjacent ferromagnetic layers and their exchange energies. Also, the magnetoresistance ratio is insensitive to the height and width of the potential barrier in the tunneling limit. Their results indicated that Slonczewski's theoretical model can be used to study wider variety of junction types than Julliere's model (Qi et al., 1998).

In these two approaches the researchers did not directly put the applied magnetic field in their calculations. The effect of the applied field magnetic field was indirectly included through the difference in the densities of states for majority spin and minority spin in Julliere's case, and through the change in the direction of magnetization of one of the ferromagnetic layers in Slonczewski's case.

Another approach one can use to study transport in such junctions is a tight-binding model. It is a quantum mechanical model that describes the properties of tightly bound electrons in solids. In this model, electrons are assumed to be tightly bound to the atom to which they belong. As a result, the wave function of the electron is similar to the atomic orbital of the free atom. The energy of the electron is therefore close to the ionization energy of the electron in the free atom due to the limitation of the interaction with potentials and states on neighboring atoms. In 1997, Mathon used a tight-binding model to investigate the tunneling magnetoresistance of two Co (001) electrodes separated by a vacuum gap (Mathon, 1997). It was based on the Kubo-Landauer formula and fully realistic tight-binding bands fitted to band structure obtained from first-principles calculation. He applied the model to a single-orbital tight-binding model to investigate analytically a continuous transition from the ballistic-current perpendicular-to-plane giant magnetoresistance of a metallic system to the tunneling magnetoresistance of a tunneling junction. He saw the transition take place when either hopping of electrons between the ferromagnetic electrodes is gradually turned off, or the on-site potentials in the nonmagnetic spacer are varied so that the Fermi level in the spacer moved into the band gap. He also found that the tunneling magnetoresistance approaches the same saturation value, when either the interelectrode hopping decreases or the height of the insulating barrier increases. When the insulating barrier is high (large band gap), the tunneling magnetoresistance depends weakly

on the thickness of the insulating layer. However, when the band gap is small compared to the conduction band width, the tunneling magnetoresistance decreases rapidly with increasing thickness of the insulator. The numerical results for a Co(001) junction, based on a fully realistic band structure of the Co electrodes, show a very similar behavior. As the tight-binding hopping matrix between the Co electrodes is turned down, the tunneling magnetoresistance ratio dropped from 280% in the metallic regime to 40% and stabilizes in the range 40–65% (Mathon, 1997). Mathon also applied similar procedure to epitaxial Fe/MgO/Fe(001) junction and found that the tunneling magnetoresistance is in excess of 1000% for an MgO barrier of 20 atomic planes and the spin polarization of the tunneling current is positive for all MgO thicknesses (Mathon and Umerski, 2001). We make notes that in all Mathon's results the effect of changing strength applied magnetic field was not investigated.

1.2.2.2 First Principles Calculations

Magnetic tunnel junction can also be studied by an atomic-scale using first-principles approach. This approach is basically using only atomic number and crystal structure as input to obtain the interaction between nucleus and electrons based on quantum mechanics principles. The solutions to the Schrödinger's equation are found through approximations and simplifications based on the density functional theory (Kohn, 1999; Khomyakov et al., 2009). From these solutions, one can obtain other physical properties, including the transport properties.

Waldron and his colleagues used first-principles calculation to calculate the tunneling magnetoresistance of the Fe(100)/MgO(100)/Fe (100) trilayer structure, shown in Figure 1.7 (Waldron et al., 2006). They found that the tunneling magnetoresistance could be as high as many thousand percent at zero bias, but this effect

was reduced to about 1000% when the Fe/MgO interface was oxidized. Miura and co-workers also used first-principles calculation to obtain the tunneling magnetoresistance of Fe/MgAl₂O₄/Fe (001) junctions in zero magnetic field (Miura et al., 2012). They obtained a tunneling magnetoresistance ratio of 160%, which is much smaller than that of the Fe/MgO/Fe junction. Although first-principles calculation approach provides very realistic electronic structure of the system of interest, its results are only specific to the system and is time consuming.

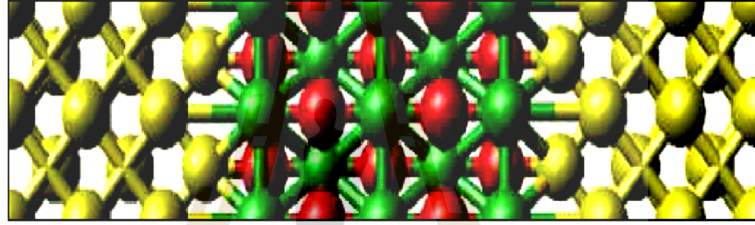


Figure 1.7 Schematic plot of the Fe (100)/MgO (100)/Fe (100) junction in an atomic scale (Waldron et al., 2006).

Table 1.1 The conductance for parallel and antiparallel magnetization of majority and minority electrons and tunneling magnetoresistance ratio for the Fe/MgAl₂O₄/Fe (001) and the Fe/MgO/Fe (001) MTJs with the same thickness of barrier ~ 1.2 nm (taken from Miura et al., 2012).

	Conductance ($S/\mu m^2$)				TMR ratio (%)
	Parallel magnetization		Antiparallel magnetization		
	Majority spin	Minority spin	Majority spin	Minority spin	
Fe/MgAl ₂ O ₄ /Fe(001) MTJ	0.5	0.02	0.1	0.1	160
Fe/MgO/Fe MTJ	0.1	0.003	0.003	0.003	1600

1.3 Outline of Thesis

In this thesis, we theoretically study ferromagnetic metal/spacer/ferromagnetic metal junctions in a small applied field through a one-dimensional tight-binding model. We specifically investigate the effect of types of the spacer, i.e metal vs insulator and the thickness of the spacer on the magnetoresistance ratio. The organization of this thesis is as follows. In Chapter II, we describe a tight-binding model of a H_2^+ molecule, one-dimensional metallic bonds, and metal/spacer/metal junction as a precursor to our model for one-dimensional ferromagnetic metal/spacer/ferromagnetic metal structure, which will be presented in Chapter III. More specifically, we will show how to obtain the transmission probability through appropriate matching conditions at the two interfaces. We will include a small external magnetic field perpendicular to the chain into the model as a perturbation and calculate the tunneling magnetoresistance ratio from the transmission probability. The results and discussion will be presented in Chapter IV and finally we will leave with the conclusions in Chapter V.

CHAPTER II

TIGHT-BINDING MODEL FOR ONE-DIMENSIONAL TUNNELING SYSTEM

There are many quantum mechanical approaches to the calculation of electronic band structure of molecules and solids. Tight-binding method, which uses an approximate set of wave functions based on superposition of eigenstates of isolated atoms at each site, is among the simplest. It generally provides less accurate results than density functional calculations. However, when a tight-binding calculation is done with a good basis set, it can provide a direct and easy-to-perceive picture of chemical bonding occurring in the systems. A tight-binding calculation requires much less computer time than other more sophisticated electronic structure calculations, but still producing qualitatively and often quantitatively correct results (Slater and Koster, 1954; Heine, 1980; Haydock, 1980; Harrison, 1989; Sutton, 1993; Goringe et al., 1997; Horsfield and Bratkovsky, 1999; Finnis, 2010; Paxton and Kohanoff, 2011; Agapito et al., 2016). We very much appreciate the efficiency and intuitive simplicity of tight-binding method. Other than using tight-binding method to get the picture of chemical bonding in a system, we can also apply it to study tunneling through a heterostructure by treating tunneling as a scattering problem, in which an incident wave on a barrier is partially reflected and transmitted.

In this chapter, we give descriptions of tight-binding pictures to three systems in order to get the reader familiar with the notations we use throughout this thesis. We start with applying tight-binding method to a Hydrogen

molecule ion (H_2^+) in Section 2.1 and a one-dimensional infinite metallic chain in Section 2.2 to obtain eigenstates and eigenenergies of both systems. In Section 2.3, we apply the tight binding model to tunneling through a one-dimensional metal/spacer/metal junction, which is a preamble to that through a ferromagnetic metal/spacer/ferromagnetic metal junction.

2.1 Hydrogen Molecule Ion

The hydrogen molecule ion is the simplest molecule we can imagine. It consists of an electron orbiting about two protons. In this section, we introduce a tight-binding approach to investigate this simple molecule before we move on to a more complicated system. We will look for a ground-state, energy of which is less than that of a hydrogen atom and a free proton.

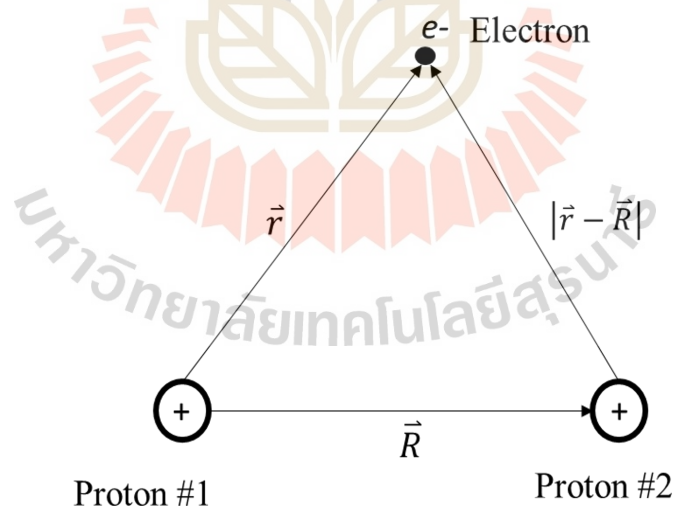


Figure 2.1 The figure shows the geometry of hydrogen molecule (H_2^+) consisting two protons and single electron.

In the following, we will approximate that the protons are essentially stationary, since their masses are 1000 times of the electron mass and particles with

bigger masses tend to moves far more slowly than those with smaller masses in the same circumstances. Suppose that the two protons are separated by a distance R (see Figure 2.1) and define the position \vec{r} of the electron with respect to proton #1. Thus, the second proton is at the position \vec{R} from proton #1. The Hamiltonian of this system takes the form:

$$\hat{H} = \frac{-\hbar^2 \nabla^2}{2m} - \frac{ke^2}{|\vec{r}|} - \frac{ke^2}{|\vec{r} - \vec{R}|} + \frac{ke^2}{|\vec{R}|}, \quad (2.1)$$

where m the electron mass, e is the electron charge and k is Coulomb's constant. The first term is the kinetic energy of an electron. The second and third terms are the coulomb attraction potential energies between the electron and each proton. The last term is the repulsion potential energy between the two protons. Let $|1\rangle, |2\rangle$ describe the $1s$ orbital states at the protons #1 and #2 respectively. That is, the wave functions of the electron in the $1s$ orbital state at the protons #1 and #2 are $\phi_1(\vec{r}) = \langle \vec{r}|1\rangle = e^{-\vec{r}/a_B}$ and $\phi_2(\vec{r}) = \langle \vec{r}|2\rangle = e^{-|\vec{r}-\vec{R}|/a_B}$, where $a_B = \frac{\hbar^2}{mke^2}$ is the Bohr radius. Thus, we write the trial ground states as

$$|\psi\rangle = c_1|1\rangle + c_2|2\rangle \quad (2.2)$$

where c_n is the amplitude that will be obtained from the variation approach (Zettili, 2009), which will be described below. In this case, the phase factor of c_n is not important; so, we take c_n to be real without losing generality.

The expectation value of the energy is equal to as

$$E = \frac{\iiint_{\text{all space}} \psi^*(\vec{r}) \hat{H} \psi(\vec{r}) d^3r}{\iiint_{\text{all space}} \psi^*(\vec{r}) \psi(\vec{r}) d^3r}, \quad (2.3)$$

where $\psi(\vec{r}) = \langle \vec{r}|\psi\rangle = c_1\langle \vec{r}|1\rangle + c_2\langle \vec{r}|2\rangle = c_1\phi_1(\vec{r}) + c_2\phi_2(\vec{r})$. We then obtain

$$E = \frac{c_1^2 E_{11} + c_2^2 E_{22} + c_1 c_2 E_{12} + c_2 c_1 E_{21}}{c_1^2 + c_2^2 + 2c_1 c_2 S}, \quad (2.4)$$

where

$$E_{11} = \iiint_{\text{all space}} \phi_1^*(\vec{r}) \hat{H} \phi_1(\vec{r}) d^3 r = E_{22} = \varepsilon_G - \Delta\epsilon + \frac{ke^2}{R}, \quad (2.5)$$

The last term is obviously the repulsion between the two protons. ε_G is the ground-state energy of a hydrogen atom, which is equal to

$$\varepsilon_G = \iiint_{\text{all space}} \phi_1^*(\vec{r}) \left[\frac{-\hbar^2 \nabla^2}{2m} - \frac{ke^2}{r} \right] \phi_1(\vec{r}) d^3 r = -13.6 \text{ eV}. \quad (2.6)$$

$\Delta\epsilon$ is the average attraction between the electron at proton #1 and proton #2 (and vice versa), which is

$$\Delta\epsilon = \iiint_{\text{all space}} \phi_1^*(\vec{r}) \left[\frac{ke^2}{|\vec{r} - \vec{R}|} \right] \phi_1(\vec{r}) d^3 r. \quad (2.7)$$

We call $E_{11} = E_{22}$ the on-site energy. Similarly, we have

$$E_{12} = \iiint_{\text{all space}} \phi_1^*(\vec{r}) \hat{H} \phi_2(\vec{r}) d^3 r = E_{21} = \left(\varepsilon_G + \frac{ke^2}{R} \right) S - t, \quad (2.8)$$

where

$$S = \iiint_{\text{all space}} \phi_1^*(\vec{r}) \phi_2(\vec{r}) d^3 r \quad (2.9)$$

is the overlap between the two states and

$$t = \iiint_{\text{all space}} \phi_1^*(\vec{r}) \frac{ke^2}{|\vec{r} - \vec{R}|} \phi_2(\vec{r}) d^3 r \quad (2.10)$$

is called the hopping energy.

We then minimize the energy E with respect to c_1 and c_2 and obtain the following results of two cases. For the eigenstate with $c_1 = c_2$, its eigenenergy is

$$E = E_B = \varepsilon_G + \frac{ke^2}{R} - \Delta\epsilon - \frac{t - S\Delta\epsilon}{1 + S}, \quad (2.11)$$

and for the eigenstate with $c_1 = -c_2$, its eigenenergy is

$$E = E_{AB} = \varepsilon_G + \frac{ke^2}{R} - \Delta\epsilon + \frac{t - S\Delta\epsilon}{1 - S}. \quad (2.12)$$

We call E_B and E_{AB} bonding and anti-bonding energy respectively.

In the tight binding limit, we will take the overlap $S = \langle 1|2\rangle = \langle 2|1\rangle = 0$ and the eigenenergies becomes

$$E = \varepsilon_0 \pm t, \quad (2.13)$$

where $\varepsilon_0 \equiv \varepsilon_G + \frac{ke^2}{R} - \Delta\epsilon$.

2.2 One-dimensional chain of metallic atoms

When atoms, like Lithium or Sodium atoms, are brought together to form a crystal, they are bonded by metallic bonds. That is, the valence electron is energetically favorable to be released from its atom, when all the atoms are brought together. These electrons are free to move anywhere in the system, leaving ions behind at the lattice sites. Their moving around helps lower the kinetic energy of the crystal and stabilizes the structure. We can understand how this can be by using a tight-binding model to consider the simplest one-dimensional model, where we have a chain of $N + 1$ ions, placed equidistantly from each other as depicted in Figure 2.2. We let $|n\rangle$, where $n = 0, 1, 2, \dots, N$, be the state, in which a valence electron is at ion n . For a tight-binding model, we have $\langle n|m\rangle = \delta_{nm}$. We also ignore the interactions among the electrons. That is, we only solve for the one-electron eigenstate.

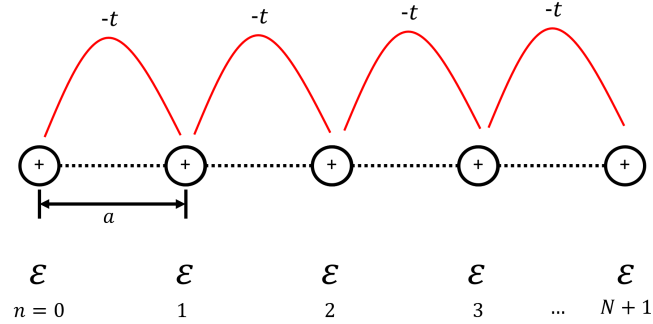


Figure 2.2 Chain of $N + 1$ ions in a one-dimensional.

The simplest Hamiltonian that describes the system is:

$$\hat{H} = \varepsilon \sum_{n=0}^N |n\rangle\langle n| - t \sum_{n=0}^{N-1} (|n\rangle\langle n+1| + |n+1\rangle\langle n|) \quad (2.14)$$

where ε is the on-site energy (the energy to have the electron at any given site) and $-t$ is the nearest-neighbor hopping energy. The second term in the Hamiltonian describes nearest-neighbor hopping. That is, if the electron is at site n , attraction (hence the negative sign) from the neighboring ions can make it move either to $n + 1$ or to $n - 1$. In reality, the electron will feel attraction from ions $n + 2$ and $n - 2$ and ions further away as well and could hop directly two or more lattice sites. However, the hopping energy decreases exponentially with the distance between the sites; so, nearest-neighbor hopping is the largest term, and in many cases it is a good approximation to ignore longer-range hopping.

We find the eigenstates and eigenenergies of the electron from

$$\hat{H}|\phi\rangle = E|\phi\rangle. \quad (2.15)$$

We write the eigenstate $|\phi\rangle$ as

$$|\phi\rangle = \sum_{n=0}^N c_n |n\rangle. \quad (2.16)$$

where c_n is an amplitude of state $|n\rangle$. Once we substitute $|\phi\rangle$ into $\hat{H}|\phi\rangle = E|\phi\rangle$, we obtain

$$Ec_n = \varepsilon c_n - t(c_{n+1} + c_{n-1}). \quad (2.17)$$

Using the periodic boundary conditions $c_n = c_{N+n}$, we then have

$$c_n(k) = \frac{1}{\sqrt{N}} e^{ikna} \quad (2.18)$$

and the corresponding eigenenergy is

$$E(k) = \varepsilon - 2t\cos(ka) \quad (2.19)$$

where $k = \frac{2\pi n}{Na}$ is a parameter with the dimension of a wave number, and $n = -\frac{N+1}{2}, \dots, -1, 0, 1, \dots, \frac{N}{2}$. We plot $E(k)$ in Figure 2.3.

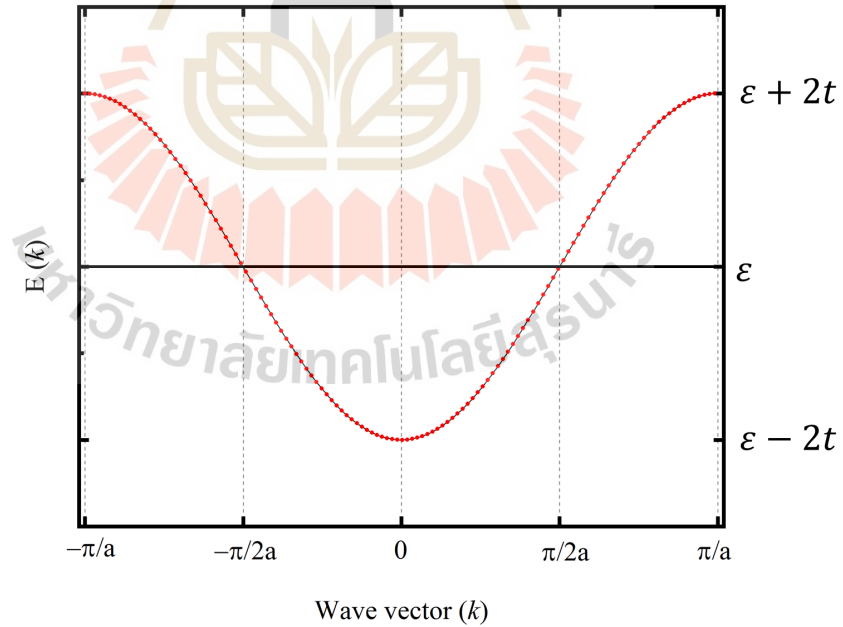


Figure 2.3 The energy dispersion of the electron in the metal with wave vector are between $-\pi/a$ and π/a .

2.3 One-dimensional metal/spacer/metal junction

Now we consider in a scattering problem for an electron tunneling through one-dimensional metal/space/metal junction in a tight-binding model. We use the following assumptions throughout our calculation.

1. Electrons in the system are not interacting with one another.
2. Electron transport through the system is ballistic (i.e. no energy lost in the process).
3. Only one atomic orbital contributes to the electron eigenstate of the system.
4. Only nearest-neighbor hopping energy is significant.
5. The lattice constant of the system is the same in all regions and we will take into account the possible unequal lattice constants by adjusting the hopping energy where it is needed.

We construct a model consisting of semi-infinite chains of metallic atoms on either side of the junction and in the middle is the chain of finite number N_M of spacer atoms that can be either insulating or metallic. This model is depicted in Figure 2.4. That is, we label each site by an index $n = -\infty, \dots, -1, 0, 1, \dots, \infty$ and let $|n\rangle$ be the orbital state of electron at site n . Particularly, the metal atoms are put together on the sites $-\infty < n < 0$, and sites $N_M < n < \infty$. The spacer atoms are on $0 \leq n \leq N_M$ sites.

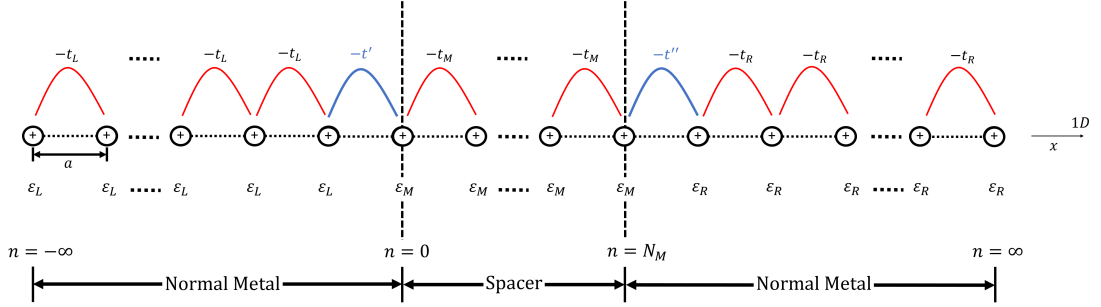


Figure 2.4 Chains of ions representing one-dimensional metal/spacer/metal junction. Each ion is a distance a apart. ε 's and t 's are on-site and hopping energies.

2.3.1 The Hamiltonian

The Hamiltonian for this system is

$$\hat{H} = \hat{H}_L + \hat{H}_M + \hat{H}_R \quad (2.20)$$

where $\hat{H}_L, \hat{H}_M, \hat{H}_R$ describe the bulk metal on the left side, the spacer in the middle, and the bulk metal on the right side of the junction respectively. That is,

$$\hat{H}_L = (\varepsilon_L - \mu) \sum_{n=-\infty}^{-1} |n\rangle\langle n| - t_L \sum_{n=-\infty}^{-2} (|n\rangle\langle n+1| + |n+1\rangle\langle n|), \quad (2.21)$$

$$\begin{aligned} \hat{H}_M = & (\varepsilon_L - \mu) | -1\rangle\langle -1| - t' (| -1\rangle\langle 0| + |0\rangle\langle -1|) + (\varepsilon_M - \mu) \sum_{n=1}^{N_M} |n\rangle\langle n| \\ & - t_M \sum_{n=1}^{N_M-1} (|n\rangle\langle n+1| + |n+1\rangle\langle n|) + (\varepsilon_R - \mu) |N_M+1\rangle\langle N_M+1| \\ & - t'' (|N_M\rangle\langle N_M+1| + |N_M+1\rangle\langle N_M|), \end{aligned} \quad (2.22)$$

$$\hat{H}_R = (\varepsilon_R - \mu) \sum_{n=N_M+1}^{\infty} |n\rangle\langle n| - t_R \sum_{n=N_M+1}^{\infty} (|n\rangle\langle n+1| + |n+1\rangle\langle n|) \quad (2.23)$$

where ε_j ($j= L, M$, or R) is the on-site energy of the electron in each region, μ is the chemical potential of the system in equilibrium, and t 's are the nearest-neighbor hopping energies between nearest-neighbor atoms in each region. Notice that we label the hopping energies between the two nearest-neighbor atoms at the two interfaces and t' and t'' .

2.3.2 The Electron State in Each Region and Matching Conditions

Considering Equation 2.14, we now have $|\phi\rangle = |\phi_L\rangle + |\phi_M\rangle + |\phi_R\rangle$ for the electron state of this one-dimensional heterostructure where

$$|\phi_L\rangle = \sum_{n=-\infty}^0 c_{nL}|n\rangle, \quad (2.24)$$

$$|\phi_M\rangle = \sum_{n=1}^{N_M} c_{nM}|n\rangle, \quad (2.25)$$

$$|\phi_R\rangle = \sum_{n=N_M+1}^{\infty} c_{nR}|n\rangle \quad (2.26)$$

are the state in each region and $|\phi\rangle$ satisfies the energy eigenequation (the same equation as Equation 2.15 above):

$$\hat{H}|\phi\rangle = E|\phi\rangle.$$

We also have additional energy eigenequations for the electron in the bulk for both metals and the spacer:

$$\hat{H}_j|\phi_{j,bulk}\rangle = E_{k,j}|\phi_{j,bulk}\rangle = E_{k,j} \sum_{n=-\infty}^{\infty} c_{nj}|n\rangle \quad (2.27)$$

where j represents L, M, R . and $E_{k,j} = (\varepsilon_j - \mu_j) - 2t_j \cos(k_j a)$. We can adjust the value of ε_M , the on-site energy of the middle region, to make the spacer becomes

either metallic or insulating layer. In the ballistic limit and the approximation that the bulk energy does not change when the material is in contact with other materials, we will take $E_{k,L} = E_{k,M} = E_{k,R} = E$.

After we make use of the energy eigenequations $\hat{H}|\phi\rangle = E|\phi\rangle$ and Equation 2.27, we obtain the following difference equations:

$$Ec_{nL} = \varepsilon_L c_{nL} - t_L(c_{n+1,L} + c_{n-1,L}); -\infty < n \leq \infty \quad (2.28)$$

$$Ec_{nM} = \varepsilon_M c_{nM} - t_M(c_{n+1,M} + c_{n-1,M}); -\infty < n \leq \infty \quad (2.29)$$

$$Ec_{nR} = \varepsilon_R c_{nR} - t_R(c_{n+1,R} + c_{n-1,R}); -\infty < n \leq \infty \quad (2.30)$$

$$Ec_{nL} = \varepsilon_L c_{nL} - t_L(c_{n+1,L} + c_{n-1,L}); -\infty < n \leq -2 \quad (2.31)$$

$$Ec_{nM} = \varepsilon_L c_{-1L} - t_L c_{-2L} - t' c_{-0M} + \varepsilon_M c_{0M} - t' c_{-1L} - t_M c_{1M} \\ + \varepsilon_M c_{N_M,M} - t_M c_{(N_M-1),M} - t'' c_{(N_M+1),M} + \varepsilon_{(N_M+1),M} \quad (2.32)$$

$$- t'' c_{N_M M} - t_R c_{(n_M+2),R}; -1 \leq n \leq N_M + 1 \\ Ec_{nR} = \varepsilon_R c_{nR} - t_R(c_{n+1,R} + c_{n-1,R}); N_M + 1 < n \leq \infty \quad (2.33)$$

After some mathematical arrangements, we obtain the following matching conditions:

$$t_L c_{0L} = t' c_{0M} \quad (2.34)$$

$$t_M c_{-1M} = t' c_{-1L} \quad (2.35)$$

$$t_L c_{N_M,M} = t'' c_{N_M,R} \quad (2.36)$$

$$t_M c_{N_M+1,M} = t'' c_{N_M+1,R}. \quad (2.37)$$

In a scattering problem we write

$$c_{n,L} = e^{ik_L n a} + \gamma e^{-ik_L n a}, \quad (2.38)$$

$$c_{n,M} = \alpha e^{ik_M na} + \beta e^{-ik_M na}, \quad (2.39)$$

and

$$c_{n,R} = \tau e^{ik_R na}. \quad (2.40)$$

Here $e^{ik_L na}$, $e^{-ik_L na}$, $e^{ik_R na}$ represent the incident, the reflected and the transmitted electron respectively. $e^{\pm ik_M na}$ represent the two waves in the spacer region. That is, γ , τ , α , β are the amplitudes of the reflected electron wave, the transmitted electron wave and the two interfering electron waves in the spacer respectively. The wave numbers, k 's, are real for electrons in metals and pure imaginary for those in insulators. Because we assume the electron transport across the structure to be an elastic process, we can obtain the values of k_j from

$$E = (\varepsilon_j - \mu_j) - 2t_j \cos(k_j a). \quad (2.41)$$

We sketch of the energy dispersion relations of the electron in all regions in Figure 2.5.

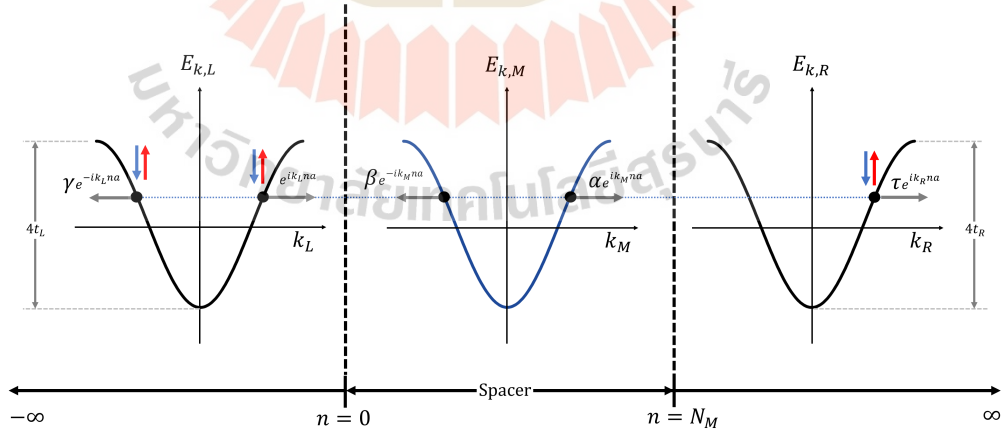


Figure 2.5 The sketch of the energy dispersion relation of an electron in each region in the case where the spacer is a metal.

From these four matching conditions, we can obtain all the amplitudes:

$\gamma, \tau, \alpha, \beta$. Once we get these amplitudes, we can obtain the reflection and the transmission probabilities (R and T respectively) from the following equations:

$$R(E) = |\gamma|^2 \quad (2.42)$$

$$T(E) = |\tau|^2 \frac{t_R \sin(k_R a)}{t_L \sin(k_L a)}. \quad (2.43)$$

2.3.3 The Conductance

Now we will show how we relate the conductance to the transmission probability in the scattering problem. We ultimately use this relation to calculate the magnetoresistance of our system of interest: a ferromagnet/spacer/ferromagnet junction. We write the net current density of spin- s electrons across a junction, with an applied voltage $V = \mathbb{E}d$ across the junction of thickness d and with electric field \mathbb{E} , as

$$j_{net}^S = \sum_k e v_s T_S(k) [f(\varepsilon_k - eV) - f(\varepsilon_k)] \quad (2.44)$$

where e is the magnitude of an electron charge, $T_s(k)$ is the transmission probability of a spin- s electron, $f(\varepsilon_k)$ is the Fermi-Dirac distribution function, and \vec{v}_s is the velocity of the spin- s electron. Changing the summation in to an integral, we have for one dimensional system,

$$j_{net}^S = \frac{Le}{2\pi} \int dk v_s T_S(k) [f(\varepsilon_k - eV) - f(\varepsilon_k)]. \quad (2.45)$$

Because $v_s = \frac{1}{\hbar} \frac{d\varepsilon_k}{dk}$,

$$j_{net}^S = \frac{Le}{2\pi\hbar} \int_{-\infty}^{\infty} d\varepsilon_k T_S(\varepsilon_k) [f(\varepsilon_k - eV) - f(\varepsilon_k)] \quad (2.46)$$

At zero temperature,

$$j_{net}^S = \frac{Le}{h} \int_{\varepsilon_F}^{\varepsilon_F + eV} d\varepsilon_k T_S(\varepsilon_k) \quad (2.47)$$

$$j_{net}^S = \frac{Le}{h} eVT_S(\varepsilon_F) \quad (2.48)$$

$$j_{net}^S = \frac{Le^2}{h} T_S(\varepsilon_F)V. \quad (2.49)$$

When the electric field \mathbb{E} is not too big, one can approximate the current density to be proportional to the electric field as

$$j = \sigma\mathbb{E}. \quad (2.50)$$

Because $j = \sigma\mathbb{E} = \sigma\frac{V}{d} = \frac{\sigma}{d}V$ and compare this equation with Equation 2.40, one obtains

$$\frac{\sigma_S}{d} = \frac{Le^2}{h} T_S(\varepsilon_F) \quad (2.51)$$

$$\sigma_S = \frac{Le^2d}{h} T_S(\varepsilon_F). \quad (2.52)$$

Once we obtain $T_S(\varepsilon_F)$ for each case, we can examine closely how physical properties of the spacer affect the magnetoresistance.

CHAPTER III

ONE-DIMENSIONAL TUNNELING FOR FERROMAGNET/SPACER/FERROMAGNET JUNCTION IN A SMALL MAGNETIC FIELD

In this chapter, we apply a tight-binding method to one-dimensional atomic chain representing ferromagnet/spacer/ferromagnet junction in a small magnetic field. We treat the tunneling through this structure as a scattering problem in the same way we did with metal/spacer/metal in Section 2.3 in the previous chapter. In addition to all the approximations mentioned in that section, we also assume that the strength of the applied field is small enough that we can consider it as a Zeeman Effect.

The infinite chain of a ferromagnet/spacer/ferromagnet junction in a small magnetic field is depicted in Figure 3.1. We label each site by an index $n = -\infty, \dots, -1, 0, 1, \dots, \infty$ and let $|n\rangle$ be the orbital state of electron at site n . There are two ferromagnetic metal regions and a spacer (barrier) which a spacer the chain of finite number of spacer atoms that can be insulating. The spacer ions is at $0 \leq n \leq N_M$ site which N_M is the thickness of insulator layer. For both ferromagnetic metal region, the ferromagnetic ions are put together on the sites $-\infty < n < 0$, and sites $N_M < n < \infty$.

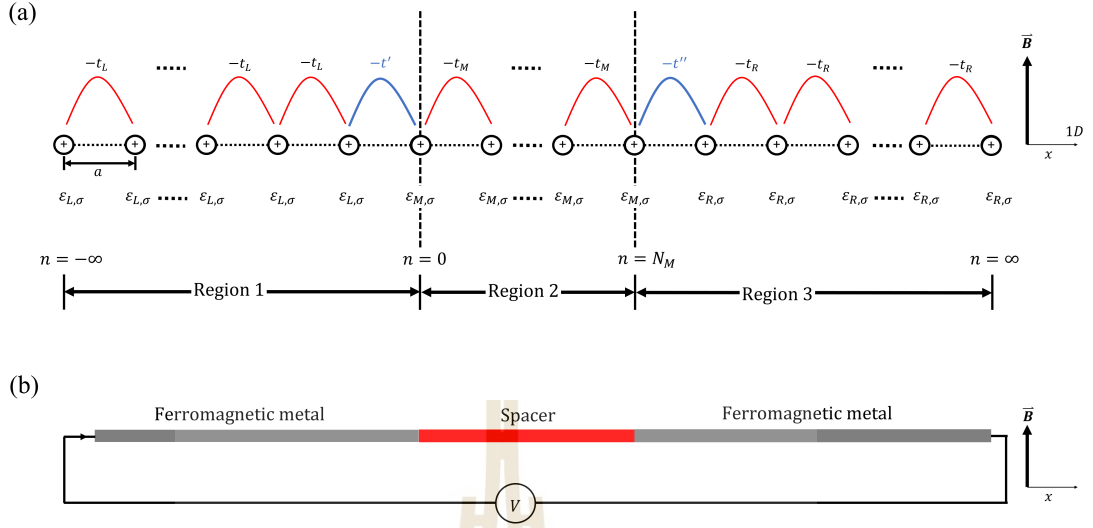


Figure 3.1 One-dimensional of ferromagnetic metal/spacer/ferromagnetic metal junction is displayed for (a) the chains of ions and (b) the geometry in a small external magnetic field perpendicular to into the model.

3.1 The Hamiltonian

In this model, we can be obtained the Hamiltonian of system by a tight-binding model, that is,

$$\hat{H} = \hat{H}_L + \hat{H}_M + \hat{H}_R, \quad (3.1)$$

where $\hat{H}_L, \hat{H}_M, \hat{H}_R$ describe the bulk ferromagnetic metal on the left side, the spacer in the middle, and the bulk ferromagnetic metal on the right side of the junction respectively. That is,

$$\begin{aligned} \hat{H}_L = & (\epsilon_L - \mu_L) \sum_{n=-\infty}^{-1} \sum_{\sigma=-\frac{1}{2}}^{\frac{1}{2}} |n\sigma\rangle\langle n\sigma| \\ & - t_L \sum_{n=-\infty}^{-2} \sum_{\sigma=-\frac{1}{2}}^{\frac{1}{2}} (|n\sigma\rangle\langle n+1, \sigma| + |n+1, \sigma\rangle\langle n, \sigma|) \\ & - (J_L + cB) \sum_{n=-\infty}^{-1} \left(\left| n\frac{1}{2} \right\rangle \left\langle n\frac{1}{2} \right| - \left| n, -\frac{1}{2} \right\rangle \left\langle n, -\frac{1}{2} \right| \right), \end{aligned} \quad (3.2)$$

$$\begin{aligned}
\hat{H}_M = & (\varepsilon_L - \mu_L) \sum_{\sigma=-\frac{1}{2}}^{\frac{1}{2}} | -1\sigma \rangle \langle -1\sigma | - t' \sum_{\sigma=-\frac{1}{2}}^{\frac{1}{2}} (| -1\sigma \rangle \langle 0\sigma | + | 0\sigma \rangle \langle -1\sigma |) \\
& + (\varepsilon_M - \mu_M) \sum_{n=1}^{N_M} \sum_{\sigma=-\frac{1}{2}}^{\frac{1}{2}} | n\sigma \rangle \langle n\sigma | \\
& - t_M \sum_{n=1}^{N_M-1} \sum_{\sigma=-\frac{1}{2}}^{\frac{1}{2}} (| n\sigma \rangle \langle n+1, \sigma | + | n+1, \sigma \rangle \langle n, \sigma |)
\end{aligned} \tag{3.3}$$

$$\begin{aligned}
& + (\varepsilon_R - \mu_R) \sum_{\sigma=-\frac{1}{2}}^{\frac{1}{2}} | N_M + 1, \sigma \rangle \langle N_M + 1, \sigma | \\
& - t'' \sum_{\sigma=-\frac{1}{2}}^{\frac{1}{2}} (| N_M \sigma \rangle \langle N_M + 1, \sigma | + | N_M + 1, \sigma \rangle \langle N_M \sigma |) \\
& - \sum_{n=1}^{N_M} cB \left(\left| n \frac{1}{2} \right\rangle \left\langle n \frac{1}{2} \right| - \left| n, -\frac{1}{2} \right\rangle \left\langle n, -\frac{1}{2} \right| \right), \\
\hat{H}_R = & (\varepsilon_R - \mu_R) \sum_{n=N_M+1}^{\infty} \sum_{\sigma=-\frac{1}{2}}^{\frac{1}{2}} | n\sigma \rangle \langle n\sigma | \\
& - t_R \sum_{n=N_M+1}^{\infty} \sum_{\sigma=-\frac{1}{2}}^{\frac{1}{2}} (| n\sigma \rangle \langle n+1, \sigma | + | n+1, \sigma \rangle \langle n, \sigma |) \\
& - (-J_R + cB) \sum_{n=N_M+1}^{\infty} \left(\left| n \frac{1}{2} \right\rangle \left\langle n \frac{1}{2} \right| - \left| n, -\frac{1}{2} \right\rangle \left\langle n, -\frac{1}{2} \right| \right)
\end{aligned} \tag{3.4}$$

where ε_M is the on-site energy at the ion acting as a barrier, ε_L is the on-site energy at the ions of the left side of the junction, ε_R is the on-site energy at the ions of the right side of the junction, J_i are the spin exchange energy, B is the magnetic field and c is an appropriate proportional constant. Notice that we label the hopping energies between the two nearest-neighbor atoms at the two interfaces as t' and t'' .

3.2 The Electron States

For the ferromagnet/spacer/ferromagnet junction, similar to the metal/spacer/metal structure in the previous chapter but only now the state is spin-dependent, the eigenenergy equation for the electron with spin σ in the system is $\hat{H}_\sigma|\phi_\sigma\rangle = E|\phi_\sigma\rangle$ and the electron state $|\phi_\sigma\rangle = |\phi_{\sigma L}\rangle + |\phi_{\sigma M}\rangle + |\phi_{\sigma R}\rangle$ with spin σ in the region j are written as a linear combination of the states at all sites in that region.

$$|\phi_{\sigma L}\rangle = \sum_{n=-\infty}^0 c_{n\sigma,L} |n\sigma\rangle, \quad (3.5)$$

$$|\phi_{\sigma M}\rangle = \sum_{n=1}^{N_M} c_{n\sigma,M} |n\sigma\rangle, \quad (3.6)$$

$$|\phi_{\sigma R}\rangle = \sum_{n=N_M+1}^{\infty} c_{n\sigma,R} |n\sigma\rangle \quad (3.7)$$

where $c_{n,L}$, $c_{n,R}$ and $c_{n,M}$ are the amplitudes of electron state with spin σ at site n . We still also have for the electron state in the bulk for both metals and the spacer similar to the case for metal/spacer/metal junction in the previous chapter.

We will later write, for example for the ferromagnetic metal on the left side,

$$C_{n,L} = \begin{bmatrix} c_{n\uparrow,L} \\ c_{n\downarrow,L} \end{bmatrix}.$$

For a scattering event, in which an incident electron injected from the left side of the junction, the energy dispersion relation of the ferromagnet/insulating/ferromagnet junction is shown in Figure 3.2.

We write a scattering of the electron state of the ferromagnet left side, ferromagnetic right side and the insulating for middle region. Therefore, we represented the wave functions (the electron scattering) of three regions.

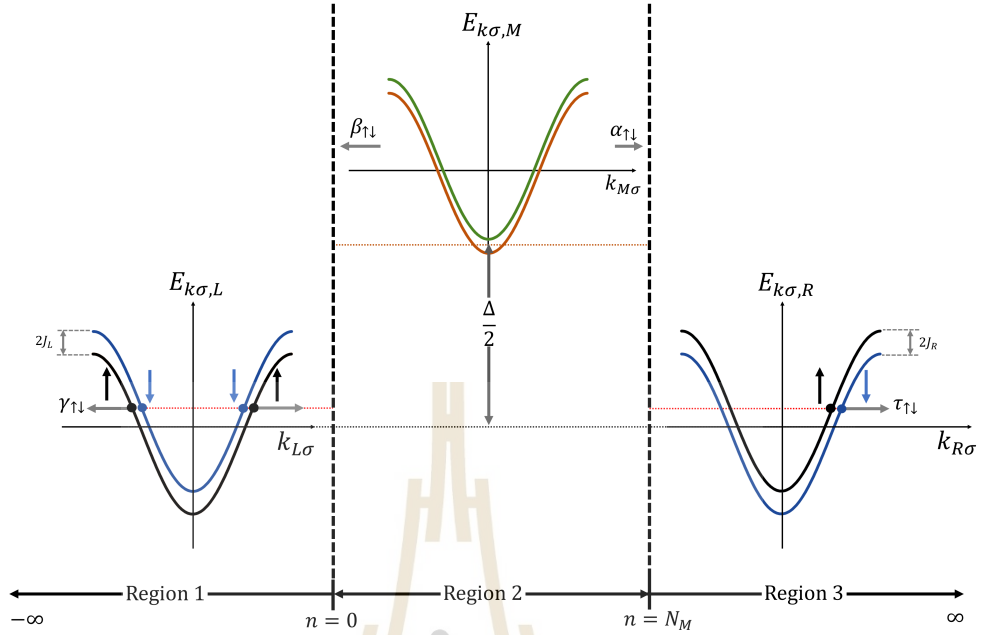


Figure 3.2 The sketches of the energy dispersion relation of an electron in each region. Notice the splits of the relation for spin-up and spin-down electrons. In this picture we take the spacer to be insulating.

In region 1 ($-\infty < n < 0$), There are the scattering of one incident electron state and two reflected electron state. The diagram of the energy dispersion relation of left ferromagnetic metal is shown in Figure 3.3.

There are two possibilities of the amplitudes of the electron wave in the metal on the left. In the case of spin-up incident electron, we have

$$\mathbb{C}_{n,L}^{\uparrow} = \begin{bmatrix} c_{n\uparrow,L} \\ c_{n\downarrow,L} \end{bmatrix} = \begin{bmatrix} 1 \\ 0 \end{bmatrix} e^{ik_{L\uparrow}na} + \gamma_{\uparrow} \begin{bmatrix} 1 \\ 0 \end{bmatrix} e^{-ik_{L\uparrow}na} + \gamma_{\downarrow} \begin{bmatrix} 0 \\ 1 \end{bmatrix} e^{-ik_{L\downarrow}na} \quad (3.8)$$

In the case of spin-down incident electron, we have

$$\mathbb{C}_{n,L}^{\downarrow} = \begin{bmatrix} c_{n\uparrow,L} \\ c_{n\downarrow,L} \end{bmatrix} = \begin{bmatrix} 0 \\ 1 \end{bmatrix} e^{ik_{L\downarrow}na} + \gamma_{\uparrow} \begin{bmatrix} 1 \\ 0 \end{bmatrix} e^{-ik_{L\uparrow}na} + \gamma_{\downarrow} \begin{bmatrix} 0 \\ 1 \end{bmatrix} e^{-ik_{L\downarrow}na} \quad (3.9)$$

where γ_σ are the reflection coefficients of the reflected electron waves with spin σ . The wave vector of a spin electrons is $k_{L\sigma}$, that is $k_{L\sigma} = \frac{1}{a} \arccos\left(\frac{(\varepsilon_L - \mu) \mp J_L \mp cB - E_L}{2t_L}\right)$ where μ is the chemical potential of the system.

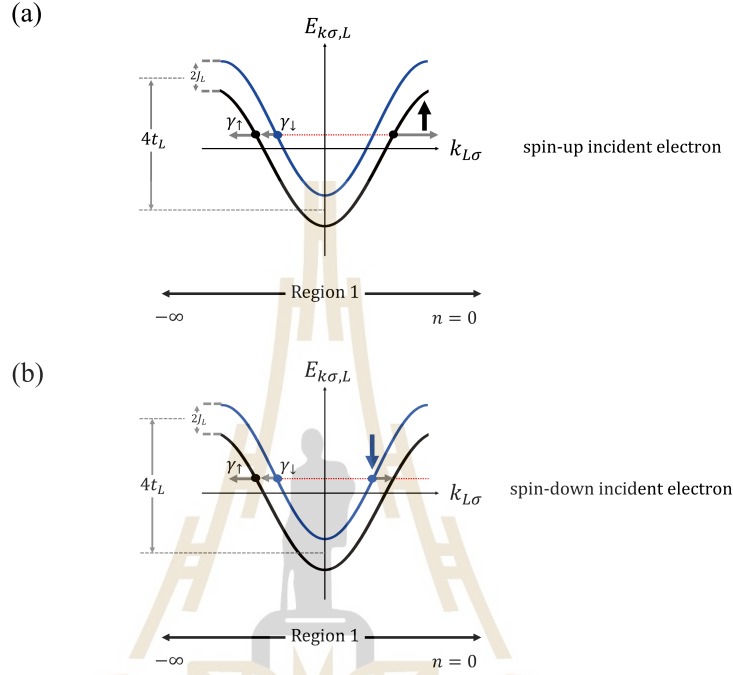


Figure 3.3 The sketches of the energy dispersion relation of a ferromagnet in left side. The arrows depict the directions of the electron spins and J_L are the spin exchange energy with (a) spin-up incident and (b) spin-down incident electron.

In region 2 ($0 \leq n \leq N_M$), the scattering of the excitation in the insulating region is represented in the energy dispersion relation of insulating region as Figure 3.4.

The amplitude of the electron wave in the spacer region takes the form for both cases of incident electron spins, $\mathbb{C}_{n,M} = \begin{bmatrix} c_{n\uparrow,M} \\ c_{n\downarrow,M} \end{bmatrix}$, we have

$$\mathbb{C}_{n,M} = \begin{bmatrix} \alpha_\uparrow \\ 0 \end{bmatrix} e^{ik_{M\uparrow}na} + \begin{bmatrix} 0 \\ \alpha_\downarrow \end{bmatrix} e^{ik_{M\downarrow}na} + \begin{bmatrix} \beta_\uparrow \\ 0 \end{bmatrix} e^{-ik_{M\uparrow}na} + \begin{bmatrix} 0 \\ \beta_\downarrow \end{bmatrix} e^{-ik_{M\downarrow}na} \quad (3.10)$$

where α_σ and β_σ are the amplitude of electron reflection and transmission state with spin σ in this region. As for the insulating, $k_{M\sigma}$ is the wave vector, that is $k_{M\sigma} = \frac{1}{a} \arccos\left(\frac{(\varepsilon_M - \mu) \mp cB - E_M}{2t_M}\right)$ at a middle region. We assumed that the on-site energy of insulator as $\varepsilon_M = \frac{\Delta}{2} + 2t_M$ where Δ is the energy gap.

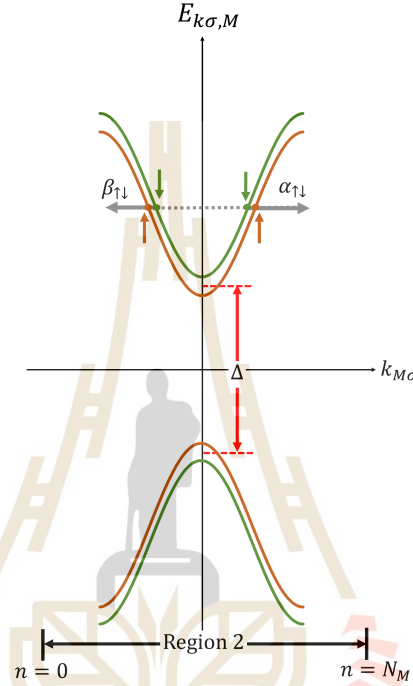


Figure 3.4 The sketches of the energy dispersion relation of the insulating and Δ is the band gap.

In region 3 ($N_M \leq n \leq \infty$), the amplitude of the electron wave in the metal in the right region takes the form for both cases of incident electron spins

$$\mathbb{C}_{n,R} = \begin{bmatrix} c_{n\uparrow,R} \\ c_{n\downarrow,R} \end{bmatrix} = \tau_\uparrow \begin{bmatrix} 1 \\ 0 \end{bmatrix} e^{ik_{R\uparrow}na} + \tau_\downarrow \begin{bmatrix} 0 \\ 1 \end{bmatrix} e^{ik_{R\downarrow}na}. \quad (3.11)$$

where τ_σ are the transmission amplitudes of the outgoing electron waves with spin σ . The wave vector of a spin electrons is $k_{R\sigma}$, that is $k_{R\sigma} = \frac{1}{a} \arccos\left(\frac{(\varepsilon_R - \mu) \pm J_R \mp cB - E_R}{2t_R}\right)$. The energy dispersion relation of insulating region shown in Figure 3.5.

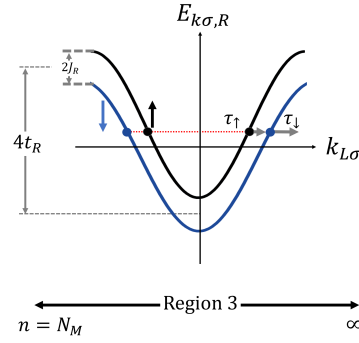


Figure 3.5 The sketches of the energy dispersion relation of a ferromagnet in right side with two transmission of electron scattering. The arrows depict the directions of the electron spins and J_R are the spin exchange energy.

3.3 The Electron State in Each Region and Matching Conditions

Considering Equations 3.2, 3.3 and 3.4, we now have $|\phi_{\sigma}\rangle = |\phi_{\sigma L}\rangle + |\phi_{\sigma M}\rangle + |\phi_{\sigma R}\rangle$ for the electron state of this one-dimensional heterostructure where

$$|\phi_{\sigma L}\rangle = \sum_{n=-\infty}^0 c_{n\sigma,L} |n\sigma\rangle, \quad (3.12)$$

$$|\phi_{\sigma M}\rangle = \sum_{n=1}^{N_M} c_{n\sigma,M} |n\sigma\rangle, \quad (3.13)$$

$$|\phi_{\sigma R}\rangle = \sum_{n=N_M+1}^{\infty} c_{n\sigma,R} |n\sigma\rangle \quad (3.14)$$

are the state in each region and $|\phi_{\sigma}\rangle$ satisfies the energy eigenequation (the same equation as Equation 2.15 above):

$$\hat{H}|\phi_{\sigma}\rangle = E_{\sigma}|\phi_{\sigma}\rangle. \quad (3.15)$$

We also have additional energy eigenequations for the electron in the bulk for both ferromagnetic metals and the spacer:

$$\hat{H}_j|\phi_{\sigma j,bulk}\rangle = E_{k\sigma,j}|\phi_{\sigma j,bulk}\rangle = E_{k\sigma,j} \sum_{n=-\infty}^{\infty} c_{n\sigma,j}|n\sigma\rangle \quad (3.16)$$

where j represents L, M, R . and we obtain ferromagnet eigenenergy and a spacer, there are

$$E_{k\sigma,L} = (\varepsilon_L - \mu_L) - 2t_L \cos(k_{L\sigma}a) \mp J_L \mp cB, \quad (3.17)$$

$$E_{k\sigma,R} = (\varepsilon_R - \mu_R) - 2t_R \cos(k_{R\sigma}a) \pm J_R \mp cB \quad (3.18)$$

and

$$E_{k\sigma,M} = (\varepsilon_M - \mu_M) - 2t_M \cos(k_{M\sigma}a) \mp cB. \quad (3.19)$$

We can adjust the value of ε_M , the on-site energy of the middle region, to make the spacer becomes either metallic or insulating layer. In the ballistic limit and the approximation that the bulk energy does not change when the material is in contact with other materials, we will take $E_{k\sigma,L} = E_{k\sigma,M} = E_{k\sigma,R} = E_\sigma$.

After we make use of the energy eigenequations $\hat{H}|\phi_\sigma\rangle = E_\sigma|\phi_\sigma\rangle$ and Equation 3.16, we obtain the following difference equations: for a bulk of ferromagnet in left side,

$$Ec_{n\uparrow,L} = \varepsilon_L c_{n\uparrow,L} - t_L(c_{n\uparrow+1,L} + c_{n\uparrow-1,L}) - J_L c_{n\uparrow,L} - cB c_{n\uparrow,L}; -\infty < n \leq \infty \quad (3.20)$$

$$Ec_{n\downarrow,L} = \varepsilon_L c_{n\downarrow,L} - t_L(c_{n\downarrow+1,L} + c_{n\downarrow-1,L}) + J_L c_{n\downarrow,L} + cB c_{n\downarrow,L}; -\infty < n \leq \infty \quad (3.21)$$

a bulk of spacer,

$$Ec_{n\uparrow,M} = \varepsilon_M c_{n\uparrow,M} - t_M(c_{n\uparrow+1,M} + c_{n\uparrow-1,M}) - cB c_{n\uparrow,M}; -\infty < n \leq \infty \quad (3.22)$$

$$Ec_{n\downarrow,M} = \varepsilon_M c_{n\downarrow,M} - t_M(c_{n\downarrow+1,M} + c_{n\downarrow-1,M}) + cB c_{n\downarrow,M}; -\infty < n \leq \infty \quad (3.23)$$

a bulk of ferromagnet in right side,

$$Ec_{n\uparrow,R} = \varepsilon_R c_{n\uparrow,R} - t_R(c_{n\uparrow+1,R} + c_{n\uparrow-1,R}) + J_R c_{n\uparrow,R} - cB c_{n\uparrow,R}; -\infty < n \leq \infty \quad (3.24)$$

$$Ec_{n\downarrow,R} = \varepsilon_R c_{n\downarrow,R} - t_R(c_{n\downarrow+1,R} + c_{n\downarrow-1,R}) - J_R c_{n\downarrow,R} + cB c_{n\downarrow,R}; -\infty < n \leq \infty \quad (3.25)$$

and,

$$Ec_{n\uparrow,L} = \varepsilon_L c_{n\uparrow,L} - t_L(c_{n\uparrow+1,L} + c_{n\uparrow-1,L}) - J_L c_{n\uparrow,L} - cB c_{n\uparrow,L}; -\infty < n \leq -2 \quad (3.26)$$

$$Ec_{n\downarrow,L} = \varepsilon_L c_{n\downarrow,L} - t_L(c_{n\downarrow+1,L} + c_{n\downarrow-1,L}) + J_L c_{n\downarrow,L} + cB c_{n\downarrow,L}; -\infty < n \leq -2 \quad (3.27)$$

$$\begin{aligned} Ec_{n\uparrow,M} = & \varepsilon_L c_{-1\uparrow,L} - t_L c_{-2\uparrow,L} - t' c_{0\uparrow,M} - J_L c_{n\uparrow,L} - cB c_{n\uparrow,L} + \varepsilon_M c_{0\uparrow,M} \\ & - t' c_{-1\uparrow,L} - t_M c_{1\uparrow,M} - cB c_{n\uparrow,L} + \varepsilon_M c_{N_M\uparrow,M} - t_M c_{(N_M-1)\uparrow,M} \\ & - t'' c_{(N_M+1)\uparrow,R} - cB c_{n\uparrow,M} + \varepsilon_M c_{(N_M+1)\uparrow,M} - t'' c_{N_M\uparrow,M} \end{aligned} \quad (3.28)$$

$$\begin{aligned} Ec_{n\downarrow,M} = & \varepsilon_L c_{-1\downarrow,L} - t_L c_{-2\downarrow,L} - t' c_{0\downarrow,M} + J_L c_{n\downarrow,L} + cB c_{n\downarrow,L} + \varepsilon_M c_{0\downarrow,M} \\ & - t' c_{-1\downarrow,L} - t_M c_{1\downarrow,M} - cB c_{n\downarrow,L} + \varepsilon_M c_{N_M\downarrow,M} - t_M c_{(N_M-1)\downarrow,M} \\ & - t'' c_{(N_M+1)\downarrow,R} - cB c_{n\downarrow,M} + \varepsilon_M c_{(N_M+1)\downarrow,M} - t'' c_{N_M\downarrow,M} \end{aligned} \quad (3.29)$$

$$- t_M c_{(N_M+2)\downarrow,R} + J_L c_{n\downarrow,R} + cB c_{n\downarrow,R} \quad ; -1 \leq n \leq N_M + 1$$

$$Ec_{n\uparrow,R} = \varepsilon_R c_{n\uparrow,R} - t_R(c_{n\uparrow+1,R} + c_{n\uparrow-1,R}) + J_R c_{n\uparrow,R} - cB c_{n\uparrow,R}; N_M + 1 < n \leq \infty \quad (3.30)$$

$$Ec_{n\downarrow,R} = \varepsilon_R c_{n\downarrow,R} - t_R(c_{n\downarrow+1,R} + c_{n\downarrow-1,R}) - J_R c_{n\downarrow,R} + cB c_{n\downarrow,R}; N_M + 1 < n \leq \infty \quad (3.31)$$

After some mathematical arrangements, we obtain the following matching

conditions. In spin-up electron, we have

$$t_L c_{0\uparrow,L} = t' c_{0\uparrow,M} \quad (3.32)$$

$$t_L c_{N_M\uparrow,M} = t'' c_{N_M\uparrow,R} \quad (3.33)$$

$$t_M c_{-1\uparrow,M} = t' c_{-1\uparrow,L} \quad (3.34)$$

$$t_M c_{(N_M+1)\uparrow,M} = t'' c_{(N_M+1)\uparrow,R}. \quad (3.35)$$

In spin-down electro, we have

$$t_L c_{0\downarrow,L} = t' c_{0\downarrow,M} \quad (3.36)$$

$$t_L c_{N_M\downarrow,M} = t'' c_{N_M\downarrow,R} \quad (3.37)$$

$$t_M c_{-1\downarrow,M} = t' c_{-1\downarrow,L} \quad (3.38)$$

$$t_M c_{(N_M+1)\downarrow,M} = t'' c_{(N_M+1)\downarrow,R}. \quad (3.39)$$

From these equations, we can obtain all the amplitudes: $\gamma'_\sigma s, \tau'_\sigma s, \alpha'_\sigma s, \beta'_\sigma s$. Once we get these amplitudes, we can obtain the reflection and the transmission probabilities (R and T respectively).

3.4 Transmission and Reflection Probabilities

The transmission and reflection probabilities can be obtained from the reflection and transmission amplitudes. They all are now spin-dependent and are described in the equations below. In the case of the incident electron with spin-up, there are two different reflection probabilities and two transmission probabilities. That is,

$$R_\uparrow^{incident\uparrow}(E) = |\gamma_\uparrow|^2 \quad (3.40)$$

$$R_\downarrow^{incident\uparrow}(E) = |\gamma_\downarrow|^2 \frac{\sin(k_L^\downarrow a)}{\sin(k_L^\uparrow a)} \quad (3.41)$$

and the two transmission probabilities are

$$T_{\uparrow}^{incident\uparrow}(E) = |\tau_{\uparrow}|^2 \frac{t_R \sin(k_R^{\uparrow} a)}{t_L \sin(k_L^{\uparrow} a)} \quad (3.42)$$

$$T_{\downarrow}^{incident\uparrow}(E) = |\tau_{\downarrow}|^2 \frac{t_R \sin(k_R^{\downarrow} a)}{t_L \sin(k_L^{\uparrow} a)}. \quad (3.43)$$

In the case of the incident electron with spin-down, the two reflection probabilities are

$$R_{\uparrow}^{incident\downarrow}(E) = |\gamma_{\uparrow}|^2 \frac{\sin(k_L^{\downarrow} a)}{\sin(k_L^{\uparrow} a)} \quad (3.44)$$

$$R_{\downarrow}^{incident\downarrow}(E) = |\gamma_{\downarrow}|^2, \quad (3.45)$$

and the two transmission probabilities are

$$T_{\uparrow}^{incident\downarrow}(E) = |\tau_{\uparrow}|^2 \frac{t_R \sin(k_R^{\uparrow} a)}{t_L \sin(k_L^{\downarrow} a)} \quad (3.46)$$

$$T_{\downarrow}^{incident\downarrow}(E) = |\tau_{\downarrow}|^2 \frac{t_R \sin(k_R^{\downarrow} a)}{t_L \sin(k_L^{\downarrow} a)}. \quad (3.47)$$

We will ultimately calculate the magnetoresistance (MR) from the conductivity (Julliere, 1975), σ . That is,

$$MR = \frac{\sigma_P - \sigma_{AP}}{\sigma_{AP}} \quad (3.48)$$

where σ_P is the sum of the spin-up conductivity σ_{\uparrow} and spin-down conductivity σ_{\downarrow} when both ferromagnetic electrodes have parallel magnetizations, and σ_{AP} is the sum of σ_{\uparrow} and σ_{\downarrow} , when both ferromagnetic electrodes have antiparallel magnetizations. We obtain σ_{\uparrow} and σ_{\downarrow} from the same way shown in Section 2.3.3 in the previous chapter.

CHAPTER IV

RESULTS AND DISCUSSION

In the previous chapter, we laid out how we obtained the electron transmission probability, electrical conductance, and the magnetoresistance ratio of a one-dimensional ferromagnetic metal/spacer/ferromagnetic metal junction from a tight-binding model. Here, we will present the numerical results of such quantities and how physical factors of interest, such as voltage bias, magnetic field, and the thickness of spacer, affect them.

For all our results, we assign all our parameters of the ferromagnetic metals with the values related to the known physical properties of Fe. All the energy terms in our model are taken to be with respect to the hopping energy of conduction electrons in Fe. Below is the list of the physical quantities of Fe we use in this thesis.

1. The exchange energy is approximately 0.089 eV, which we approximate from the Curie temperature of Fe.
2. The hopping energy of Fe is taken to be about 0.93 eV which we approximate the Fe *d*-bandwidth (Walter et al., 2010; Yamasaki and Fujiwara, 2002).
3. The proportional constant *c* related to the applied field is taken to be the magnetic dipole moment of Fe which is equal to $2.22\mu_B = 0.13 \text{ meV/T}$, where μ_B is the Bohr magneton.

4.1 Ferromagnetic metal/ Normal metal /Ferromagnet metal Structure

4.1.1 Transmission probability for different metals

For a metal as a spacer, we can take $\varepsilon_M - \mu$ to be equal to greater than and less than to represent half-filled, more than half-filled bands and less than half-filled respectively as depicted in Figure 4.1.

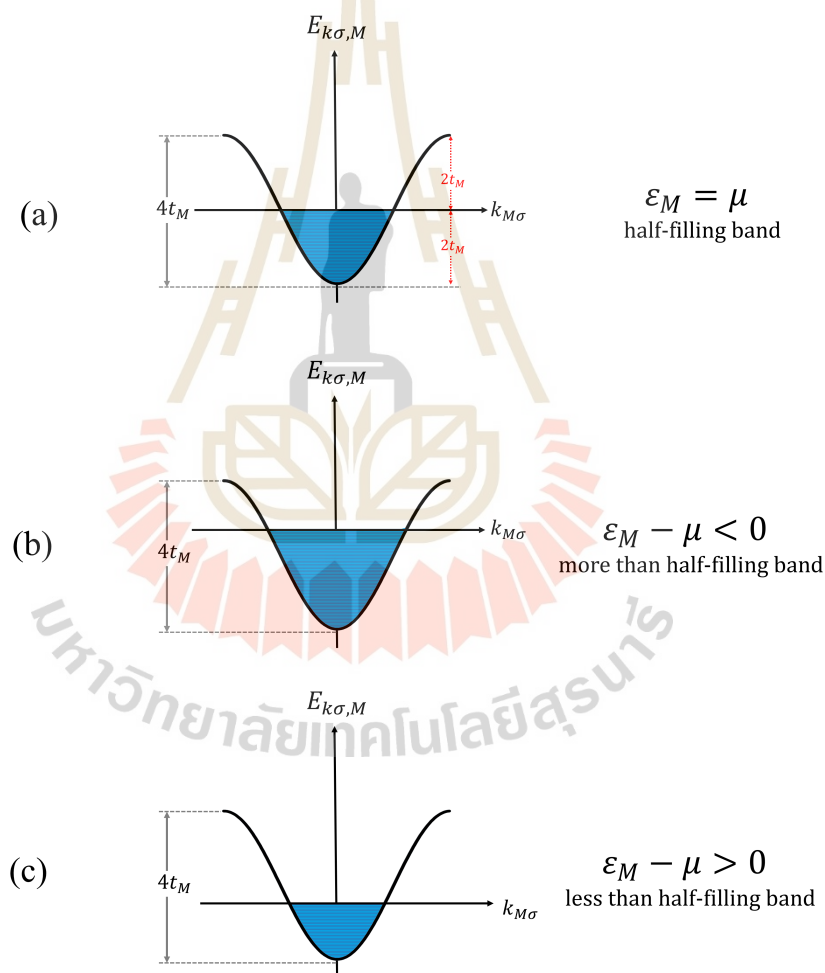


Figure 4.1 The sketches of the energy dispersion relation of a metallic spacer at (a) $\varepsilon_M = \mu$ (half-filling), (b) $\varepsilon_M - \mu < 0$ (more than half filling) and (c) $\varepsilon_M - \mu > 0$ (less than half filling).

Below, we show the plot of the total transmission probability a function of the energy, equivalent to the applied voltage across the junction, for $N_M = 7$ atoms in zero field for the three values of $\varepsilon_M - \mu = 0, -0.5t_L, 0.5t_L$. For all the plots in Figure 4.2, we use the hopping energy of the ferromagnet in the left side to compare with all energy parameters and we approximate that the hopping energies of both ferromagnetic metals (t_L and t_R) are same the hopping energy of a spacer ($t_M = t_L = t_R$). We also take the hopping energy of an electron between two atoms of two interfaces ($t' = t''$) of metal to be $1.5t_L$. As can be seen in the plots, the transmission probability is oscillating with the energy with a different period in energy; the smaller the filling the larger the period.

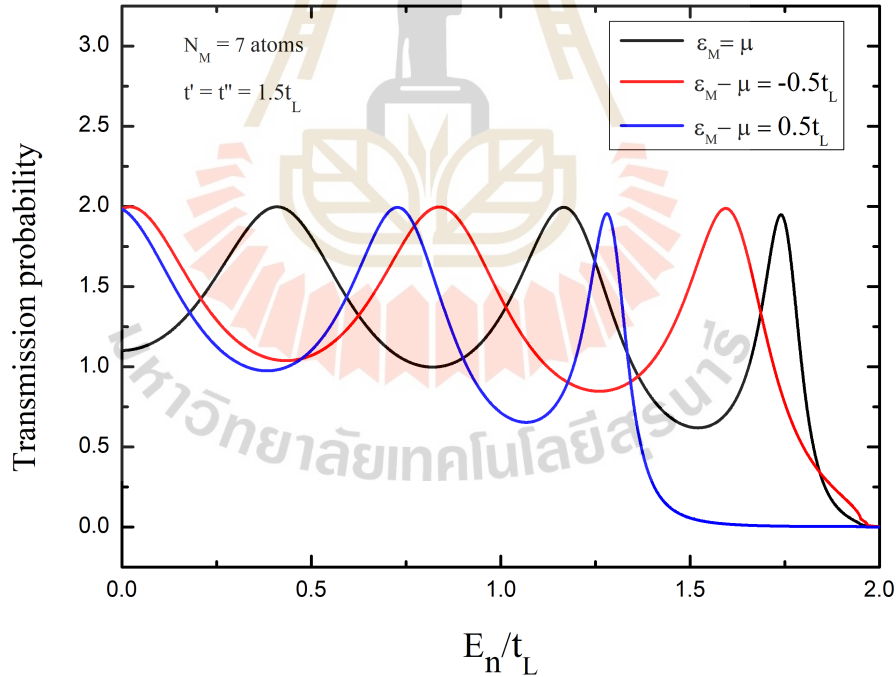


Figure 4.2 The transmission probability as a function of energy (E_n/t_L) with 7 metallic spacer atoms.

4.1.2 The effect of a metal thickness on magnetoresistance

We show the results of magnetoresistance as a function of an applied magnetic field for the various value of N_M atoms in Figure 4.3.

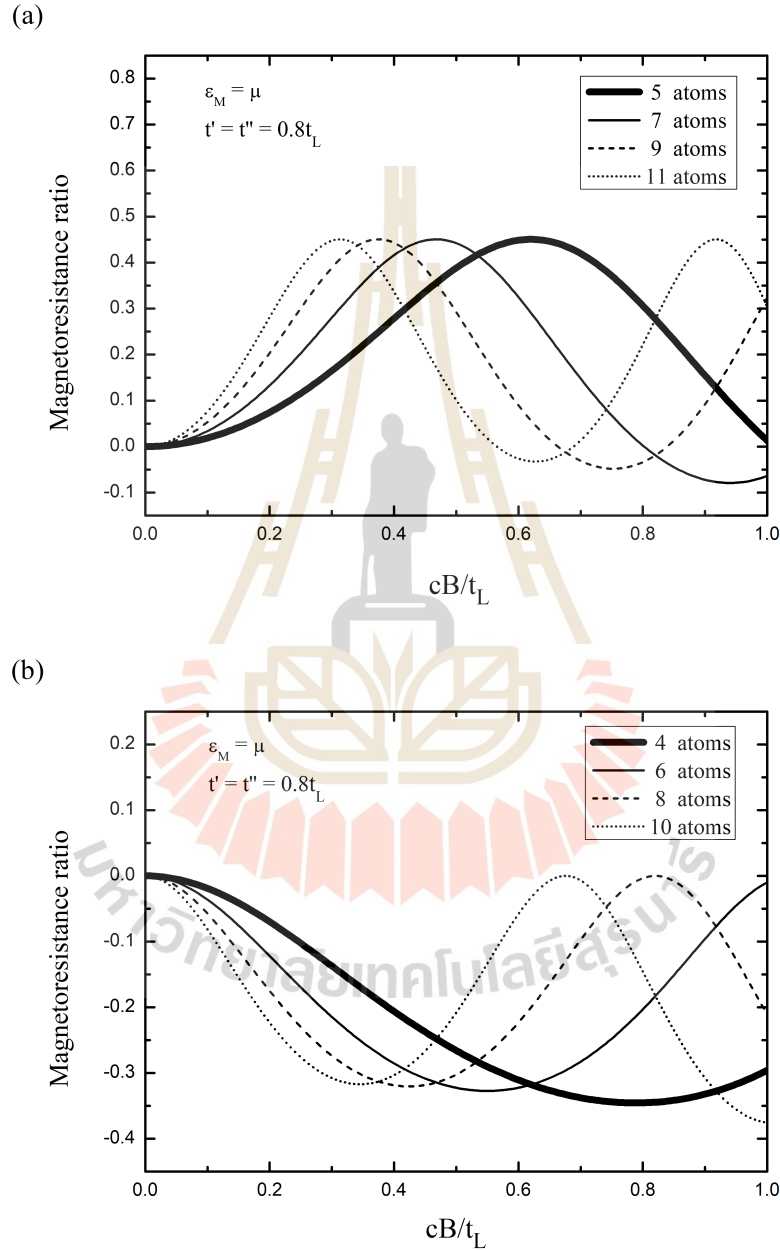


Figure 4.3 The magnetoresistance ratio as a function of magnetic field with various thicknesses of the metal layers (a) $N_M = 5, 7, 9$ and 11 atoms and (b) $N_M = 4, 6, 8$ and 10 atoms.

We take the hopping energy of an electron at the two interfaces to be $t' = t'' = 0.8t_L$ and we use a metallic spacer to have half-filling band. As can be seen in Figure 4.3, the odd and even numbers N_M give different results of the plots. For all odd numbers, the magnetoresistance ratio are increased with the magnitude of the field, reach maxima at some critical value, which is decreased with the number of the atoms N_M , and are then decreased with the magnitude of the field. When the number of the atoms are even the magnetoresistance ratios are negative and decreased with the magnitude of the field. The negative magnetoresistance ratio is surprising; it has not been observed in experiments.

For example, we will make a substitution of the related parameters in order to set the thickness to be in the range of 0.9 to 1.8 nm (Binasch et al., 1989; Grünberg et al., 1986) which is consistent with most experiments. We plot the magnetoresistance as a function of a metal thickness with the magnetic field at 1.0 and 1.5 times t_L which is shown in Figure 4.4. We also take the hopping energy of an electron at the interfaces ($t' = t''$) to be $0.3t_L$. We show the magnetoresistance as a function of the thickness of metal as the energy at zero. We found that the magnetoresistances are the negative and positive value which these magnetoresistances depend on the number atomic of the metal layer. Also, we represent the negative magnetoresistance ratio when the thickness of the metal layer is even number.

For experimental work, the magnetoresistance ratio of Fe/Cr multilayers as a function of Cr thickness is represented (Piroux et al., 1994; Fert and Piroux, 1999). They found the oscillation of magnetoresistance with the thickness of Cr which is measured at low temperature. The magnetoresistance effect is periodic in nature and it varies with the thickness Cr which is shown in Figure 4.5(a). For our model, we take that the spacer is Cr metallic layer as the bandwidth of Cr

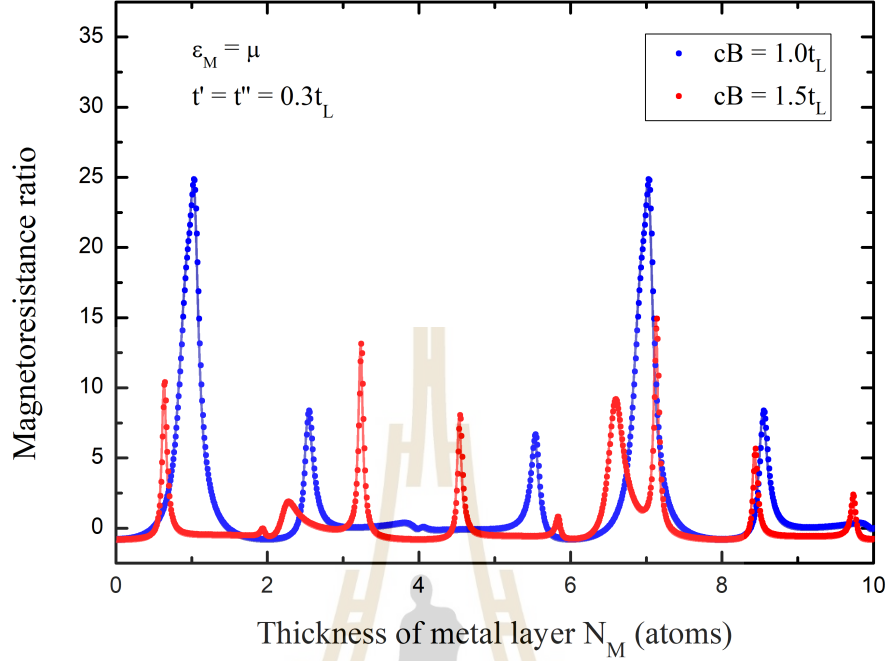


Figure 4.4 The magnetoresistance of Fe/metal/Fe junction plotted as a function of the thickness of metal with the magnetic field at 1.0 and 1.5 times t_L .

is higher more than Fe and we obtain the hopping energy at the metal in 2.5 eV (Soulaïrol et al., 2010). We take the hopping energy of the metal region to be $2.5t_L$. We plot the magnetoresistance as a function of thickness N_M with $\varepsilon_M = \mu$ and a small magnetic field is $1.5t_L$ which is shown in Figure 4.5(b). We can obtain that both results of the magnetoresistance ratio are oscillation behavior. For our model, the negative magnetoresistance depends on the even number. From oscillation behavior, we can explain by the Ruderman-Kittel-Kasuya-Yosida (RKKY) interaction which is the interaction between the spin electron of two ferromagnetic electrodes. The RKKY interaction is the electron through a spacer as nonmagnetic and exchange coupling between magnetic moments in ferromagnetic metals.

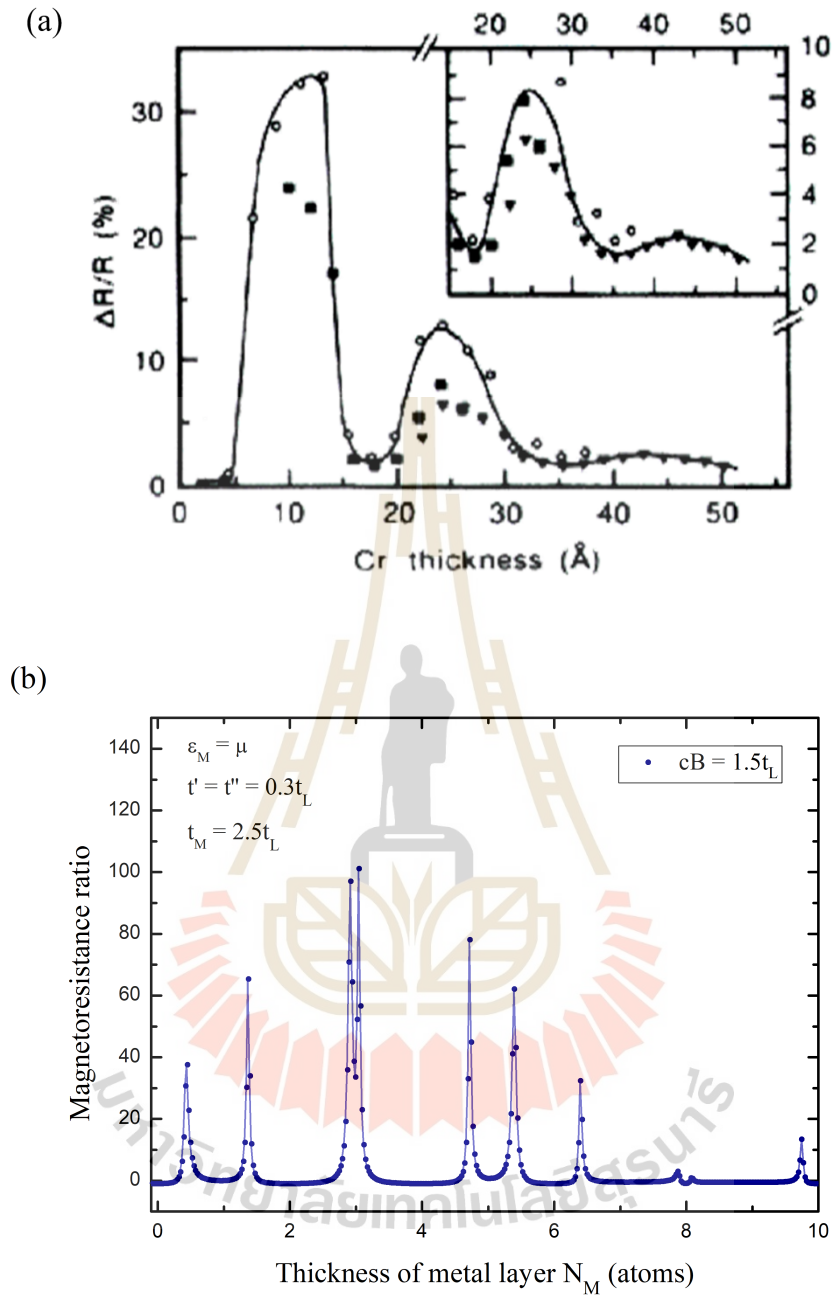
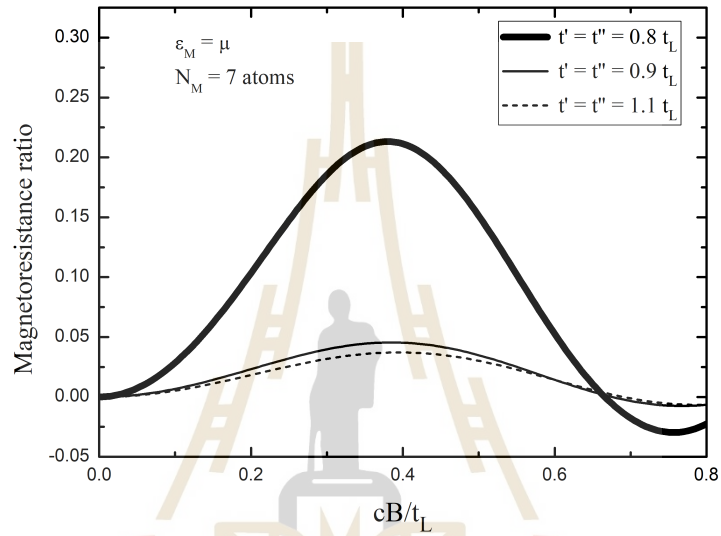


Figure 4.5 The magnetoresistance of Fe/Cr/Fe junction plotted as a function of the thickness of Cr. Also shown are the oscillation magnetoresistance (a) in at low temperature of experimental work and (b) our model, when $\epsilon_M = \mu$ and $cB = 1.5t_L$.

4.1.3 The effect of the hopping energy between two atoms of two interfaces on magnetoresistance

We plot the magnetoresistance ratio as a function magnetic field with the barrier potential for $t' = t''$ and $t' \neq t''$ which shows in Figure 4.6.

(a)



(b)

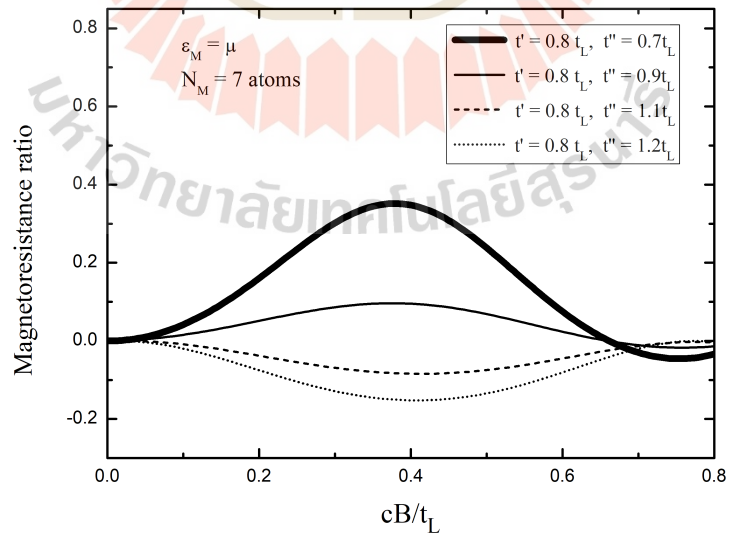


Figure 4.6 Show the result of magnetoresistance as a function of external magnetic field (cB/t_L) with (a) $t' = t''$ and (b) $t' \neq t''$.

For the $t' = t''$, We show the result of magnetoresistance as a magnetic field with $t' = t'' = 0.8, 0.9$ and 1.1 times t_L . The magnetoresistance ratio is increased when the hopping energy between the interfaces is decreased as which means the state of the electron has good scattering through the interface as a low potential barrier. For $t' \neq t''$, we found that the magnetoresistance is the negative value when the hopping energy at the interface as t'' is increased. We obtain that the magnetoresistance is same value when we alternate the hopping energy between two atoms of two interfaces.

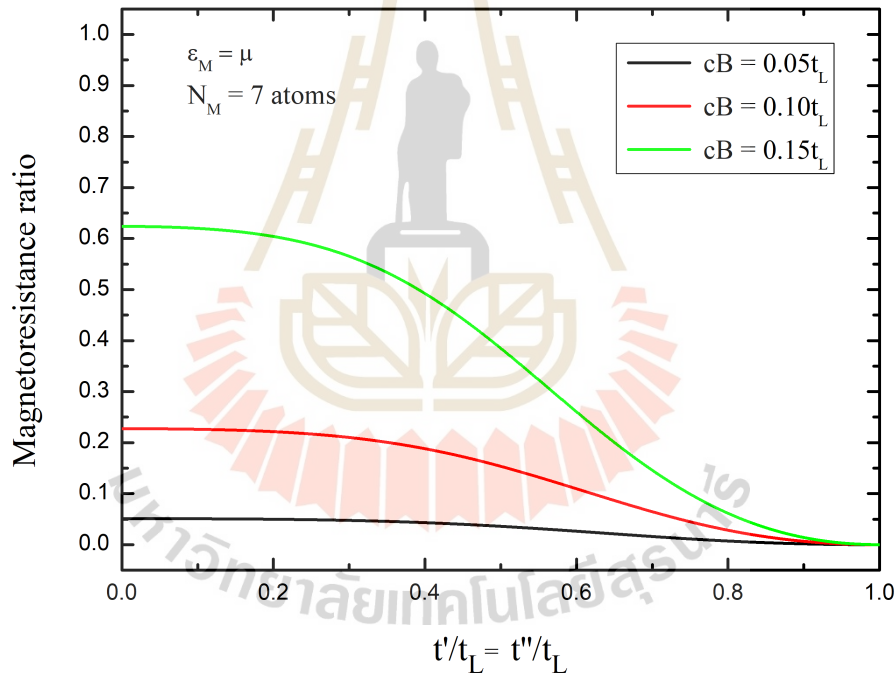


Figure 4.7 The result of magnetoresistance as a function of the hopping energy between two atoms of two interfaces with the magnetic field.

In Figure 4.7, we plot of the magnetoresistance as the hopping energy between two atoms of two interfaces ($t' = t''$) with the thickness as 7 atoms. We take the magnetic field $cB = 0.05t_L, 0.1t_L$ and $0.15t_L$. We found the large magnetore-

sistance when $t' = t''$ is a small value. The magnetoresistance becomes saturated by varying $t' = t''$. The magnetoresistance is decreased when the hopping energy of the interfaces has increased until the magnetoresistance is in the saturation value and when we increase the magnetic field (cB) then the magnetoresistance is quite high value. Thus, we can see that this hopping energy significantly affects the magnetoresistance and the quality of the interface is good with the metallic spacer when we obtain the negative magnetoresistance ratio.

4.2 Ferromagnetic metal/Insulating/Ferromagnet metal Structure

4.2.1 Transmission probability for insulating

From the previous results, the transmission probability as a function of energy is high value when we applied $\varepsilon_M - \mu$ equal to zero then the spacer is metal. The spacer of on-site energy between two ferromagnetic electrodes ($\varepsilon_M - \mu$) is large enough which the spacer is the barrier height (band gap) of insulating. For insulating spacer, we show the transmission probability as a function of the energy (or voltage) for various $\varepsilon_M - \mu = 2.01, 2.25$ and 2.5 times t_L . We also take the hopping energy of an electron at the interfaces ($t' = t''$) to be $1.5t_L$.

In Figure 4.8, we represent the electron scattering on high barrier when we take $\varepsilon_M - \mu > 2t_L$. We obtain the transmission probabilities are the less value at the energy equal to zero bias which means the spacer to be insulating. For the energy at zero bias voltage, the insulating spacer is a high barrier (band gap) which the electron scattering is weakly on the junction. Thus, the transmission probability depends on the band gap of the insulating layer. From preview 4.1.1, we know that the spacer can be adjusted by the on-site energy parameter ($\varepsilon_M - \mu$)

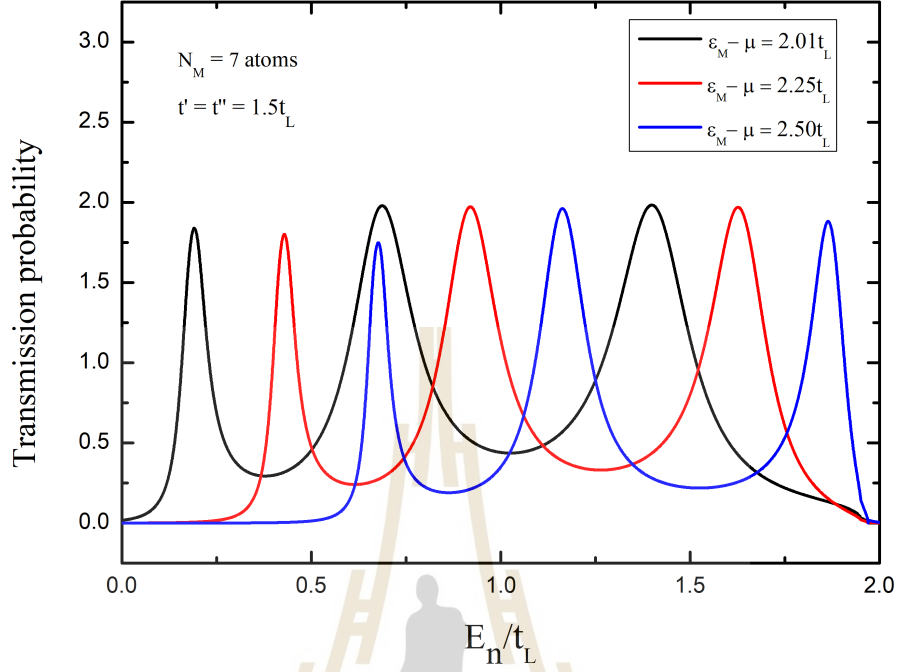


Figure 4.8 The transmission probability as a function of the energy (E_n/t_L) with thickness of the insulating layer as 7 atoms.

of the middle region, to make the spacer becomes an either metallic or insulating layer. We can analyze from the results that the metal can become insulating when the $\varepsilon_M - \mu$ should be greater than $2t_L$. We found that the transmission probabilities show oscillation behavior.

4.2.2 The effect of insulating thickness on magnetoresistance

The results of the magnetoresistance as a function of the external magnetic field with $\varepsilon_M - \mu = 2.01t_L$ and $t' = t''$ to be $0.8t_L$ shown in Figure 4.9. We obtain the magnetoresistance ratio is increased by varying the magnetic field and the maximum magnetoresistances ratio value as a critical magnetic field (cB_c)

are decreased when we increase the number of thicknesses. For insulating, the magnetoresistance ratios are the positive value when the number of thickness is even number in Figure 4.9(b).

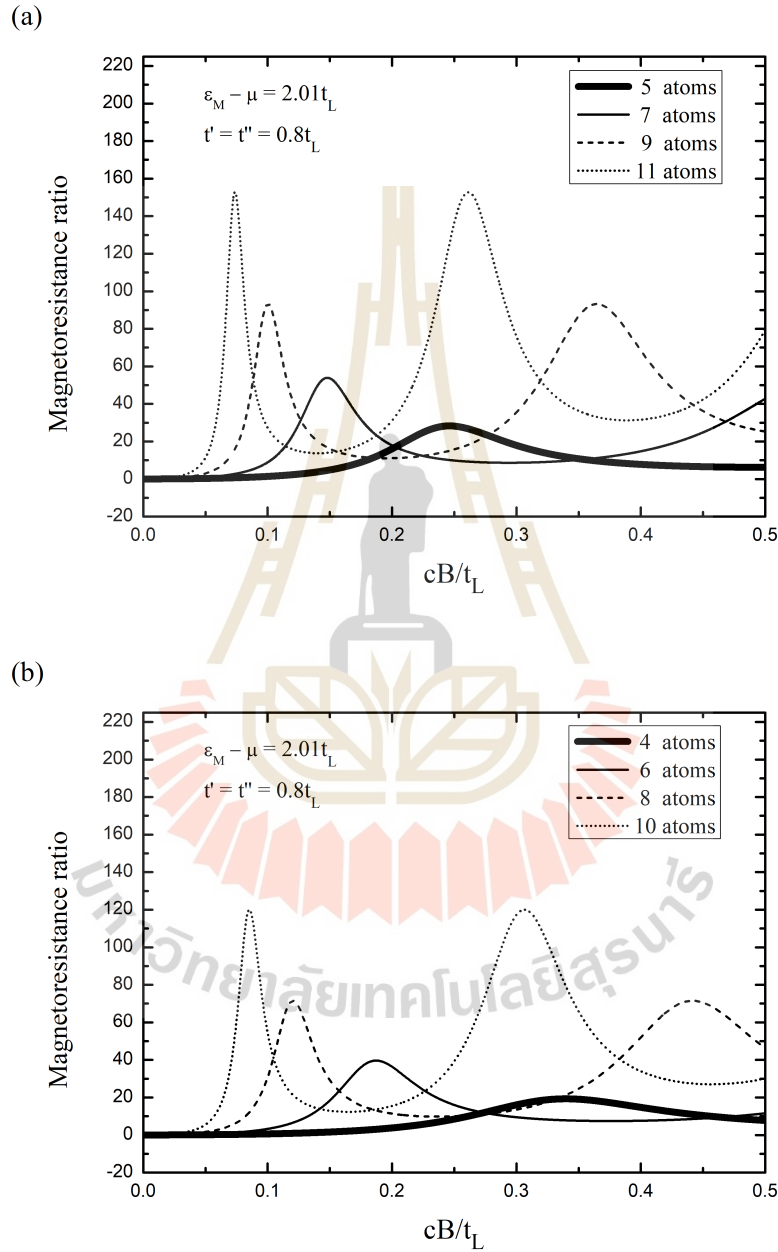


Figure 4.9 The magnetoresistance ratio as a function of magnetic field with thickness of the insulating layer for various thickness (a) $N_M = 5, 7, 9$ and 11 atoms and (b) $N_M = 4, 6, 8$ and 10 atoms.

In addition, we substitute the related parameters in order to set the thickness to be in the range of 1.0 nm to 1.6 nm, which is around 3 to 8 the number of atoms with most experiments. For example, we plot the magnetoresistance as a function of the insulating thickness with the magnetic field at 0.1 and 0.15 times t_L which is shown in Figure 4.10.

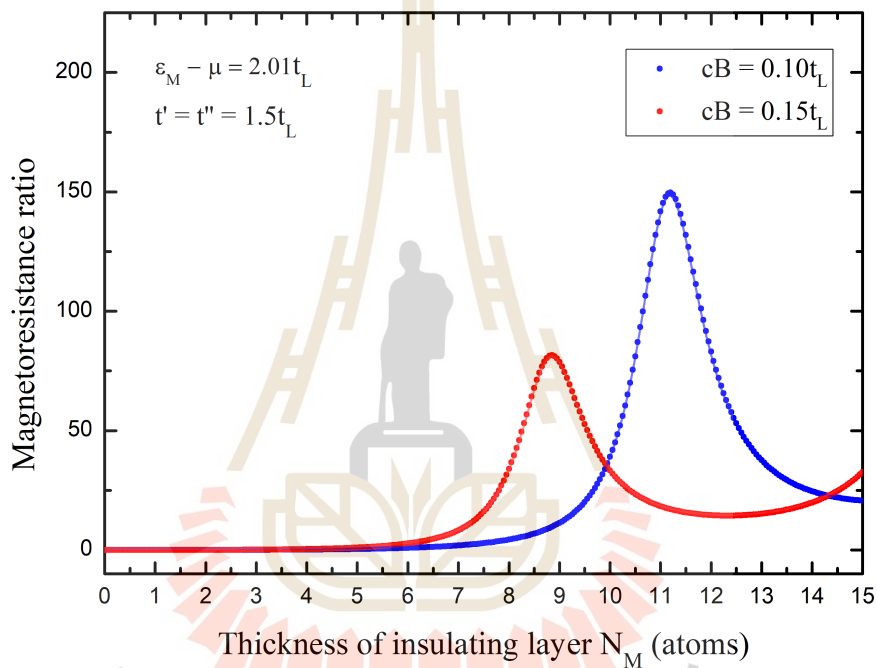


Figure 4.10 The magnetoresistance ratio as a function of thickness of the insulating layer for as $cB = 0.1t_L$ and $0.15t_L$ and $\varepsilon_M - \mu = 2.01t_L$.

We found that the maximum value of an external magnetic field is shifted by the effect of the insulating layer thickness is increased. When the magnetic field is increased, the magnetoresistances will have an increase in the maximum value, one of which tends to vibrate like the previous value.

However, the experimental work for investigating about the effect of the thickness of insulating on tunneling magnetoresistance in Fe/MgO/Fe junction

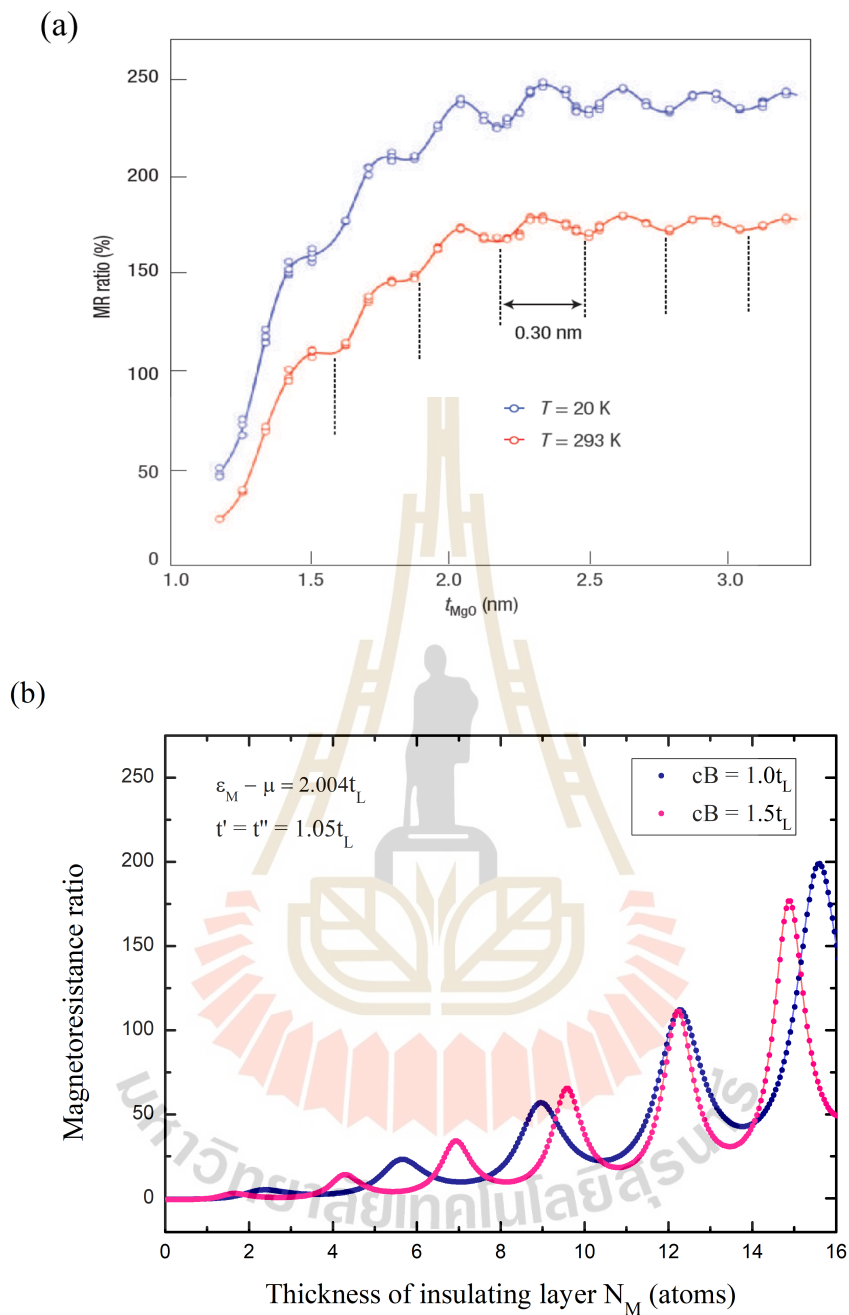


Figure 4.11 The magnetoresistance of Fe(001)/MgO (001)/Fe(001) junction plotted as a function of the thickness of MgO (t_{MgO}). Also shown are (a) the oscillation in 1.2 to 3.2 nm at temperature 293 K and 20 K and (b) the magnetoresistance as a function of the number of atoms, when $\varepsilon_{\text{M}} - \mu = 2.004t_{\text{L}}$.

is shown in Figure 4.11(a). We present the results of our model to compare with experimental results of the tunnel magnetic junction which is Fe/MgO/Fe junction at the barrier height (band gap) of the junction is considerably lower than the values in the literature part. The plots of the magnetoresistance as a function of the number of atoms as $cB = 1.0t_L$ and $1.5t_L$ with $\varepsilon_M - \mu = 2.004t_L$ shown in Figure 4.11(b).

For the experimental work, Yuasa and co-workers (Yuasa et al., 2005) studied Fe(001)/MgO(001)/Fe(001) junctions with varying MgO-layer thickness between 1.2 nm and 3.2 nm. They found that the tunneling magnetoresistance can reach up to 180% at 293 K and 247% at 20 K. This shows the tunneling magnetoresistance oscillations which this shows the oscillation period (0.30 nm). For our model predicts that the magnetoresistance is increased with the insulating layer thickness which is also the tunneling magnetoresistance oscillations and it is the oscillation period around 2 atoms. We can explain the both of oscillation results that the thickness of the insulating layer was too big for the RKKY interaction between the two ferromagnetic metals which this interaction depends on the thickness of the adjacent ferromagnetic layer.

4.2.3 The effect of the band gap on magnetoresistance

We show the transmission probability as a function of the on-site energy of spacer in Figure 4.12 for the small magnetic field as parameter $cB = 0.01t_L$ and $0.05t_L$ and the hopping energy of the electron at the interfaces ($t' = t''$) to be $0.8t_L$.

We consider two regions of these results which consist as large and small probability regions. For large transmission probability region, that means the metallic spacer because the spacer is non-barrier height as $\varepsilon_M - \mu$ parameter less

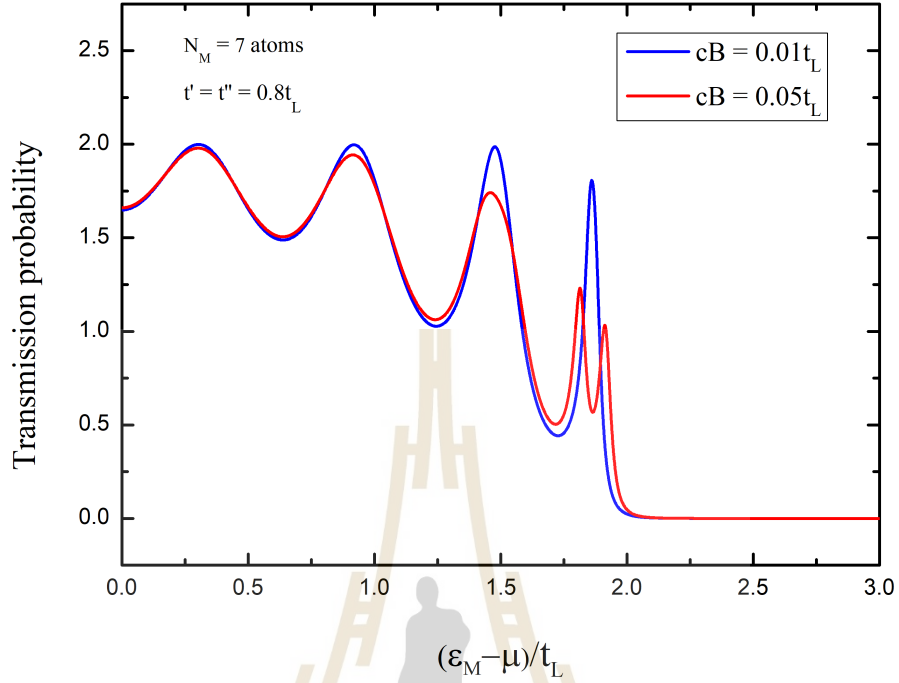


Figure 4.12 The transmission probability as the on-site energy of the spacer at the thickness layer as 7 atoms.

then $2t_L$ which it is strongly the electron can be scattered in metallic regime. For small transmission value, the transmission probability is low value come to zero at $\epsilon_M - \mu$ larger than $2t_L$ which the region is the insulating spacer. We will explain more specifically for the insulating with the low transmission probability. When the on-site energy of insulating regime is a large value, the transmission probability is zero value that means the electrons do have to scatter thought the barrier which the insulating barrier is high (large band gap). Thus, the electron can be scattered in barrier potential of a spacer which the height barrier of insulating depends on band gap. Next, we will show the result of the magnetoresistance as a function of band gap energy (Δ/t_L) in order to determine that the band gap should be in the range of energy. We take the small magnetic field cB equal to 0.17 and 0.23 times

t_L in Figure 4.13. We found that the magnetoresistance ratio is decreasing with band gap which shows the maximum of the magnetoresistance for some band gap. Thus, in our model can consider that each insulating has some band gap make to good insulating because it exhibits a high magnetoresistance ratio.

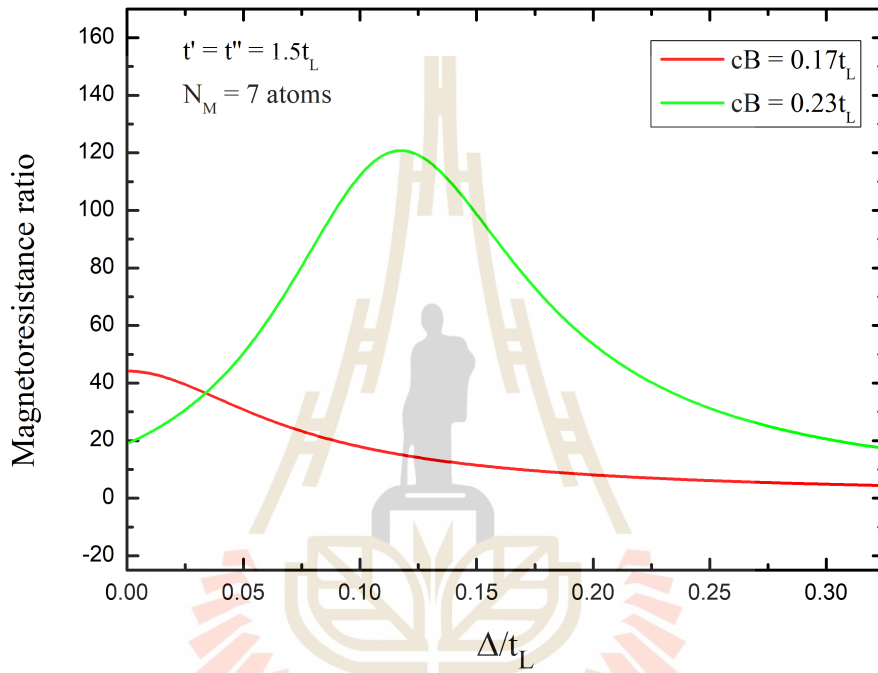


Figure 4.13 The result of the magnetoresistance as a function of band gap energy (Δ/t_L) at the thickness layer as 7 atoms.

4.2.4 The effect of the hopping energy between two atoms of two interfaces on magnetoresistance

Now, we show the effect of the barrier potential of interfaces on the magnetoresistance in a small applied field. We consider the barrier potential for (a) $t' = t''$ and (b) $t' \neq t''$ which shows in Figure 4.14. For $t' = t''$, when we increase the hopping energy as interfaces, the magnetoresistance value will decrease. For

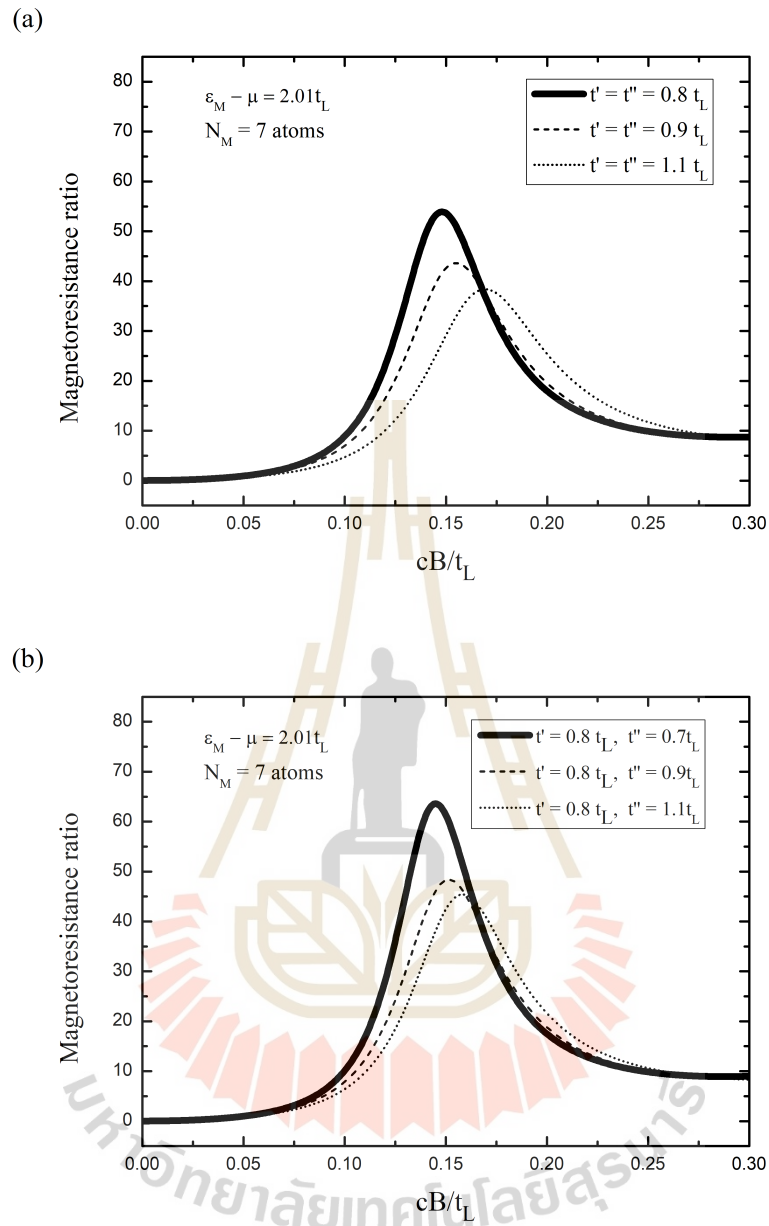


Figure 4.14 Show the result of magnetoresistance a function of external magnetic field (cB/t_L) with (a) $t' = t''$ and (b) $t' \neq t''$.

$t' \neq t''$, we found that the magnetoresistance value decreases with increasing the t' parameter. However, both results of magnetoresistance have not changed much trend.

Also, we plot of the magnetoresistance as the hopping energy between two

atoms of two interfaces with the magnetic field which shows in Figure 4.15. We found that the magnetoresistance depends on the hopping energy of the interfaces, the magnetoresistances ratio will have a decrease in the saturation value which tends to show like the metallic spacer in the previous value.

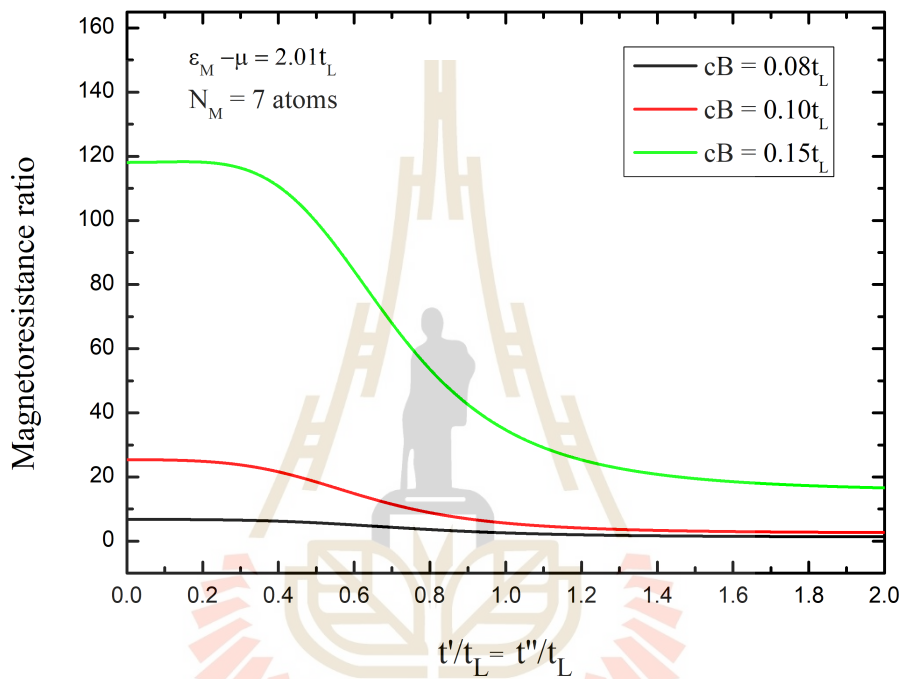


Figure 4.15 The result of magnetoresistance as a function of the hopping energy between two atoms of two interfaces with an external magnetic field.

CHAPTER V

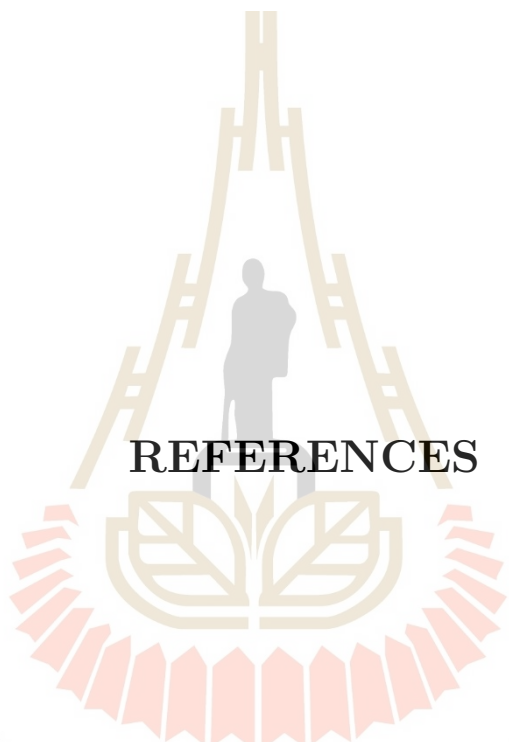
CONCLUSION

In this work, we investigate the magnetoresistance of the ferromagnetic metal/spacer/ferromagnetic metal junction based on quantum principles to calculate the theoretical values under a small external magnetic field. We use a tight binding model for the tunneling magnetoresistance calculation of our junction devices. This consists of two ferromagnetic layers separated by the spacer barrier which is metal and the insulating layer. We take into account many factors that may affect the magnetoresistance, such as the thickness of the spacer layer (N_M), strength of the barrier ($\varepsilon_M - \mu$), and the effect of the hopping energy of electron between two atoms in two interfaces (t' and t'').

First of all, we present the results of the ferromagnetic metal/metal/ferromagnetic metal. We show the results of transmission probability for the definition of the spacer to be a metal. For metallic spacer, the magnetoresistance ratio shows oscillation behavior depends on the small external magnetic field (cB) and we found the negative of the magnetoresistances which these magnetoresistances depend on the number atomic of the metal layer which is even. The magnetoresistance ratio shows oscillating behavior as a function of thickness. Thus, the magnetoresistances depend on the number atomic of the metal layer. For the hopping energy of electron between two atoms of two interfaces, we show that the quality of the two ferromagnet and metal interfaces has a huge effect on magnetoresistance which is good with the metallic spacer when we obtain the negative magnetoresistance ratio.

The second case, we also show the results of transmission probability for the definition of the spacer to be insulating. For the ferromagnetic metal/insulating/ferromagnetic metal junctions have the result of magnetoresistance looks like the junction of the ferromagnetic metal/metal/ferromagnetic metal such as the effect of an external magnetic field (cB) and the thickness (N_M) on the magnetoresistance which shows oscillating behavior.

When we consider the effect of the barrier height (band gap) of insulating, our model predicts that the magnetoresistance is increased with the strength of the barrier of insulator which the magnitude of magnetoresistance qualitatively agrees with the experiment. Moreover, it suggests that certain values of the barrier potential, or the band gap of the insulating layer, give the high magnetoresistance ratio. For the effect of the thickness of the insulating layer, the magnetoresistance for the thickness of insulating is shifted to increase when the insulating layer thickness is increased. In we work show that our theoretical model predicts the right trend of the magnetoresistance on the thickness of the insulating layer, it predicts the tunneling magnetoresistance value. Also in our model, certain thicknesses give the maximum magnetoresistance, which is consistent with experimental work.



REFERENCES

มหาวิทยาลัยเทคโนโลยีสุรนารี

REFERENCES

- Agapito, L. A., Ismail-Beigi, S., Curtarolo, S., Fornari, M., and Nardelli, M. B. (2016). Accurate tight-binding hamiltonian matrices from ab initio calculations: Minimal basis sets. **Phys. Rev. B.** 93: 035104.
- Awschalom, D. D. and Flatté, M. E. (2007). Challenges for semiconductor spintronics. **Nat. Phys.** 3: 153–159.
- Baibich, M. N., Broto, J. M., Fert, A., Van Dau, F. N., Petroff, F., Etienne, P., Creuzet, G., Friederich, A., and Chazelas, J. (1988). Giant magnetoresistance of (001)Fe/(001)Cr magnetic superlattices. **Phys. Rev. Lett.** 61: 2472–2475.
- Bardeen, J. (1961). Tunnelling from a many-particle point of view. **Phys. Rev. Lett.** 6: 57–59.
- Binasch, G., Grünberg, P., Saurenbach, F., and Zinn, W. (1989). Enhanced magnetoresistance in layered magnetic structures with antiferromagnetic interlayer exchange. **Phys. Rev. B.** 39: 4828–4830.
- Butler, W. H., Zhang, X.-G., Schulthess, T. C., and MacLaren, J. M. (2001). Spin-dependent tunneling conductance of Fe|MgO|Fe sandwiches. **Phys. Rev. B.** 63: 054416.
- Chappert, C., F. A. and Van Dau, F. (2007). The emergence of spin electronics in data storage. **Nat. Mater.** 6: 813–823.
- Dexin Wang, Nordman, C., Daughton, J. M., Zhenghong Qian, and Fink, J. (2004). 70% TMR at room temperature for SDT sandwich junctions

- with CoFeB as free and reference layers. **IEEE Trans. Magn.** 40(4): 2269–2271.
- Fert, A. and Campbell, I. A. (1968). Two-current conduction in nickel. **Phys. Rev. Lett.** 21: 1190–1192.
- Fert, A. and Piraux, L. (1999). Magnetic nanowires. **J. Magn. Magn. Mater.** 200(1): 338–358.
- Finnis, M. (2010). **Interatomic Forces in Condensed Matter.** Oxford.
- Goringe, C. M., Bowler, D. R., and Hernández, E. (1997). Tight-binding modelling of materials. **Rep. Prog. Phys.** 60(12): 1447–1512.
- Grollier, J., Cros, V., Hamzic, A., George, J. M., Jaffrès, H., Fert, A., Faini, G., Ben Youssef, J., and Legall, H. (2001). Spin-polarized current induced switching in Co/Cu/Co pillars. **Appl. Phys. Lett.** 78(23): 3663–3665.
- Grollier, J., Cros, V., Jaffrès, H., Hamzic, A., George, J. M., Faini, G., Ben Youssef, J., Le Gall, H., and Fert, A. (2003). Field dependence of magnetization reversal by spin transfer. **Phys. Rev. B.** 67: 174402.
- Grünberg, P., Schreiber, R., Pang, Y., Brodsky, M. B., and Sowers, H. (1986). Layered magnetic structures: Evidence for antiferromagnetic coupling of Fe layers across Cr interlayers. **Phys. Rev. Lett.** 57: 2442–2445.
- Harrison, W. (1989). **Electronic structure and the properties of solids: the physics of the chemical bond.** Dover Publications.
- Haydock, R. (1980). The recursive solution of the schrödinger equation. **Comput. Phys. Commun.** 20(1): 11–16.

- Heine, V. (1980). **Solid State Physics: Electronic Structure from the Point of View of the Local Atomic Environment**. Academic Press.
- Horsfield, A. P. and Bratkovsky, A. M. (1999). Ab initio tight binding. **J. Phys. Condens. Matter**. 12(2): R1–R24.
- Julliere, M. (1975). Tunneling between ferromagnetic films. **Phys. Lett.** 54(3): 225–226.
- Kasuya, T. (1956). A Theory of Metallic Ferro- and Antiferromagnetism on Zener's Model. **Prog. Theor. Exp. Phys.** 16(1): 45–57.
- Katine, J. A., Albert, F. J., Buhrman, R. A., Myers, E. B., and Ralph, D. C. (2000). Current-driven magnetization reversal and spin-wave excitations in Co /Cu /Co pillars. **Phys. Rev. Lett.** 84: 3149–3152.
- Khomyakov, P. A., Giovannetti, G., Rusu, P. C., Brocks, G., van den Brink, J., and Kelly, P. J. (2009). First-principles study of the interaction and charge transfer between graphene and metals. **Phys. Rev. B**. 79: 195425.
- Kohn, W. (1999). Nobel lecture: Electronic structure of matter—wave functions and density functionals. **Rev. Mod. Phys.** 71: 1253–1266.
- LeClair, P., Ha, J. K., Swagten, H. J. M., Kohlhepp, J. T., van de Vin, C. H., and de Jonge, W. J. M. (2002). Large magnetoresistance using hybrid spin filter devices. **Appl. Phys. Lett.** 80(4): 625–627.
- Mathon, J. (1997). Tight-binding theory of tunneling giant magnetoresistance. **Phys. Rev. B**. 56: 11810–11819.
- Mathon, J. and Umerski, A. (2001). Theory of tunneling magnetoresistance of an epitaxial Fe/MgO/Fe(001) junction. **Phys. Rev. B**. 63: 220403.

- Matsumoto, R., Fukushima, A., Yakushiji, K., Yakata, S., Nagahama, T., Kubota, H., Katayama, T., Suzuki, Y., Ando, K., Yuasa, S., Georges, B., Cros, V., Grollier, J., and Fert, A. (2009). Spin-torque-induced switching and precession in fully epitaxial Fe/MgO/Fe magnetic tunnel junctions. **Phys. Rev. B.** 80: 174405.
- Miura, Y., Muramoto, S., Abe, K., and Shirai, M. (2012). First-principles study of tunneling magnetoresistance in Fe/MgAl₂O₄/Fe(001) magnetic tunnel junctions. **Phys. Rev. B.** 86: 024426.
- Moodera, J. S., Kinder, L. R., Wong, T. M., and Meservey, R. (1995). Large magnetoresistance at room temperature in ferromagnetic thin film tunnel junctions. **Phys. Rev. Lett.** 74: 3273–3276.
- Mosca, D., Petroff, F., Fert, A., Schroeder, P., Pratt, W., and Laloe, R. (1991). Oscillatory interlayer coupling and giant magnetoresistance in Co/Cu multilayers. **J. Magn. Magn. Mater.** 94(1): L1–L5.
- Parkin, S. S. P., Kaiser, C., Panchula, A., Rice, P. M., Hughes, B., Samant, M., and Yang, S.-H. (2004). Giant tunnelling magnetoresistance at room temperature with MgO (100) tunnel barriers. **Nat. Mater.** 3: 862–867.
- Parkin, S. S. P., More, N., and Roche, K. P. (1990). Oscillations in exchange coupling and magnetoresistance in metallic superlattice structures: Co/Ru, Co/Cr, and Fe/Cr. **Phys. Rev. Lett.** 64: 2304–2307.
- Paxton, A. T. and Kohanoff, J. J. (2011). A tight binding model for water. **J. Chem. Phys.** 134(4): 044130.
- Piroux, L., George, J. M., Despres, J. F., Leroy, C., Ferain, E., Legras, R., Ounad-

- jela, K., and Fert, A. (1994). Giant magnetoresistance in magnetic multilayered nanowires. **Appl. Phys. Lett.** 65(19): 2484–2486.
- Qi, Y., Xing, D. Y., and Dong, J. (1998). Relation between julliere and slonczewski models of tunneling magnetoresistance. **J. Phys. Condens. Matter.** 58: 2783–2787.
- Ruderman, M. A. and Kittel, C. (1954). Indirect exchange coupling of nuclear magnetic moments by conduction electrons. **Phys. Rev.** 96: 99–102.
- Slater, J. C. and Koster, G. F. (1954). Simplified LCAO method for the periodic potential problem. **Phys. Rev.** 94: 1498–1524.
- Slonczewski, J. C. (1989). Conductance and exchange coupling of two ferromagnets separated by a tunneling barrier. **Phys. Rev. B.** 39: 6995–7002.
- Soulaïrol, R., Fu, C.-C., and Barreateau, C. (2010). Structure and magnetism of bulk Fe and Cr: from plane waves to LCAO methods. **J. Phys.: Condens. Matter.** 22(29): 295502.
- Sutton, A. (1993). **Electronic Structure of Materials.** Clarendon Press.
- van 't Erve, O. M. J., Kioseoglou, G., Hanbicki, A. T., Li, C. H., and Jonker, B. T. (2006). Remanent electrical spin injection from Fe into AlGaAs/GaAs light emitting diodes. **Appl. Phys. Lett.** 89(7): 072505.
- Waldron, D., Timoshevskii, V., Hu, Y., Xia, K., and Guo, H. (2006). First principles modeling of tunnel magnetoresistance of Fe/MgO/Fe trilayers. **Phys. Rev. Lett.** 97: 226802.
- Walter, A. L., Riley, J. D., and Rader, O. (2010). Theoretical limitations to the

determination of bandwidth and electron mass renormalization: the case of ferromagnetic iron. **New J. Phys.** 12(1): 013007.

Yamasaki, A. and Fujiwara, T. (2002). Electronic structure of the MO oxides (M=Mg, Ca, Ti, V) in the GW approximation. **Phys. Rev. B.** 66: 245108.

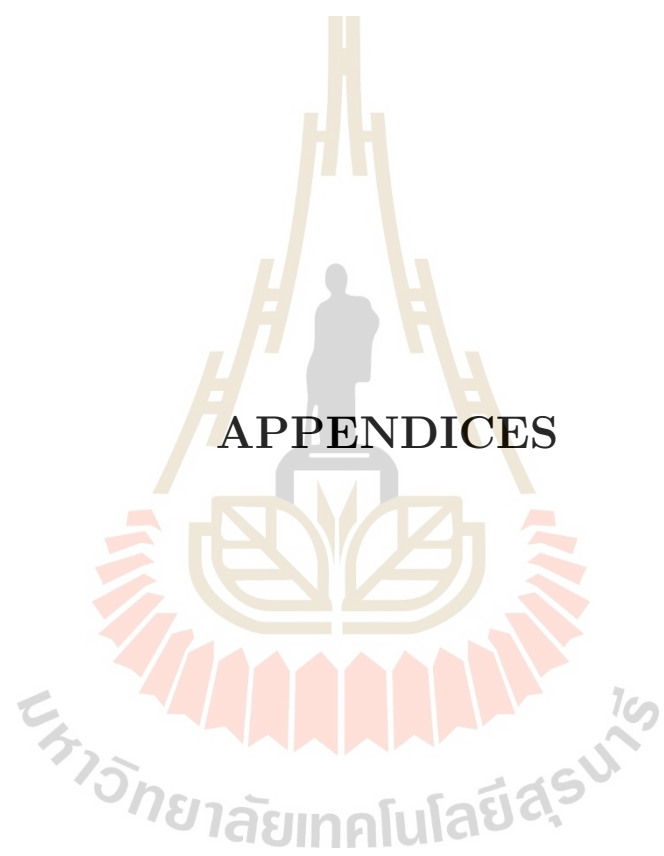
Yosida, K. (1957). Magnetic properties of Cu-Mn alloys. **Phys. Rev.** 106: 893–898.

Yuasa, S., Nagahama, T., Fukushima, A., Suzuki, Y., and Ando, K. (2005). Giant room-temperature magnetoresistance in single-crystal Fe/MgO/Fe magnetic tunnel junctions. **Nat. Mater.** 3: 868–871.

Yuasa, S., Sato, T., Tamura, E., Suzuki, Y., Yamamori, H., Ando, K., and Katayama, T. (2000). Magnetic tunnel junctions with single-crystal electrodes: A crystal anisotropy of tunnel magneto-resistance. **EPL.** 52(3): 344–350.

Zettili, N. (2009). **Quantum Mechanics: Concepts and Applications.** 2nd Edition. John Wiley and Sons.

Zhu, M., Chong, H., Vu, Q. B., Vo, T., Brooks, R., Stamper, H., Bennett, S., and Piccirillo, J. (2015). A CoFeB/MgO/CoFeB perpendicular magnetic tunnel junction coupled to an in-plane exchange-biased magnetic layer. **Appl. Phys. Lett.** 106(21): 212405.



APPENDICES

APPENDIX A

WOLFRAM MATHEMATICA PROGRAM

CALCULATION RELATED TO

METAL/SPACER/METAL JUNCTION

Below, this is Wolfram Mathematica program calculation, we use in this thesis after the program and we present the results of transmission probability as a function of the energy.

We present all our parameters of the system in the list as

- The energy (Voltage bias) is $En = \frac{E}{t_L}$.
- The on-site energy of each regions are $e1 = \frac{(\epsilon_L - \mu)}{t_L}$, $e2 = \frac{(\epsilon_R - \mu)}{t_L}$ and $e0 = \frac{(\epsilon_M - \mu)}{t_L}$.
- The hopping energies are $t0 = \frac{t_M}{t_L}$, $t2 = \frac{t_R}{t_L}$, $tp = \frac{t'}{t_L}$ and $tdp = \frac{t''}{t_L}$.
- Thickness (Spacer) is $m \equiv$ Number of atoms.

Code:

```
ClearAll["Global*"]
```

```
Off[General::spell]; Off[LinearSolve::luc]; On[General::stop];
```

```
(*Wave vector*)
```

```
k1[En_, e1_] := ArcCos[(e1 - En)/2]
```

```
q[En_, t0_, e0_] := ArcCos [  $\frac{e0*t0 - En}{2*t0}$  ]
```

```
k2[En_, t2_, e2_] := ArcCos [  $\frac{e2*t2 - En}{2*t2}$  ]
```

(*Matrix*)

$$M11:=1$$

$$M12[tp_]:= - tp$$

$$M13[tp_]:= - tp$$

$$M14:=0$$

$$M21[En_, tp_, t0_, e1_]:= - \frac{tp}{t0} * e^{i*k1[En,e1]}$$

$$M22[En_, t0_, e0_]:= e^{-i*q[En,t0,e0]}$$

$$M23[En_, t0_, e0_]:= e^{i*q[En,t0,e0]}$$

$$M24:=0$$

$$M31:=0;$$

$$M32[En_, t0_, e0_, m_]:= e^{i*q[En,t0,e0]*(m+1)}$$

$$M33[En_, t0_, e0_, m_]:= e^{-i*q[En,t0,e0]*(m+1)}$$

$$M34[En_, tdp_, t0_, t2_, e2_, m_]:= - \frac{tdp}{t0} * e^{i*k2[En,t2,e2]*(m+1)}$$

$$M41:=0$$

$$M42[En_, tdp_, t2_, t0_, e0_, m_]:= - \frac{tdp}{t2} * e^{i*q[En,t0,e0]*m}$$

$$M43[En_, tdp_, t2_, t0_, e0_, m_]:= - \frac{tdp}{t2} * e^{-i*q[En,t0,e0]*m}$$

$$M44[En_, t2_, e2_, m_]:= e^{i*k2[En,t2,e2]*m}$$

$$M[En_, t0_, t2_, tp_, tdp_, e0_, e1_, e2_, m_]:=$$

$$\begin{pmatrix} M11 & M12[tp] & M13[tp] & M14 \\ M21[En, tp, t0, e1] & M22[En, t0, e0] & M23[En, t0, e0] & M24 \\ M31 & M32[En, t0, e0, m] & M33[En, t0, e0, m] & M34[En, tdp, t0, t2, e2, m] \\ M41 & M42[En, tdp, t2, t0, e0, m] & M43[En, tdp, t2, t0, e0, m] & M44[En, t2, e2, m] \end{pmatrix};$$

$$A[En_, tp_, t0_, e1_]:=$$

$$\begin{pmatrix} -1 \\ \frac{tp}{t0} * e^{-i*k1[En,e1]} \\ 0 \\ 0 \end{pmatrix};$$

$$\text{Answer1}[En_, t0_, t2_, tp_, tdp_, e0_, e1_, e2_, m_]:=$$

$$\text{LinearSolve}[M[En, t0, t2, tp, tdp, e0, e1, e2, m], A[En, tp, t0, e1]]$$

(*Solve the amplitudes*)

$\gamma[\text{En_}, \text{t0_}, \text{t2_}, \text{tp_}, \text{tdp_}, \text{e0_}, \text{e1_}, \text{e2_}, \text{m_}] :=$

First[Answer1[En, t0, t2, tp, tdp, e0, e1, e2, m][[1]]]

C1[En_, t0_, t2_, tp_, tdp_, e0_, e1_, e2_, m_] :=

First[Answer1[En, t0, t2, tp, tdp, e0, e1, e2, m][[2]]]

C2[En_, t0_, t2_, tp_, tdp_, e0_, e1_, e2_, m_] :=

First[Answer1[En, t0, t2, tp, tdp, e0, e1, e2, m][[3]]]

$\tau[\text{En_}, \text{t0_}, \text{t2_}, \text{tp_}, \text{tdp_}, \text{e0_}, \text{e1_}, \text{e2_}, \text{m_}] :=$

First[Answer1[En, t0, t2, tp, tdp, e0, e1, e2, m][[4]]]

(*Transmission and Reflection Probabilities*)

T1[En_, t0_, t2_, tp_, tdp_, e0_, e1_, e2_, m_] :=

If[Abs[Im[k1[En, e1]]] >

0, 0, Abs[$\tau[\text{En}, \text{t0}, \text{t2}, \text{tp}, \text{tdp}, \text{e0}, \text{e1}, \text{e2}, \text{m}]^2 * \text{t2} * \frac{\text{Sin}[\text{k2}[\text{En}, \text{t2}, \text{e2}]]}{\text{Sin}[\text{k1}[\text{En}, \text{e1}]}$]

R[En_, t0_, t2_, tp_, tdp_, e0_, e1_, e2_, m_] :=

If[Abs[Im[k1[En, e1]]] > 0, 1, Abs[$\gamma[\text{En}, \text{t0}, \text{t2}, \text{tp}, \text{tdp}, \text{e0}, \text{e1}, \text{e2}, \text{m}]^2$]

(*Check*)

Ck1 = Table[{En, T1[En, 1, 1, 1, 1, 1.0, 1.0, 1.0, 0] + R[En, 1, 1, 1, 1, 1.0, 1.0, 1.0, 0]},
{En, 0.01, 2.01, 0.1}]

{{0.01, 1.}, {0.11, 1.}, {0.21, 1.}, {0.31, 1.}, {0.41, 1.}, {0.51, 1.}, {0.61, 1.},

{0.71, 1.}, {0.81, 1.}, {0.91, 1.}, {1.01, 1.}, {1.11, 1.}, {1.21, 1.}, {1.31, 1.},

{1.41, 1.}, {1.51, 1.}, {1.61, 1.}, {1.71, 1.}, {1.81, 1.}, {1.91, 1.}, {2.01, 1.}}

Ck2 = Style[Table[{En, T1[En, 1, 1, 1, 1, 1, 1, 1, 1] + R[En, 1, 1, 1, 1, 1, 1, 1, 1]},

{En, 0.01, 2.01, 0.1}], Tiny]

{{0.01, 1.}, {0.11, 1.}, {0.21, 1.}, {0.31, 1.}, {0.41, 1.}, {0.51, 1.}, {0.61, 1.},

{0.71, 1.}, {0.81, 1.}, {0.91, 1.}, {1.01, 1.}, {1.11, 1.}, {1.21, 1.}, {1.31, 1.},

{1.41, 1.}, {1.51, 1.}, {1.61, 1.}, {1.71, 1.}, {1.81, 1.}, {1.91, 1.}, {2.01, 1.}}

We show the results of transmission and reflection probabilities (T_1) as a function of energy (E_n/t_L)

(*Graph*)

```
G1 = Plot[T1[En, 1.3, 1, 1.1, 1.1, 0, 0, 0, 1] + R[En, 1.3, 1, 1.1, 1.1, 0, 0, 0, 1],
{En, 0.0001, 3.0001}, PlotRange -> {0, 1.2}, PlotStyle -> {Blue},
```

```
PlotLabel -> "Total Probability", Frame -> True,
```

```
LabelStyle -> Directive[Bold, Black]]
```

```
G2 = Plot[T1[En, 1.3, 1, 1.1, 1.1, 0, 0, 0, 1],
```

```
{En, 0.5001, 3.001}, PlotRange -> {0, 1.2}, PlotStyle -> {Red},
```

```
PlotLabel -> "Transmission Probability", Frame -> True,
```

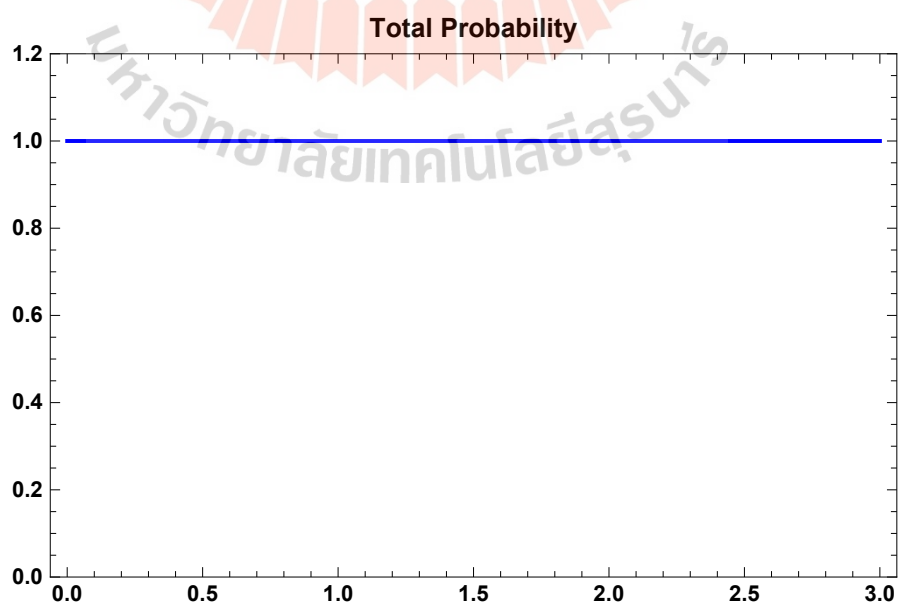
```
LabelStyle -> Directive[Bold, Black]]
```

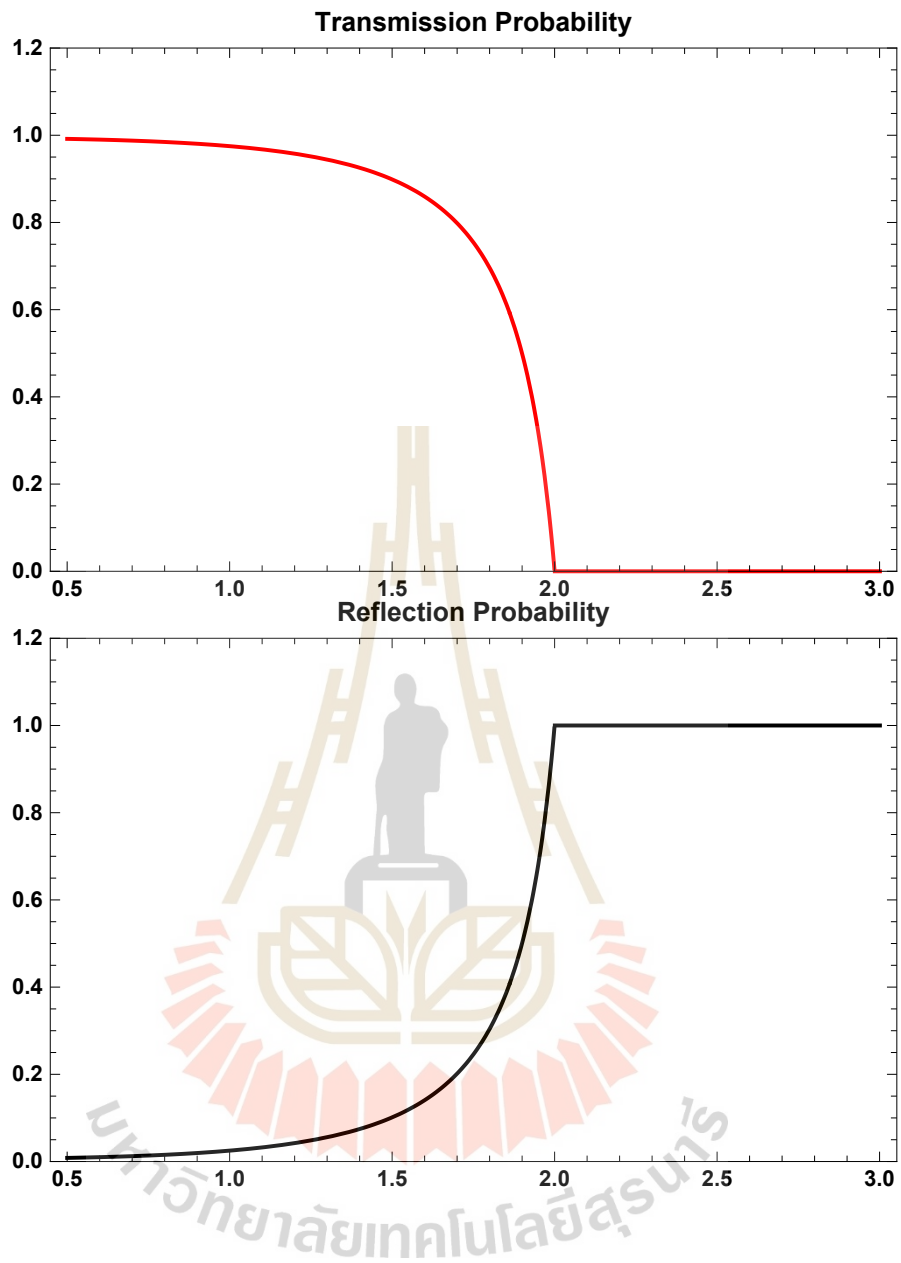
```
G3 = Plot[R[En, 1.3, 1, 1.1, 1.1, 0, 0, 0, 1],
```

```
{En, 0.5001, 3.001}, PlotRange -> {0, 1.2}, PlotStyle -> {Black},
```

```
PlotLabel -> "Reflection Probability", Frame -> True,
```

```
LabelStyle -> Directive[Bold, Black]]
```





APPENDIX B

WOLFRAM MATHEMATICA PROGRAM CALCULATION RELATED TO FERRO- MAGNETIC METAL/ SPACER/ FERRO- MAGNETIC METAL JUNCTION

Below, this is Wolfram Mathematica program calculation, we use in this thesis after the program. We present the results of transmission probability as a function of the energy and the magnetoresistance as a function of magnetic field.

We present all our parameters of the system in the list as

- The energy (Voltage bias) is $E_n = \frac{E}{t_L}$.
- The on-site energy of each regions are $e1 = \frac{(\varepsilon_L - \mu)}{t_L}$, $e2 = \frac{(\varepsilon_R - \mu)}{t_L}$ and $e0 = \frac{(\varepsilon_M - \mu)}{t_L}$.
- The exchange energies are $J1 = \frac{J_L}{t_L}$ and $J2 = \frac{J_R}{t_L}$.
- The magnetic field is $cB = \frac{cB}{t_L}$.
- The hopping energies are $t0 = \frac{t_M}{t_L}$, $t2 = \frac{t_R}{t_L}$, $tp = \frac{t'}{t_L}$ and $tdp = \frac{t''}{t_L}$.
- Thickness (Spacer) is $m = \text{Number of atoms}$.

Code:

```
ClearAll["Global*"]
```

```
Off[General::spell]; Off[LinearSolve::luc]; On[General::stop];
```

(*Left Region*)

$$ku[En_, e1_, J1_, cB_] := \text{ArcCos} \left[\frac{e1 - J1 - cB - En}{2} \right]$$

$$kd[En_, e1_, J1_, cB_] := \text{ArcCos} \left[\frac{e1 + J1 + cB - En}{2} \right]$$

(* A spacer *)

$$kmu[En_, t0_, e0_, cB_] := \text{ArcCos} \left[\frac{e0 * t0 - cB - En}{2 * t0} \right]$$

$$kmd[En_, t0_, e0_, cB_] := \text{ArcCos} \left[\frac{e0 * t0 + cB - En}{2 * t0} \right]$$

(*Right Region*)

$$qu[En_, t2_, e2_, J2_, cB_] := \text{ArcCos} \left[\frac{e2 * t2 + J2 - cB - En}{2 * t2} \right]$$

$$qd[En_, t2_, e2_, J2_, cB_] := \text{ArcCos} \left[\frac{e2 * t2 - J2 + cB - En}{2 * t2} \right]$$

$$k1 := \text{Plot}[\{ku[0, 0, 0.04, x], kd[0, 0, 0.04, x],$$

$$qu[0, 1, 0, 0.04, x], qd[0, 1, 0, 0.04, x]\},$$

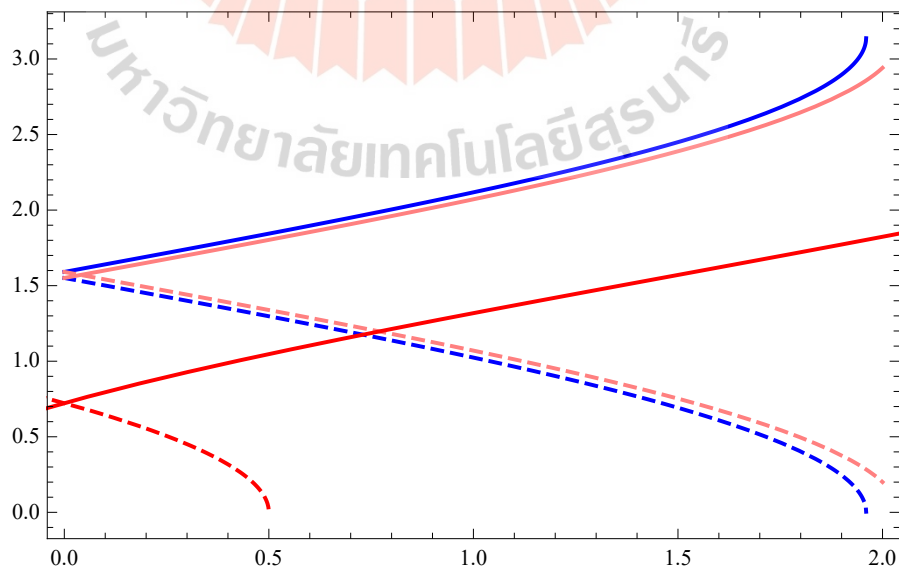
$$\{x, 0, 2\}, \text{PlotStyle} \rightarrow \{\text{Blue}, \{\text{Blue}, \text{Dashed}\}, \text{Pink}, \{\text{Pink}, \text{Dashed}\}\}]$$

$$k3 := \text{Plot}[\{kmu[0, 1, 1.5, x], kmd[0, 1, 1.5, x]\},$$

$$\{x, -3, 3\}, \text{PlotStyle} \rightarrow \{\text{Red}, \{\text{Red}, \text{Dashed}\}\}]$$

$$\text{Show}[\{k1, k3\}, \text{Frame} \rightarrow \text{True}]$$

We show the wave vectors as a function of a magnetic field (cB)



CASE I: an electron spin-up incident

(*Matrix*)

M11:=1

M12:=0

M13[tp_]:= - tp

M14:=0

M15[tp_]:= - tp

M16:=0

M17:=0

M18:=0

M21:=0

M22:=1

M23:=0

M24[tp_]:= - tp

M25:=0

M26[tp_]:= - tp

M27:=0

M28:=0

M31[En_, tp_, t0_, e1_, J1_, cB_]:= - $\frac{tp}{t0} * e^{i*ku[En,e1,J1,cB]}$

M32:=0

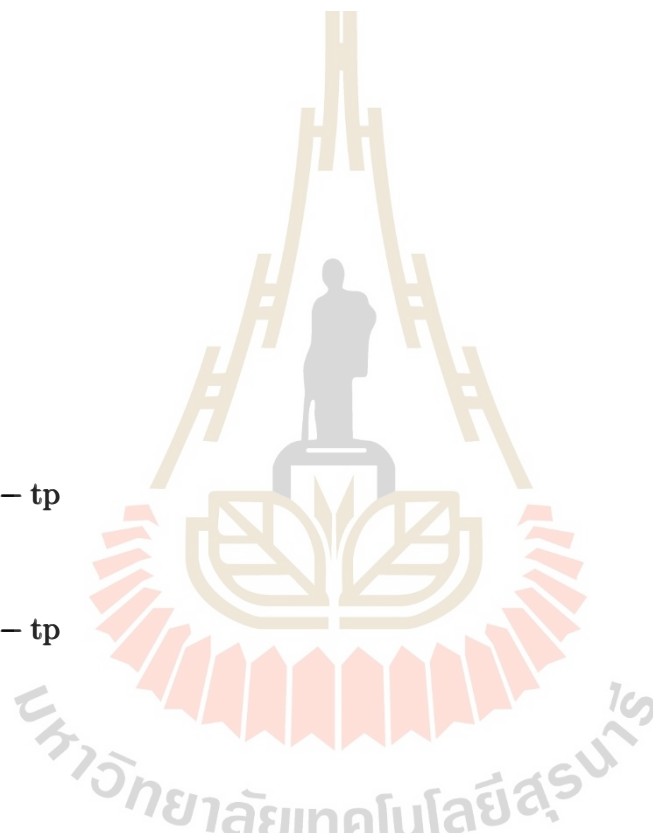
M33[En_, t0_, e0_, cB_]:= $e^{-i*kmu[En,t0,e0,cB]}$

M34:=0

M35[En_, t0_, e0_, cB_]:= $e^{i*kmu[En,t0,e0,cB]}$

M36:=0

M37:=0



$$M38:=0$$

$$M41:=0$$

$$M42[En_ , tp_ , t0_ , e1_ , J2_ , cB_]:= - \frac{tp}{t0} * e^{i*kd[En,e1,J2,cB]}$$

$$M43:=0$$

$$M44[En_ , t0_ , e0_ , cB_]:=e^{-i*kmd[En,t0,e0,cB]}$$

$$M45:=0$$

$$M46[En_ , t0_ , e0_ , cB_]:=e^{i*kmd[En,t0,e0,cB]}$$

$$M47:=0$$

$$M48:=0$$

$$M51:=0$$

$$M52:=0$$

$$M53[En_ , t0_ , e0_ , m_ , cB_]:=e^{i*kmu[En,t0,e0,cB]*(m+1)}$$

$$M54:=0$$

$$M55[En_ , t0_ , e0_ , m_ , cB_]:=e^{-i*kmu[En,t0,e0,cB]*(m+1)}$$

$$M56:=0$$

$$M57[En_ , tdp_ , t0_ , t2_ , e2_ , J2_ , m_ , cB_]:= - \frac{tdp}{t0} * e^{i*qu[En,t2,e2,J2,cB]*(m+1)}$$

$$M58:=0$$

$$M61:=0$$

$$M62:=0$$

$$M63:=0$$

$$M64[En_ , t0_ , e0_ , m_ , cB_]:=e^{i*kmd[En,t0,e0,cB]*(m+1)}$$

$$M65:=0$$

$$M66[En_ , t0_ , e0_ , m_ , cB_]:=e^{-i*kmd[En,t0,e0,cB]*(m+1)}$$

$$M67:=0$$

$$M68[En_ , tdp_ , t0_ , t2_ , e2_ , J2_ , m_ , cB_]:= -\frac{tdp}{t0} * e^{i*qd[En,t2,e2,J2,cB]*(m+1)}$$

$$M71:=0$$

$$M72:=0$$

$$M73[En_ , tdp_ , t2_ , t0_ , e0_ , m_ , cB_]:=\frac{-tdp}{t2} * e^{i*kmu[En,t0,e0,cB]*m}$$

$$M74:=0$$

$$M75[En_ , tdp_ , t2_ , t0_ , e0_ , m_ , cB_]:=\frac{-tdp}{t2} * e^{-i*kmu[En,t0,e0,cB]*m}$$

$$M76:=0$$

$$M77[En_ , t2_ , e2_ , J2_ , m_ , cB_]:=e^{i*qu[En,t2,e2,J2,cB]*m}$$

$$M78:=0$$

$$M81:=0$$

$$M82:=0$$

$$M83:=0$$

$$M84[En_ , tdp_ , t2_ , t0_ , e0_ , m_ , cB_]:=\frac{-tdp}{t2} * e^{i*kmd[En,t0,e0,cB]*m}$$

$$M85:=0$$

$$M86[En_ , tdp_ , t2_ , t0_ , e0_ , m_ , cB_]:=\frac{-tdp}{t2} * e^{-i*kmd[En,t0,e0,cB]*m}$$

$$M87:=0$$

$$M88[En_ , t2_ , e2_ , J2_ , m_ , cB_]:=e^{i*qd[En,t2,e2,J2,cB]*m}$$

$$M[En_ , t0_ , t2_ , tp_ , tdp_ , e0_ , e1_ , e2_ , J1_ , J2_ , m_ , cB_]:=$$

$$\begin{pmatrix} M11 & M12 & M13 & M14 & M15 & M16 & M17 & M18 \\ M21 & M22 & M23 & M24 & M25 & M26 & M27 & M28 \\ M31 & M32 & M33 & M34 & M35 & M36 & M37 & M38 \\ M41 & M42 & M43 & M44 & M45 & M46 & M47 & M48 \\ M51 & M52 & M53 & M54 & M55 & M56 & M57 & M58 \\ M61 & M62 & M63 & M64 & M65 & M66 & M67 & M68 \\ M71 & M72 & M73 & M74 & M75 & M76 & M77 & M78 \\ M81 & M82 & M83 & M84 & M85 & M86 & M87 & M88 \end{pmatrix};$$

$\text{Ans}[\text{En}_-, \text{tp}_-, \text{t0}_-, \text{e1}_-, \text{J1}_-, \text{cB}_-] :=$

$$\begin{pmatrix} -1 \\ 0 \\ \frac{\text{tp}_-}{\text{t0}_-} * e^{-i * \text{ku}[\text{En}_-, \text{e1}_-, \text{J1}_-, \text{cB}_-]} \\ 0 \\ 0 \\ 0 \\ 0 \\ 0 \end{pmatrix};$$

$A[\text{En}_-, \text{t0}_-, \text{t2}_-, \text{tp}_-, \text{tdp}_-, \text{e0}_-, \text{e1}_-, \text{e2}_-, \text{J1}_-, \text{J2}_-, \text{m}_-, \text{cB}_-] :=$
 $\text{LinearSolve}[M[\text{En}_-, \text{t0}_-, \text{t2}_-, \text{tp}_-, \text{tdp}_-, \text{e0}_-, \text{e1}_-, \text{e2}_-, \text{J1}_-, \text{J2}_-, \text{m}_-, \text{cB}_-],$
 $\text{Ans}[\text{En}_-, \text{tp}_-, \text{t0}_-, \text{e1}_-, \text{J1}_-, \text{cB}_-]$

$\gamma_{uu}[\text{En}_-, \text{t0}_-, \text{t2}_-, \text{tp}_-, \text{tdp}_-, \text{e0}_-, \text{e1}_-, \text{e2}_-, \text{J1}_-, \text{J2}_-, \text{m}_-, \text{cB}_-] :=$
 $\text{First}[A[\text{En}_-, \text{t0}_-, \text{t2}_-, \text{tp}_-, \text{tdp}_-, \text{e0}_-, \text{e1}_-, \text{e2}_-, \text{J1}_-, \text{J2}_-, \text{m}_-, \text{cB}_-][[1]]]$

$\gamma_{ud}[\text{En}_-, \text{t0}_-, \text{t2}_-, \text{tp}_-, \text{tdp}_-, \text{e0}_-, \text{e1}_-, \text{e2}_-, \text{J1}_-, \text{J2}_-, \text{m}_-, \text{cB}_-] :=$
 $\text{First}[A[\text{En}_-, \text{t0}_-, \text{t2}_-, \text{tp}_-, \text{tdp}_-, \text{e0}_-, \text{e1}_-, \text{e2}_-, \text{J1}_-, \text{J2}_-, \text{m}_-, \text{cB}_-][[2]]]$

$\text{cu1}[\text{En}_-, \text{t0}_-, \text{t2}_-, \text{tp}_-, \text{tdp}_-, \text{e0}_-, \text{e1}_-, \text{e2}_-, \text{J1}_-, \text{J2}_-, \text{m}_-, \text{cB}_-] :=$
 $\text{First}[A[\text{En}_-, \text{t0}_-, \text{t2}_-, \text{tp}_-, \text{tdp}_-, \text{e0}_-, \text{e1}_-, \text{e2}_-, \text{J1}_-, \text{J2}_-, \text{m}_-, \text{cB}_-][[3]]]$

$\text{cu1}[\text{En}_-, \text{t0}_-, \text{t2}_-, \text{tp}_-, \text{tdp}_-, \text{e0}_-, \text{e1}_-, \text{e2}_-, \text{J1}_-, \text{J2}_-, \text{m}_-, \text{cB}_-] :=$
 $\text{First}[A[\text{En}_-, \text{t0}_-, \text{t2}_-, \text{tp}_-, \text{tdp}_-, \text{e0}_-, \text{e1}_-, \text{e2}_-, \text{J1}_-, \text{J2}_-, \text{m}_-, \text{cB}_-][[4]]]$

$\text{du2}[\text{En}_-, \text{t0}_-, \text{t2}_-, \text{tp}_-, \text{tdp}_-, \text{e0}_-, \text{e1}_-, \text{e2}_-, \text{J1}_-, \text{J2}_-, \text{m}_-, \text{cB}_-] :=$
 $\text{First}[A[\text{En}_-, \text{t0}_-, \text{t2}_-, \text{tp}_-, \text{tdp}_-, \text{e0}_-, \text{e1}_-, \text{e2}_-, \text{J1}_-, \text{J2}_-, \text{m}_-, \text{cB}_-][[5]]]$

$\text{du2}[\text{En}_-, \text{t0}_-, \text{t2}_-, \text{tp}_-, \text{tdp}_-, \text{e0}_-, \text{e1}_-, \text{e2}_-, \text{J1}_-, \text{J2}_-, \text{m}_-, \text{cB}_-] :=$

```

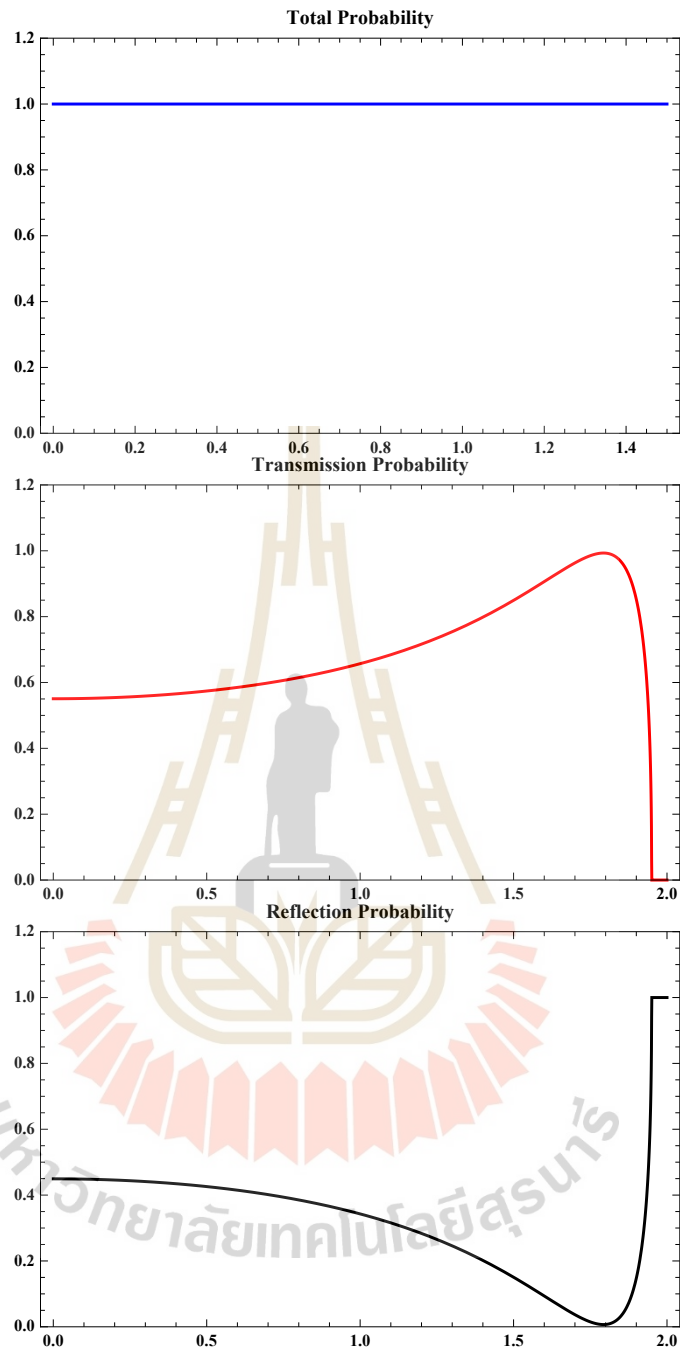
First[A[En, t0, t2, tp, tdp, e0, e1, e2, J1, J2, m, cB][[6]]]
 $\tau_{uu}[En_, t0_, t2_, tp_, tdp_, e0_, e1_, e2_, J1_, J2_, m_, cB_] :=$ 
First[A[En, t0, t2, tp, tdp, e0, e1, e2, J1, J2, m, cB][[7]]]
 $\tau_{ud}[En_, t0_, t2_, tp_, tdp_, e0_, e1_, e2_, J1_, J2_, m_, cB_] :=$ 
First[A[En, t0, t2, tp, tdp, e0, e1, e2, J1, J2, m, cB][[8]]]
(*Transmission and Reflection Probabilities*)
Tuu[En_, t0_, t2_, tp_, tdp_, e0_, e1_, e2_, J1_, J2_, m_, cB_] :=
If[Abs[Im[ku[En, e1, J1, cB]]] > 0, 0,
Abs[ $\tau_{uu}[En, t0, t2, tp, tdp, e0, e1, e2, J1, J2, m, cB]$ ]^2 * t2 *
Abs[ $\frac{\text{Sin}[qu[En, t2, e1, J1, cB]]}{\text{Sin}[ku[En, e1, J1, cB]]}$ ]]]
Tud[En_, t0_, t2_, tp_, tdp_, e0_, e1_, e2_, J1_, J2_, m_, cB_] :=
If[Abs[Im[kd[En, e1, J1, cB]]] > 0, 0,
Abs[ $\tau_{ud}[En, t0, t2, tp, tdp, e0, e1, e2, J1, J2, m, cB]$ ]^2 *
Abs[ $\frac{\text{Sin}[qd[En, t2, e1, J1, cB]]}{\text{Sin}[ku[En, e1, J1, cB]]}$ ] * t2]
Ruu[En_, t0_, t2_, tp_, tdp_, e0_, e1_, e2_, J1_, J2_, m_, cB_] :=
If[Abs[Im[ku[En, e1, J1, cB]]] > 0, 1,
Abs[ $\gamma_{uu}[En, t0, t2, tp, tdp, e0, e1, e2, J1, J2, m, cB]$ ]^2]
Rud[En_, t0_, t2_, tp_, tdp_, e0_, e1_, e2_, J1_, J2_, m_, cB_] :=
If[Abs[Im[kd[En, e1, J1, cB]]] > 0, 0,
Abs[ $\gamma_{ud}[En, t0, t2, tp, tdp, e0, e1, e2, J1, J2, m, cB]$ ]^2 *
Abs[ $\frac{\text{Sin}[kd[En, e1, J1, cB]]}{\text{Sin}[ku[En, e1, J1, cB]]}$ ]]]
Ck1 = Table[{En, Tuu[En, 1.2, 1, 2, 2, 0, 0, 0, 0.04, 0.04, 1, 0.1]+
Tud[En, 1.2, 1, 2, 2, 0, 0, 0, 0.04, 0.04, 1, 0.1]+
Ruu[En, 1.2, 1, 2, 2, 0, 0, 0, 0.04, 0.04, 1, 0.1]+
Rud[En, 1.2, 1, 2, 2, 0, 0, 0, 0.04, 0.04, 1, 0.1]}],
{En, 0.001, 3.0001, 0.1}]

```

```
{0.001, 1.}, {0.101, 1.}, {0.201, 1.}, {0.301, 1.}, {0.401, 1.}, {0.501, 1.}, {0.601, 1.}, {0.701, 1.}, {0.801, 1.}, {0.901, 1.}, {1.001, 1.},
{1.101, 1.}, {1.201, 1.}, {1.301, 1.}, {1.401, 1.}, {1.501, 1.}, {1.601, 1.}, {1.701, 1.}, {1.801, 1.}, {1.901, 1.}, {2.001, 1.}, {2.101, 1.},
{2.201, 1.}, {2.301, 1.}, {2.401, 1.}, {2.501, 1.}, {2.601, 1.}, {2.701, 1.}, {2.801, 1.}, {2.901, 1.}}
```

```
G1 = Plot[Tuu[En, 1.2, 1, 2, 2, 0, 0, 0, 0.04, 0.04, 1, 0]+
Tud[En, 1.2, 1, 2, 2, 0, 0, 0, 0.04, 0.04, 1, 0]+
Ruu[En, 1.2, 1, 2, 2, 0, 0, 0, 0.04, 0.04, 1, 0]+
Rud[En, 1.2, 1, 2, 2, 0, 0, 0, 0.04, 0.04, 1, 0],
{En, 0, 1.5}, PlotRange → {0, 1.2}, PlotStyle → {Blue},
PlotLabel → “ Total Probability”, Frame → True,
LabelStyle → Directive[Bold, Black]]
G2 = Plot[Tuu[En, 1, 1, 1.5, 1.5, 0, 0, 0, 0.05, 0.05, 1, 0]+
Tud[En, 1, 1, 1.5, 1.5, 0, 0, 0, 0.05, 0.05, 1, 0],
{En, 0, 2}, PlotRange → {0, 1.2}, PlotStyle → {Red},
PlotLabel → “Transmission Probability”, Frame → True,
LabelStyle → Directive[Bold, Black]]
G3 = Plot[Ruu[En, 1, 1, 1.5, 1.5, 0, 0, 0, 0.05, 0.05, 1, 0]+
Rud[En, 1, 1, 1.5, 1.5, 0, 0, 0, 0.05, 0.05, 1, 0],
{En, 0, 2}, PlotRange → {0, 1.2}, PlotStyle → {Black},
PlotLabel → “Reflection Probability”, Frame → True,
LabelStyle → Directive[Bold, Black]]
```

We show the results of transmission probability as a function of energy.



CASE II: an electron spin-down incident

(*Matrix*)

A11:=1

A12:=0

A13[tp_]:= - tp

A14:=0

$$A15[tp_]:= - tp$$

$$A16:=0$$

$$A17:=0$$

$$A18:=0$$

$$A21:=0$$

$$A22:=1$$

$$A23:=0$$

$$A24[tp_]:= - tp$$

$$A25:=0$$

$$A26[tp_]:= - tp$$

$$A27:=0$$

$$A28:=0$$

$$A31[En_, tp_, t0_, e1_, J1_, cB_] := - \frac{tp}{t0} * e^{i*ku[En,e1,J1,cB]}$$

$$A32:=0$$

$$A33[En_, t0_, e0_, cB_] := e^{-i*kmu[En,t0,e0,cB]}$$

$$A34:=0$$

$$A35[En_, t0_, e0_, cB_] := e^{i*kmu[En,t0,e0,cB]}$$

$$A36:=0$$

$$A37:=0$$

$$A38:=0$$

$$A41:=0$$

$$A42[En_, tp_, t0_, e1_, J2_, cB_] := - \frac{tp}{t0} * e^{i*kd[En,e1,J2,cB]}$$

$$A43:=0$$

$$A44[En_, t0_, e0_, cB_] := e^{-i*kmd[En,t0,e0,cB]}$$

$$A45:=0$$

$$A46[En_ , t0_ , e0_ , cB_]:=e^{i*kmd[En,t0,e0,cB]}$$

$$A47:=0$$

$$A48:=0$$

$$A51:=0$$

$$A52:=0$$

$$A53[En_ , t0_ , e0_ , m_ , cB_]:=e^{i*kmu[En,t0,e0,cB]*(m+1)}$$

$$A54:=0$$

$$A55[En_ , t0_ , e0_ , m_ , cB_]:=e^{-i*kmu[En,t0,e0,cB]*(m+1)}$$

$$A56:=0$$

$$A57[En_ , tdp_ , t0_ , t2_ , e2_ , J2_ , m_ , cB_]:= -\frac{tdp}{t0} * e^{i*qu[En,t2,e2,J2,cB]*(m+1)}$$

$$A58:=0$$

$$A61:=0$$

$$A62:=0$$

$$A63:=0$$

$$A64[En_ , t0_ , e0_ , m_ , cB_]:=e^{i*kmd[En,t0,e0,cB]*(m+1)}$$

$$A65:=0$$

$$A66[En_ , t0_ , e0_ , m_ , cB_]:=e^{-i*kmd[En,t0,e0,cB]*(m+1)}$$

$$A67:=0$$

$$A68[En_ , tdp_ , t0_ , t2_ , e2_ , J2_ , m_ , cB_]:= -\frac{tdp}{t0} * e^{i*qd[En,t2,e2,J2,cB]*(m+1)}$$

$$A71:=0$$

$$A72:=0$$

$$A73[En_ , tdp_ , t2_ , t0_ , e0_ , m_ , cB_]:=\frac{-tdp}{t2} * e^{i*kmu[En,t0,e0,cB]*m}$$

$$A74:=0$$

$$A75[En_ , tdp_ , t2_ , t0_ , e0_ , m_ , cB_] := \frac{-tdp}{t2} * e^{-i*kmu[En,t0,e0,cB]*m}$$

$$A76 := 0$$

$$A77[En_ , t2_ , e2_ , J2_ , m_ , cB_] := e^{i*qu[En,t2,e2,J2,cB]*m}$$

$$A78 := 0$$

$$A81 := 0$$

$$A82 := 0$$

$$A83 := 0$$

$$A84[En_ , tdp_ , t2_ , t0_ , e0_ , m_ , cB_] := \frac{-tdp}{t2} * e^{i*kmd[En,t0,e0,cB]*m}$$

$$A85 := 0$$

$$A86[En_ , tdp_ , t2_ , t0_ , e0_ , m_ , cB_] := \frac{-tdp}{t2} * e^{-i*kmd[En,t0,e0,cB]*m}$$

$$A87 := 0$$

$$A88[En_ , t2_ , e2_ , J2_ , m_ , cB_] := e^{i*qd[En,t2,e2,J2,cB]*m}$$

$$M2[En_ , t0_ , t2_ , tp_ , tdp_ , e0_ , e1_ , e2_ , J1_ , J2_ , m_ , cB_] :=$$

$$\begin{pmatrix} A11 & A12 & A13 & A14 & A15 & A16 & A17 & A18 \\ A21 & A22 & A23 & A24 & A25 & A26 & A27 & A28 \\ A31 & A32 & A33 & A34 & A35 & A36 & A37 & A38 \\ A41 & A42 & A43 & A44 & A45 & A46 & A47 & A48 \\ A51 & A52 & A53 & A54 & A55 & A56 & A57 & A58 \\ A61 & A62 & A63 & A64 & A65 & A66 & A67 & A68 \\ A71 & A72 & A73 & A74 & A75 & A76 & A77 & A78 \\ A81 & A82 & A83 & A84 & A85 & A86 & A87 & A88 \end{pmatrix};$$

$$B[En_ , tp_ , t0_ , e1_ , J1_ , cB_] :=$$

$$\begin{pmatrix} 0 \\ -1 \\ 0 \\ \frac{tp}{t0} * e^{-i*kd[En,e1,J1,cB]} \\ 0 \\ 0 \\ 0 \\ 0 \end{pmatrix};$$

$$Answer2[En_ , t0_ , t2_ , tp_ , tdp_ , e0_ , e1_ , e2_ , J1_ , J2_ , m_ , cB_] :=$$

```

LinearSolve[M2[En, t0, t2, tp, tdp, e0, e1, e2, J1, J2, m, cB],
B[En, tp, t0, e1, J1, cB]]
γdu[En_, t0_, t2_, tp_, tdp_, e0_, e1_, e2_, J1_, J2_, m_, cB_] :=
First[Answer2[En, t0, t2, tp, tdp, e0, e1, e2, J1, J2, m, cB][[1]]]
γdd[En_, t0_, t2_, tp_, tdp_, e0_, e1_, e2_, J1_, J2_, m_, cB_] :=
First[Answer2[En, t0, t2, tp, tdp, e0, e1, e2, J1, J2, m, cB][[2]]]
cd1[En_, t0_, t2_, tp_, tdp_, e0_, e1_, e2_, J1_, J2_, m_, cB_] :=
First[Answer2[En, t0, t2, tp, tdp, e0, e1, e2, J1, J2, m, cB][[3]]]
cd1[En_, t0_, t2_, tp_, tdp_, e0_, e1_, e2_, J1_, J2_, m_, cB_] :=
First[Answer2[En, t0, t2, tp, tdp, e0, e1, e2, J1, J2, m, cB][[4]]]
dd2[En_, t0_, t2_, tp_, tdp_, e0_, e1_, e2_, J1_, J2_, m_, cB_] :=
First[Answer2[En, t0, t2, tp, tdp, e0, e1, e2, J1, J2, m, cB][[5]]]
dd2[En_, t0_, t2_, tp_, tdp_, e0_, e1_, e2_, J1_, J2_, m_, cB_] :=
First[Answer2[En, t0, t2, tp, tdp, e0, e1, e2, J1, J2, m, cB][[6]]]
τdu[En_, t0_, t2_, tp_, tdp_, e0_, e1_, e2_, J1_, J2_, m_, cB_] :=
First[Answer2[En, t0, t2, tp, tdp, e0, e1, e2, J1, J2, m, cB][[7]]]
τdd[En_, t0_, t2_, tp_, tdp_, e0_, e1_, e2_, J1_, J2_, m_, cB_] :=
First[Answer2[En, t0, t2, tp, tdp, e0, e1, e2, J1, J2, m, cB][[8]]]
(*Transmission and Reflection Probabilities*)
Tdu[En_, t0_, t2_, tp_, tdp_, e0_, e1_, e2_, J1_, J2_, m_, cB_] :=
If[Abs[Im[kd[En, e1, J1, cB]]] > 0, 0,
Abs[τdu[En, t0, t2, tp, tdp, e0, e1, e2, J1, J2, m, cB]]^2*
Abs [ Sin[qu[En,t2,e1,J1,cB]] / Sin[kd[En,e1,J1,cB]] ] * t2]
Tdd[En_, t0_, t2_, tp_, tdp_, e0_, e1_, e2_, J1_, J2_, m_, cB_] :=
If[Abs[Im[ku[En, e1, J1, cB]]] > 0, 0,
Abs[τdd[En, t0, t2, tp, tdp, e0, e1, e2, J1, J2, m, cB]]^2 * t2*

```

```

Abs  $\left[ \frac{\text{Sin}[\text{qd}[\text{En}, \text{t2}, \text{e1}, \text{J1}, \text{cB}]]}{\text{Sin}[\text{kd}[\text{En}, \text{e1}, \text{J1}, \text{cB}]]} \right]$ 
Rdu[En_, t0_, t2_, tp_, tdp_, e0_, e1_, e2_, J1_, J2_, m_, cB_] :=
If[Abs[Im[kd[En, e1, J1, cB]]] > 0, 0,
Abs[ $\gamma_{\text{du}}[\text{En}, \text{t0}, \text{t2}, \text{tp}, \text{tdp}, \text{e0}, \text{e1}, \text{e2}, \text{J1}, \text{J2}, \text{m}, \text{cB}]$ ]^2*
Abs  $\left[ \frac{\text{Sin}[\text{ku}[\text{En}, \text{e1}, \text{J1}, \text{cB}]]}{\text{Sin}[\text{kd}[\text{En}, \text{e1}, \text{J1}, \text{cB}]]} \right]$ 
Rdd[En_, t0_, t2_, tp_, tdp_, e0_, e1_, e2_, J1_, J2_, m_, cB_] :=
If[Abs[Im[ku[En, e1, J1, cB]]] > 0, 1,
Abs[ $\gamma_{\text{dd}}[\text{En}, \text{t0}, \text{t2}, \text{tp}, \text{tdp}, \text{e0}, \text{e1}, \text{e2}, \text{J1}, \text{J2}, \text{m}, \text{cB}]$ ]^2]
Ck2 = Table[{En, Tdu[En, 1, 1, 1, 1, 0, 0, 0, 1, 1, 1, 0]+
Tdd[En, 1, 1, 1, 1, 0, 0, 0, 1, 1, 1, 0]+
Rdu[En, 1, 1, 1, 1, 0, 0, 0, 1, 1, 1, 0]+
Rdd[En, 1, 1, 1, 1, 0, 0, 0, 1, 1, 1, 0]},
{En, 0.001, 3.0001, 0.1}
{0.001, 1.}, {0.101, 1.}, {0.201, 1.}, {0.301, 1.}, {0.401, 1.}, {0.501, 1.}, {0.601, 1.}, {0.701, 1.}, {0.801, 1.}, {0.901, 1.}, {1.001, 1.},
{1.101, 1.}, {1.201, 1.}, {1.301, 1.}, {1.401, 1.}, {1.501, 1.}, {1.601, 1.}, {1.701, 1.}, {1.801, 1.}, {1.901, 1.}, {2.001, 1.}, {2.101, 1.},
{2.201, 1.}, {2.301, 1.}, {2.401, 1.}, {2.501, 1.}, {2.601, 1.}, {2.701, 1.}, {2.801, 1.}, {2.901, 1.}
G1 = Plot[Tdu[En, 1, 1, 1, 1, 0.0, 0.0, 0.0, 0, 0, 1, 1]+
Tdd[En, 1, 1, 1, 1, 0.0, 0.0, 0.0, 0, 0, 1, 1]+
Rdu[En, 1, 1, 1, 1, 0.0, 0.0, 0.0, 0, 0, 1, 1]+
Rdd[En, 1, 1, 1, 1, 0.0, 0.0, 0.0, 0, 0, 1, 1],
{En, 0, 1.5}, PlotRange → {0, 1.2}, PlotStyle → {Blue},
PlotLabel → "Total Probability", Frame → True,
LabelStyle → Directive[Bold, Black]
G2 = Plot[Tdu[En, 1, 1, 1.5, 1.5, 0, 0, 0, 0.05, 0.05, 1, 0]+
Tdd[En, 1, 1, 1.5, 1.5, 0, 0, 0, 0.05, 0.05, 1, 0],
{En, 0, 2}, PlotRange → {0, 1.2}, PlotStyle → {Red},

```

PlotLabel → “Transmission Probability”, Frame → True,

LabelStyle → Directive[Bold, Black]]

G3 = Plot[Rdu[En, 1, 1, 1.5, 1.5, 0, 0, 0, 0.05, 0.05, 1, 0]+

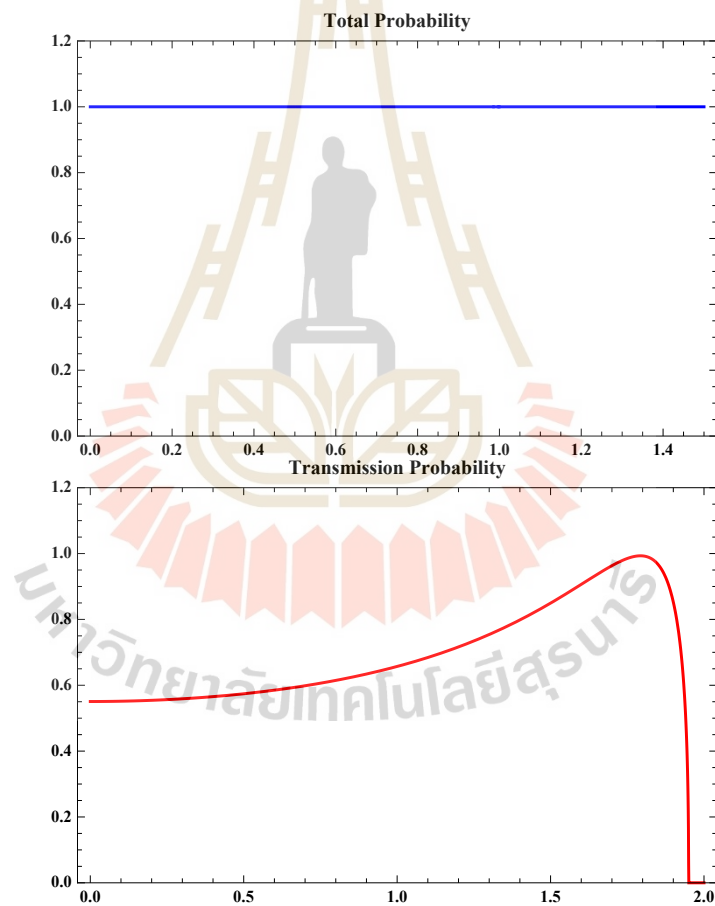
Rdd[En, 1, 1, 1.5, 1.5, 0, 0, 0, 0.05, 0.05, 1, 0],

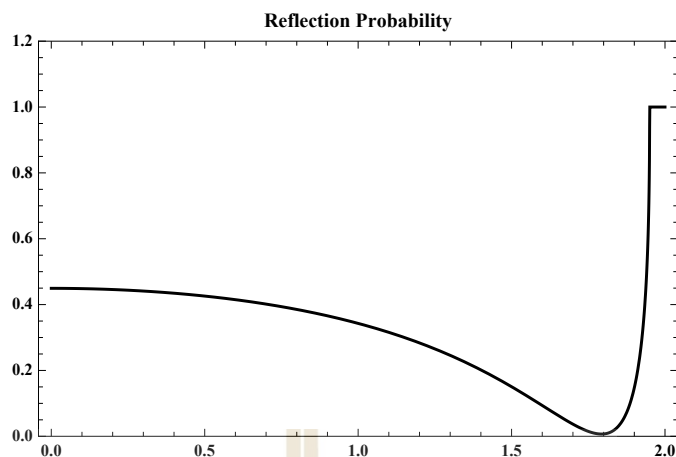
{En, 0, 2}, PlotRange → {0, 1.2}, PlotStyle → {Black},

PlotLabel → “Reflection Probability”, Frame → True,

LabelStyle → Directive[Bold, Black]]

We show the results of transmission probability as a function of energy.





Below is all result of our system.

Ck1 + Ck2

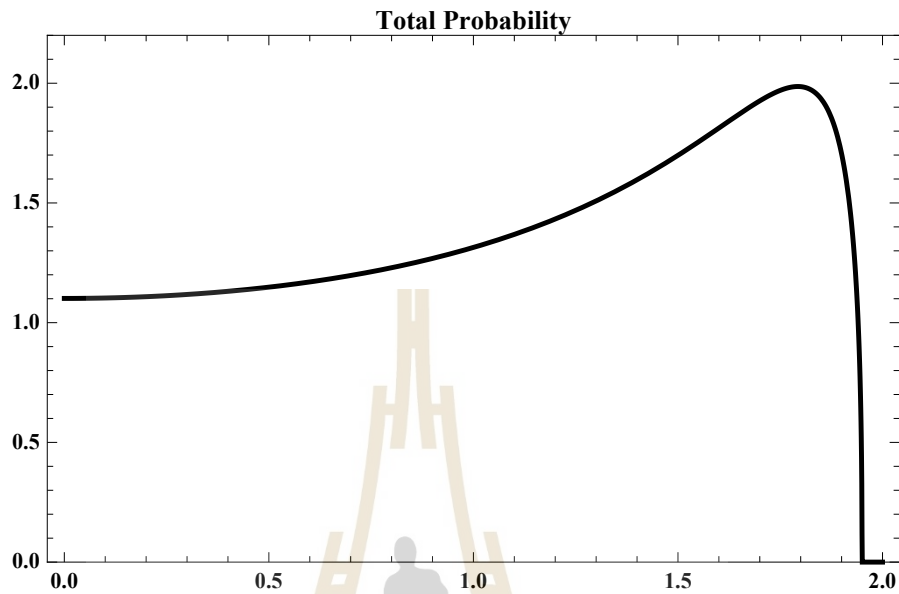
```
{0.002, 2.}, {0.202, 2.}, {0.402, 2.}, {0.602, 2.}, {0.802, 2.}, {1.002, 2.}, {1.202, 2.}, {1.402, 2.}, {1.602, 2.}, {1.802, 2.},
{2.002, 2.}, {2.202, 2.}, {2.402, 2.}, {2.602, 2.}, {2.802, 2.}, {3.002, 2.}, {3.202, 2.}, {3.402, 2.}, {3.602, 2.}, {3.802, 2.},
{4.002, 2.}, {4.202, 2.}, {4.402, 2.}, {4.602, 2.}, {4.802, 2.}, {5.002, 2.}, {5.202, 2.}, {5.402, 2.}, {5.602, 2.}, {5.802, 2.}
```

```
Ttotu[En_, t0_, t2_, tp_, tdp_, e0_, e1_, e2_, J1_, J2_, m_, cB_] :=
Tuu[En, t0, t2, tp, tdp, e0, e1, e2, J1, J2, m, cB] +
Tud[En, t0, t2, tp, tdp, e0, e1, e2, J1, J2, m, cB];
Ttotd[En_, t0_, t2_, tp_, tdp_, e0_, e1_, e2_, J1_, J2_, m_, cB_] :=
Tdu[En, t0, t2, tp, tdp, e0, e1, e2, J1, J2, m, cB] +
Tdd[En, t0, t2, tp, tdp, e0, e1, e2, J1, J2, m, cB];
```

We show the result of total probability as a function of energy.

```
GTotal = Plot[{
  Ttotd[En, 1, 1, 1.5, 1.5, 0, 0, 0, 0.05, 0.05, 1, 0] +
  Ttotu[En, 1, 1, 1.5, 1.5, 0, 0, 0, 0.05, 0.05, 1, 0]},
{En, 0, 2}, PlotRange → {0, 2.2}, PlotStyle → {Red, {Black, Thick}},
PlotLabel → "Total Probability", Frame → True,
```

LabelStyle → Directive[Bold, Black]]

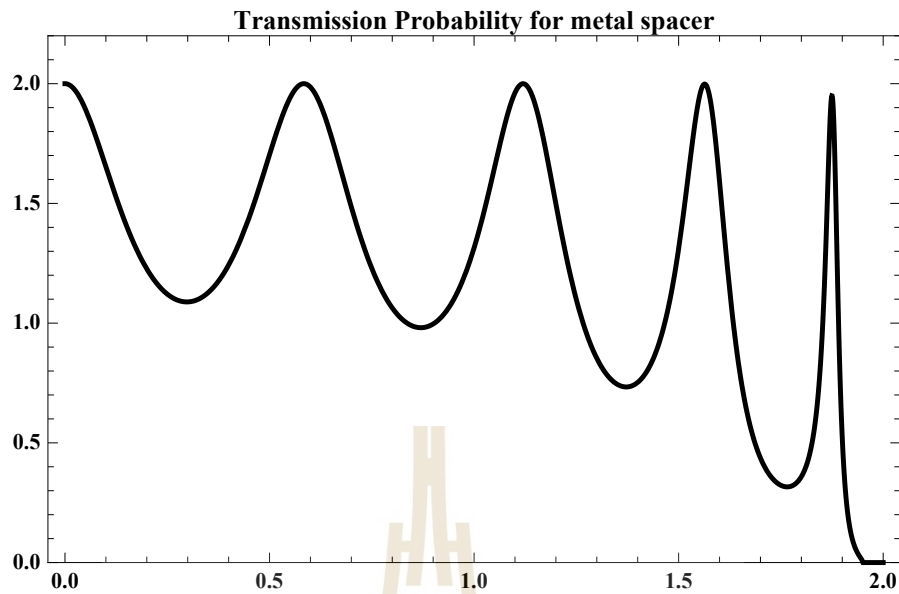


(*TotalTransmissionProbability::Ttot*)

```
Ttot[En_, t0_, t2_, tp_, tdp_, e0_, e1_, e2_, J1_, J2_, m_, cB_] :=
Ttotu[En, t0, t2, tp, tdp, e0, e1, e2, J1, J2, m, cB] +
Ttotd[En, t0, t2, tp, tdp, e0, e1, e2, J1, J2, m, cB]
```

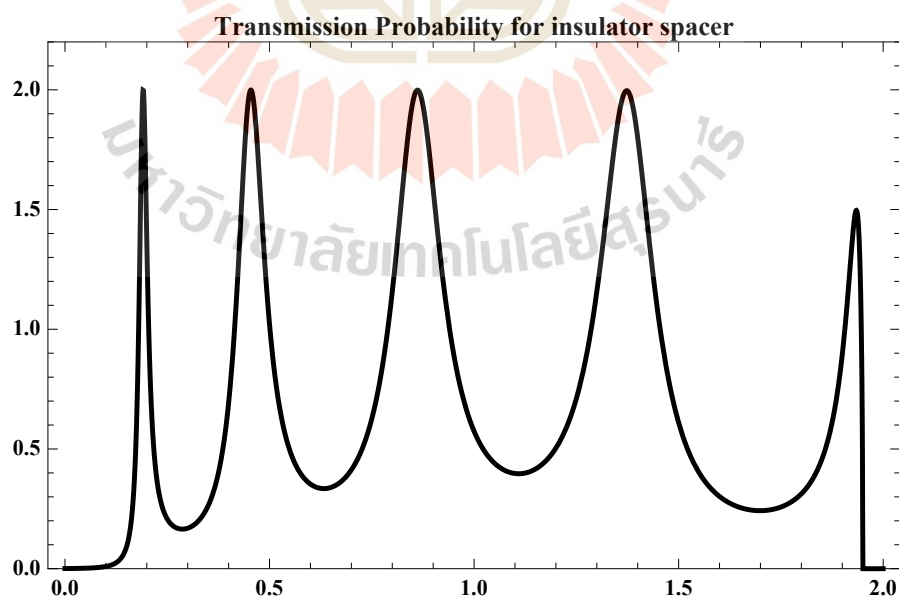
For a spacer is a metal.

```
G4 = Plot[Ttot[En, 1, 1, 1.5, 1.5, 0, 0, 0, 0.05, 0.05, 10, 0],
{En, 0, 2}, PlotRange → {0, 2.2}, PlotStyle → {Red, {Black, Thick}},
PlotLabel → "Transmission Probability for metal spacer", Frame → True,
LabelStyle → Directive[Bold, Black]]
```



For a spacer is an insulator.

```
G5 = Plot[Ttot[En, 1, 1, 1.5, 1.5, 2.1, 0, 0, 0.05, 0.05, 10, 0],
{En, 0, 2}, PlotRange -> {0, 2.2}, PlotStyle -> {Red, {Black, Thick}},
PlotLabel -> "Transmission Probability for insulator spacer", Frame -> True,
LabelStyle -> Directive[Bold, Black]]
```



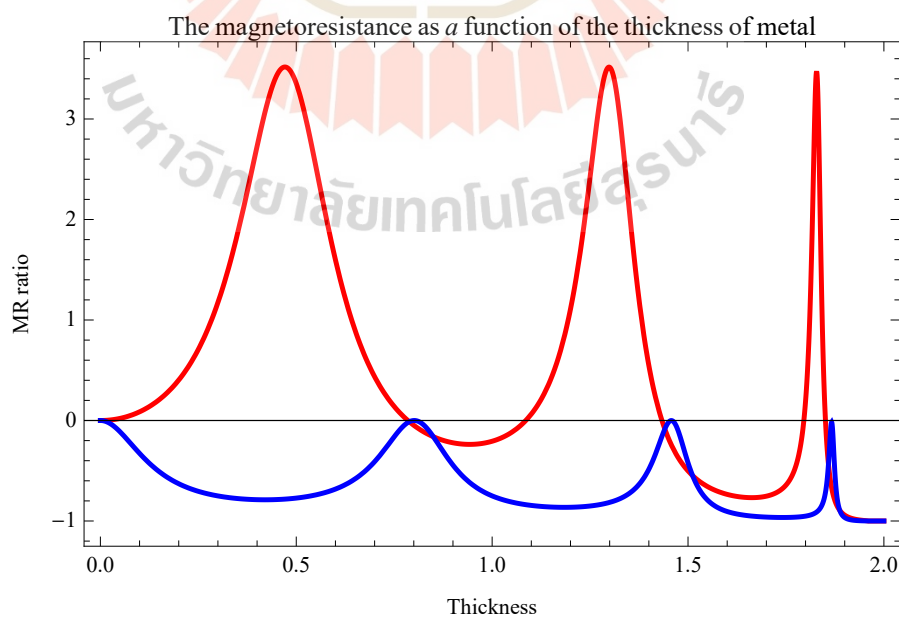
Next, we show the result of the magnetoresistance as a function of magnetic field.

(*Tunneling magnetoresistance::TMR*)

```
TMR[En_, t0_, t2_, tp_, tdp_, e0_, e1_, e2_, J1_, J2_, m_, cB_] :=
(Ttot[En, t0, t2, tp, tdp, e0, e1, e2, J1, J2, m, cB] -
Ttot[En, t0, t2, tp, tdp, e0, e1, e2, J1, J2, m, 0]) /
Ttot[En, t0, t2, tp, tdp, e0, e1, e2, J1, J2, m, 0]
```

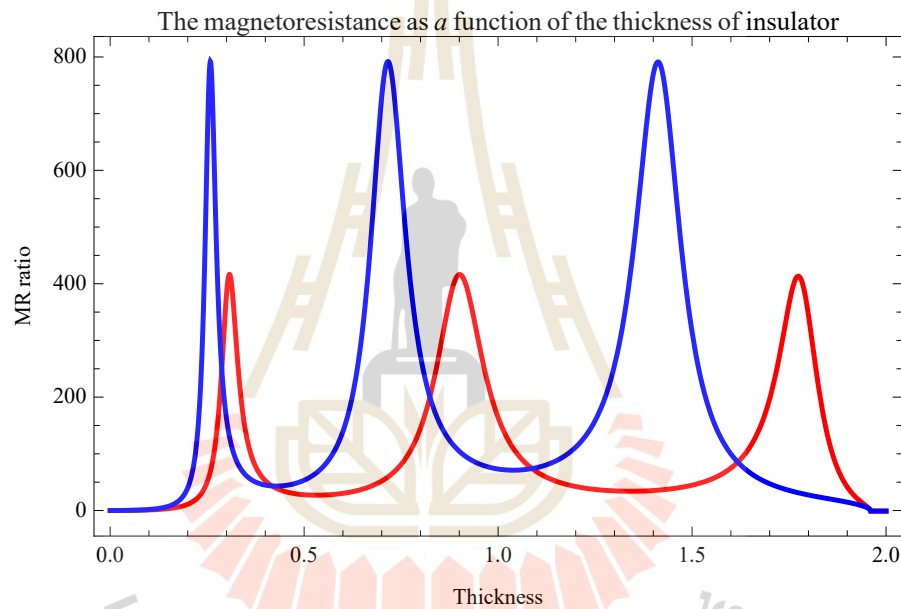
For a spacer is a metal.

```
G6:=Plot[{
TMR[0, 1, 1, 0.5, 0.5, 0, 0, 0, 0.04, 0.04, 5, x],
TMR[0, 1, 1, 0.5, 0.5, 0, 0, 0, 0.04, 0.04, 6, x]},
{x, 0, 2}, PlotStyle -> {{Red, Thick}, {Blue, Thick}},
PlotLabel -> "Magnetoresistance", Frame -> True,
LabelStyle -> Directive[Bold, Black]]
```



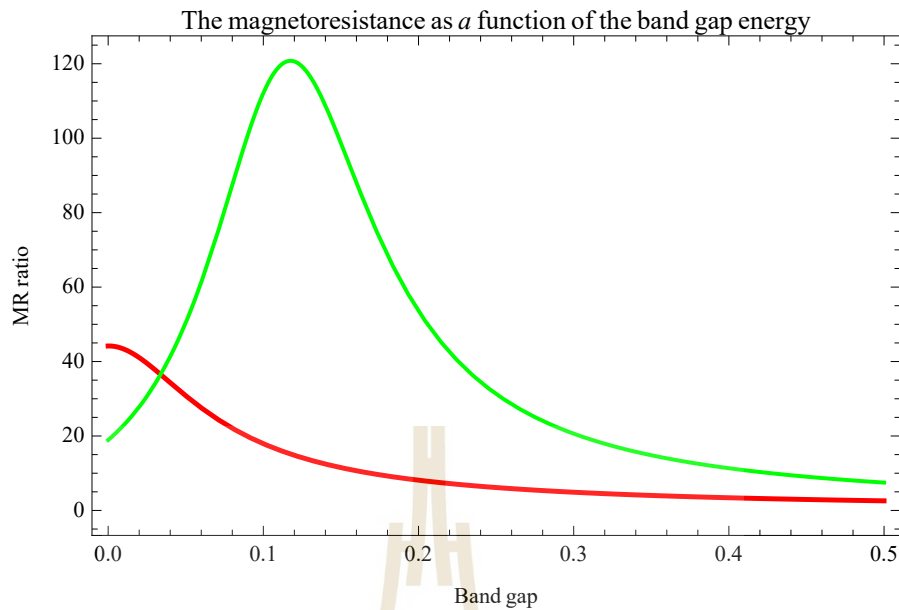
For a spacer is an insulator.

```
G7:=Plot[{
TMR[0, 1, 1, 0.5, 0.5, 2.1, 0, 0, 0.04, 0.04, 5, x],
TMR[0, 1, 1, 0.5, 0.5, 2.1, 0, 0, 0.04, 0.04, 6, x]},
{x, 0, 2}, PlotStyle → {{Red, Thick}, {Blue, Thick}},
PlotLabel → "Magnetoresistance", Frame → True,
LabelStyle → Directive[Bold, Black]]
```



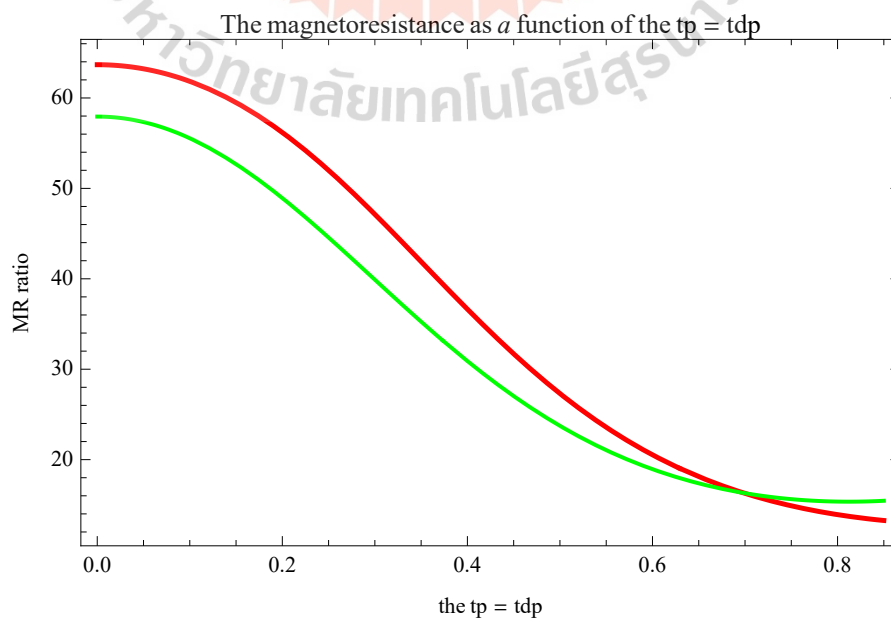
Below, we present the result of the magnetoresistance as a function of Band gap energy.

```
G8:=Plot[{
TMR[0, 1, 1, 1.5, 1.5, x/2 + 2, 0, 0, 0.04, 0.04, 7, 0.17],
TMR[0, 1, 1, 1.5, 1.5, x/2 + 2, 0, 0, 0.04, 0.04, 7, 0.23]},
{x, 0, 0.5}, PlotStyle → {{Red, Thick}, Green, Black, Blue},
PlotLabel → "Magnetoresistance", Frame → True,
LabelStyle → Directive[Bold, Black]]
```



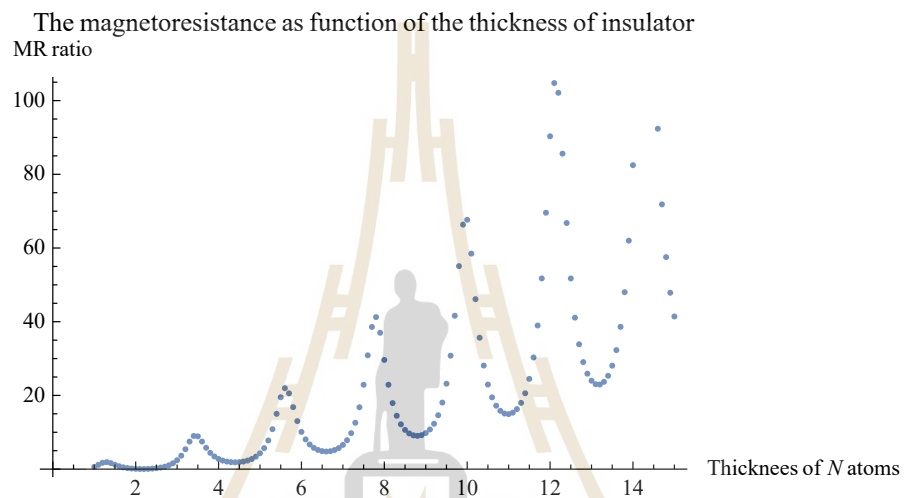
We show the result of the magnetoresistance as a function of $t' = t''$.

```
G9:=Plot[{
TMR[0, 0.8, 1, x, x, 2.001, 0, 0, 0.04, 0.04, 7, 0.7],
TMR[0, 0.8, 1, x, x, 2.001, 0, 0, 0.04, 0.04, 7, 1.2]},
{x, 0, 0.85}, PlotStyle → {{Red, Thick}, Green, Black, Blue},
PlotLabel → "Magnetoresistance", Frame → True,
LabelStyle → Directive[Bold, Black]]
```

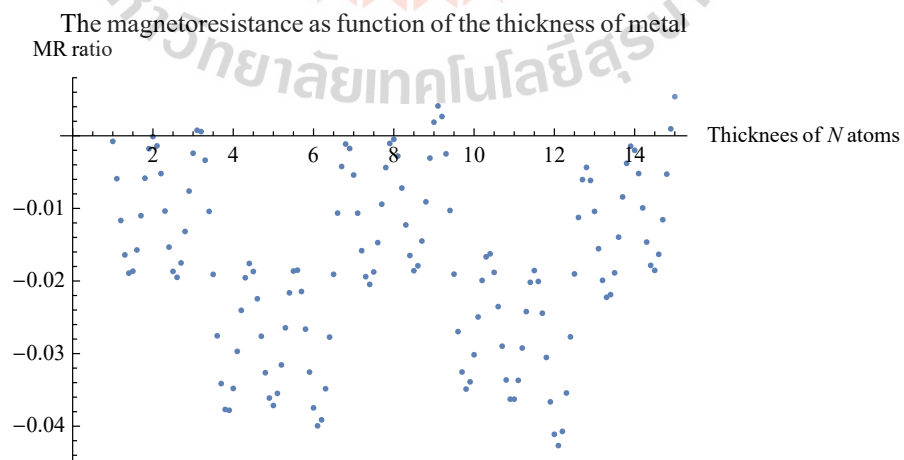


The effect of thickness on magnetoresistance for a spacer to be insulating and metallic.

```
L1:=ListPlot[Table[{m, TMR[0, 1, 1, 1.05, 1.05, 2.004, 0, 0, 0.04, 0.04, m, 1.75]}],
{m, 1, 15, 0.1}]]
```



```
L2:=ListPlot[Table[{m, TMR[0, 1, 1, 1.05, 1.05, 0, 0, 0, 0.04, 0.04, m, 1.75]}],
{m, 1, 15, 0.1}]]
```



CURRICULUM VITAE

NAME: Natthagrittha Nakhonthong **GENDER:** Female

NATIONALITY: Thai

DATE OF BIRTH: February 16, 1992

E-MAIL: nakhonthong.n@gmail.com

EDUCATIONS:

- March 2014 Bachelor of Science, Department of Physics, Mahasarakham University, Mahasarakham, Thailand
- March 2009 Finished Senior High School (Grade 12, Roi-Et Wittayalai School)
- March 2006 Finished Junior High School (Grade 9, Strisuksa Roi-Et School)



มหาวิทยาลัยเทคโนโลยีสุรนารี